



**Università
degli Studi
di Ferrara**

**DOTTORATO DI RICERCA IN
SCIENZE BIOMEDICHE E BIOTECNOLOGICHE**

CICLO XXXIV

COORDINATORE Prof. Pinton Paolo

*Biomolecular approaches to endocrine-related
cancers: from diagnostics to targeted therapies*

Settore Scientifico Disciplinare MED/13

Dottoranda

Dott. Borges de Souza Patricia

(firma)

Tutore

Prof. Zatelli Maria Chiara

(firma)

Anni 2018/2022

Abstract

The aim of this PhD thesis was to investigate molecular approaches to improve the treatment and diagnosis of endocrine-related cancer. Chapter one focused on the challenges of treating typical bronchial carcinoids (TBC) and the differences between TBC and atypical bronchial carcinoids (ABC). We found that TBC can be resistant to treatment and that targeting certain proteins and pathways, such as PI3K/mTOR and TGF- β , may improve the progression-free survival in patients with advanced typical carcinoids. Chapter two examined the mechanism of action of a chemical inhibitor, Compound 5, which enhances the sensitivity of chemoresistant cells to pro-apoptotic stimuli. Our findings indicated that Compound 5 may sensitize cells to pro-apoptotic stimuli by disrupting the physical interaction between Tim16 and Tim14 proteins. Chapter three explored the use of next-generation sequencing (NGS) to diagnose thyroid nodules and identified genetic alterations in intronic regions of the PI3KCA and HRAS genes in samples with Bethesda III or IV cytology, which were associated with follicular thyroid carcinoma phenotype. Overall, these results highlight the potential for new approaches to improve the treatment and diagnosis of cancer, including targeting specific proteins and pathways, identifying ways to overcome chemoresistance, and using advanced technologies such as NGS.

For my partner in life who has always supported me.

Acknowledgements

Firstly, thank you to Professor Maria Chiara Zatelli for the endless support and friendship, you have made my PhD one of the most challenging and fulfilling years of my life. Special thank you to Anna and Stefania who were always available for helping me with the Clinical Engineering department. And in that matter, a special thank you to Giulio who was always available to fix urgently the lab's machinery.

Thank you to Professor Christopher McCabe and all the members of the McCabe's lab who were so welcoming during my time at University of Birmingham, even during the pandemic. This was an invaluable experience for me. A special thanks to Cait and her precious NanoBiT insights.

To B, you probably did not expect so many lab-related frustrations to come your way when you naively invited me to have some coffee but thank you for always believing it would work out in the end, you have been my rock. To my mom and Valter who gave me the support I needed. To my Alprazolam friends, thank you for always being ready to eliminate all stress, virtually or physically at the all-you-can-eat giappo. And finally, thank you to life. I am very grateful to all the mistakes and accomplishments that have brought me here today.

Table of Contents

CHAPTER 1 NEUROENDOCRINE NEOPLASMS	1
INTRODUCTION	1
<i>Classification: a little bit of history</i>	2
<i>Classification: World Health Organisation</i>	5
<i>Epidemiology</i>	10
<i>Risk factors</i>	15
<i>Biomarkers Landscape</i>	16
Non-specific biomarkers	20
Specific biomarkers	21
RNAs	23
Genomic biomarkers	24
Immune Response Biomarkers	26
<i>Neuroendocrine Neoplasms of the Lung</i>	27
Bronchial Carcinoids	28
<i>Signalling Pathways</i>	33
Cell-cycle	33
PI3K/Akt/mTOR	33
TGF- β	34
AIMS	36
MATERIALS & METHODS	38
<i>Drugs & Reagents</i>	38
<i>Cell culture</i>	38
<i>Cell viability</i>	38
<i>Caspase activation</i>	39
<i>Migration capacity assay</i>	40
<i>Protein isolation</i>	40
<i>Western blot analysis</i>	41
<i>Statistical analysis</i>	42
RESULTS	42
<i>TBC vs. ABC cell-cycle protein profile</i>	42

<i>Increased expression of the canonical TGF-β signalling in typical carcinoids</i>	43
<i>TGF-β increases cell malignancy features in typical carcinoids</i>	43
Cell migration	43
EMT marker N-cadherin is more expressed in typical carcinoids	43
Cell viability, caspase activation and apoptosis	48
<i>Inhibition of mTOR and TGF-β signalling reduce TBC malignancy features</i>	49
CONCLUSIONS	54
CHAPTER 2 COMPOUND 5 MECHANISM OF ACTION	57
INTRODUCTION	57
<i>Magmas</i>	58
Magmas Inhibitor: Compound 5	59
AIMS	60
MATERIALS & METHODS	62
<i>Drugs and reagents</i>	62
<i>Cell culture</i>	62
<i>NanoLuc[®] Binary Technology (NanoBiT)</i>	62
<i>Vectors, Plasmids & Primers</i>	63
<i>Transformation of DNA into E. coli</i>	64
<i>Miraprep: purification of plasmid DNA</i>	65
<i>Sequencing</i>	65
<i>Cell transfection & Plate reading</i>	66
RESULTS	67
CONCLUSIONS	68
CHAPTER 3 NGS IN THE PREOPERATIVE DIAGNOSIS OF INDETERMINATE THYROID	
NODULES	69
INTRODUCTION	69
<i>Thyroid nodules</i>	69
<i>Epidemiology</i>	70
<i>Diagnosis & Management</i>	71
Molecular Testing	72
AIMS	74
MATERIALS & METHODS	75

<i>Study Cohort</i>	75
<i>DNA extraction from cytology samples</i>	75
<i>Multi-gene NGS panel design</i>	76
<i>Determining Sensitivity, Specificity, and Predictive Values</i>	77
<i>Principal Component Analysis</i>	78
<i>Logistic regression</i>	79
RESULTS	79
<i>NGS panel as rule-out test</i>	79
<i>Logistic regression results</i>	80
<i>PCA results</i>	81
CONCLUSIONS	82
OVERALL CONCLUSIONS	84
REFERENCES	85

List of Figures

FIGURE 1 SCHEMATIC DISTRIBUTION OF PRIMARY NEN IN THE HUMAN BODY AND COMMON SITES OF METASTASIS	5
FIGURE 2 NEN INCIDENCE BY PRIMARY SITE IN ENGLAND FROM 1995 TO 2018	12
FIGURE 3 NEN INCIDENCE TREND FROM IN ENGLAND 1995 TO 2018 VS. ALL MALIGNANT NEOPLASIA.....	13
FIGURE 4 NET AND NEC 5-YEAR SURVIVAL BY PRIMARY SITE	14
FIGURE 5 NEN PREDICTED 5-YEAR SURVIVAL OF 40,534 NEUROENDOCRINE TUMOURS BY SITE OVER TIME FROM 1995–2018 IN ENGLAND.....	15
FIGURE 6 NEN RISK FACTORS AT A GLANCE FROM A SYSTEMATIC REVIEW	17
FIGURE 7 ENETS GUIDELINES FOR TCs AND ACs.....	32
FIGURE 8 SIMPLIFIED DEPICTION OF THE PI3K/AKT/MTOR AND TGF-B PATHWAYS CROSSTALK.	37
FIGURE 9 CELL-CYCLE PROTEINS PROFILE IN TBC VS. ABC AT BASELINE.....	44
FIGURE 10 TIME COURSE OF CELL CYCLE PROTEINS IN NCI-H727 CELLS.....	45
FIGURE 11 TIME COURSE OF CELL CYCLE PROTEINS IN NCI-H720 CELLS.....	46
FIGURE 12 BASAL LEVELS OF TGF-B PATHWAY'S PROTEINS IN BRONCHIAL CARCINOIDS FRESH TISSUE.	47
FIGURE 13 TGF-B-INDUCED MIGRATION IN ATYPICAL CARCINOIDS.....	48
FIGURE 14 E- AND N-CADHERINS EXPRESSION IN BRONCHIAL CARCINOIDS	50
FIGURE 15 N-CADHERIN EXPRESSION IN BC CELL LINES AFTER TREATMENT WITH EVEROLIMUS AND/OR TGF-B	51
FIGURE 16 TBC AND ABC FUNCTIONAL RESPONSES TO TREATMENT AND CASPASE 3 EXPRESSION	52
FIGURE 17 PI3K/MTOR AND TGF-B PATHWAY INHIBITION REDUCE MALIGNANCY FEATURES IN TYPICAL CARCINOIDS	53
FIGURE 18 MITOCHONDRIAL TIM23 COMPLEX, ITS SUBSTRATES AND COOPERATING TRANSLOCASES.	60
FIGURE 19 MODEL OF MAGMAS INHIBITOR BINDING IN THE TIM14–TIM16 INTERFACE POCKET	61
FIGURE 20 COMPOUND 5 CHEMICAL FORMULA	61
FIGURE 21 OVERVIEW OF THE PROTEIN:PROTEIN INTERACTION SYSTEM	62
FIGURE 22 MAPS OF THE VECTORS CONTAINING THE GENES OF INTEREST	64
FIGURE 23 NANOBIT® MCS STARTER SYSTEM	65
FIGURE 24 EFFECT OF COMPOUND 5 ON TIM16-TIM14 INTERACTION	67
FIGURE 25 SCHEMATIC REPRESENTATION OF THE TEST RESULTS.....	80
FIGURE 26 PRINCIPAL COMPONENT ANALYSIS.....	81

List of Tables

TABLE 1 LIST OF BIOPRODUCTS SECRETED BY GASTROINTESTINAL AND PANCREATIC NEUROENDOCRINE CELLS AND RESPECTIVE TUMOUR TYPES.....	4
TABLE 2 ENETS STAGING AND TNM CLASSIFICATION PROPOSAL FOR PANCREATIC NEN.....	7
TABLE 3 ENETS 2006/2007 GRADING PROPOSAL ENDORSED BY THE WHO 2010 CLASSIFICATION	7
TABLE 4 WHO GEP-NEN CLASSIFICATION	8
TABLE 5 LUNG NEN CLASSIFICATION	9
TABLE 6 THE 2022 WHO/IARC UNIVERSAL TAXONOMY FOR EPITHELIAL NEUROENDOCRINE NEOPLASIA ...	10
TABLE 7 NEN REPORTED INCIDENCE AMONG STUDIES.....	13
TABLE 8 LIST OF NETEST 51 MARKER GENES.....	25
TABLE 9 LIST OF PRIMARY ANTIBODIES	41
TABLE 10 AREA UNDER THE CURVE OF TIME COURSE OF CELL CYCLE PROTEINS IN TBC AND ABC CELL LINES	47
TABLE 11 PRIMERS DESIGNED TO FIT THE NANOBIT VECTORS.....	63
TABLE 12 EXPRESSION CONSTRUCTS THAT WERE CREATED.	67
TABLE 13 NGS PANEL	76
TABLE 14 DEFINITION OF PERFORMANCE PARAMETERS USED TO DESCRIBE DIAGNOSTIC TESTS	77
TABLE 15 CONTINGENCY MATRIX USED FOR DERIVING SENSITIVITY, SPECIFICITY, PPV AND NPV.....	78
TABLE 16 PERFORMANCE OF THE NGS PANEL USED AS A DIAGNOSTIC TOOL.....	80

Abbreviations

AC	Atypical Carcinoid
APUD	Amine Precursor Uptake and Decarboxylation
AUS	Atypia of Undetermined Significance
BP-NEN	Bronchopulmonary NEuroendocrine Neoplasm
CDK	Cyclin-Dependent Kinases
cfDNA	Cell-Free DNA
CgA	Chromogranin A
ctDNA	Circulating Tumour DNA
CytC	Cytochrome C
DNES	Diffuse (Neuro)Endocrine System
EC	Enterochromaffin Cells
EMT	Epithelial-Mesenchymal Transition
ENETS	European Neuroendocrine Tumor Society
eve	Everolimus
FLUS	Follicular Lesion of Undetermined Significance
FN	Follicular Neoplasm
FNA	Fine Needle Aspiration
GEP	Gastro-Entero-Pancreatic
GI	GastroIntestinal
GM-CSF	Granulocyte-Macrophage-Colony Stimulating Factor
GOI	Gene Of Interest
IGF-1	Insulin-like Growth Factor 1
LCNEC	Large Cell NEuroendocrine Carcinoma
LgBiT	Large Bit
lncRNA	Long Non-Coding RNA
MEN	Multiple Endocrine Neoplasia
miRNA	MIcroRNA
mTOR	Mammalian Target Of Rapamycin
NanoBiT	Nanoluc Binary Technology
NE	NEuroendocrine
NEC	NEuroendocrine Carcinoma
NEN	NEuroendocrine Neoplasms
NET	NEuroendocrine Tumour
NGS	Next Generation Sequencing
NPV	Negative Predictive Value
OR	Odds Ratio
PA	Pituitary Adenomas
PAC	Paclitaxel
PCA	Principal Component Analysis
PCR	Polyerase Chain Reaction
PNEC	Pulmonary NE Cells
pNET	Pancratic NET
POI	Protein Of Interest

PPV	Positive Predictive Value
SCLC	Small-Cell Lung Carcinoma
SFN	Suspicious Follicular Neoplasm
SmBiT	Small Bit
SNP	Single Nucleotide Polymorphism
SSA	SomatoStatin Analogue
TBSRTC	The Bethesda System for Reporting Thyroid Cytopathology
TC	Typical Carcinoids
TC	Thyroid Cancer
TGF-β	Transforming Growth Factor Beta
TN	Thyroid Nodule
TNM	Tumour-Node-Metastasis
WHO	World Health Organisation

CHAPTER 1

NEUROENDOCRINE NEOPLASMS

INTRODUCTION

Neuroendocrine neoplasms (NEN) are a group of relatively rare neoplasms arising from the diffuse (neuro)endocrine system (DNES) (1). The DNES may be divided into two divisions: central and peripheral. The central DNES comprise cells of the hypothalamo-pituitary-pineal complex whereas DNES cells located in the peripheral division are scattered throughout the entire body, isolated or grouped to form aggregates, such as the islets of Langerhans in the pancreas, the C cells of the thyroid or neuroepithelial bodies in the bronchopulmonary tract (2).

Neuroendocrine (NE) cells are epithelial cells having both “neuro” and “endocrine” properties (3). The majority of them originate from epithelial progenitors’ cells of their respective tissue sites (4), i.e., the endoderm, including cells of the adrenal medulla and C cells of the thyroid, whereas paraganglia cells probably originate from neural crest precursors (5). NE cells may be identified on the presence of dense core granules similar to those found in serotonergic neurons storing monoamines, which they synthesise and secrete (3). The first described NE cells were the enterochromaffin cells (EC) of the small intestine in the late nineteenth century. Based on their distinct reaction to histological stains NE cells began to be identified in the years to come revealing their presence throughout the intestinal mucosa, but also in other epithelial tissues including the lungs and the urogenital tract. These histological studies led to the proposal that NE cells make up the DNES, a peculiar functional system sharing biochemical, cytological and secretory properties, as well as control mechanisms. Thus, much like neurons, NE cells are able to metabolise, produce and secrete bioactive compounds in a coordinated fashion with the surrounding environment and with the nervous system, functioning as a diffuse hormonal system composed of cells scattered throughout the body (6, 7). NE cells are able to metabolise, produce and secrete bioactive compounds in a coordinated fashion with the surrounding environment and with the nervous

system, functioning as a diffuse hormonal system composed of cells scattered throughout the body (6, 7).

Owing to their diversity of location, types and biological roles, classification of NE cells is very challenging. In fact, with exception for the pancreatic islet cells, the cells of the adrenal medulla, and parafollicular cells (C cells), whose function is well-established, other NE cells are less well defined, and the list of secretory products secreted by these cells is continuously being updated (**Table 1**). Researchers started to give special attention to NE cells and the DNES due to their behaviour in disease. NEN sparked a great deal of interest in NE cells pathophysiology as it as it might relate to them and explain the tumorigenesis and behavioural characteristics of these neoplasms. As NE cells-derived, NEN are epithelial neoplasms with neuroendocrine differentiation capable of producing and secreting a variety of hormones and active peptides/amines showing a wide spectrum of morphological, functional and behavioural characteristics difficult to manage and classify (3, 8). NEN have been observed in almost all tissues (**Figure 1**) but are frequently found in the gastrointestinal (GI) tract and the bronchopulmonary system, reflecting the density of NE cells in these tissues. The majority, however, are of gastro-entero-pancreatic (GEP) origin including NEN of the stomach, pancreas, small bowel, appendix, colon and rectum (3, 9) (**Table 1**).

Classification: a little bit of history

Classification and nomenclature of NEN has been complex and confusing. In the early 1800s, NEN belonged to the group of epithelial tumours. These were further subdivided in large-cell and small-cell tumours, the latter being more difficult to characterise. In the beginning of the 20th century, Siegfried Oberndorfer coined the term *karzinoide* to describe a “carcinoma-like” tumour with benign behaviour (10, 11), although the fact that they only described benign lesions soon proved to be incorrect. (12). As limiting as it was (and is) to define such a wide range of tumours, the term carcinoid is difficult to abandon to this day.

Between 1870 and 1900 it was believed that some cells identified in the intestinal mucosa were the source of carcinoids. Given their resemblance to endocrine cells which could retain special stains, these cells were termed “enterochromaffin” and “argentaaffin” NE cells (13). By the time EC cells and the term carcinoid related to NE cells, a small-cell tumour identified in the mediastinum was named “oat-celled carcinoma” in 1926 (14). The terms “oat-celled

carcinoma”, “small-cell carcinoma”, “ana-plastic-cell carcinoma”, “oat-cell sarcoma”, were synonyms later used to describe other extra-pulmonary NE malignant neoplasms with similar microscopic features: resemblance to lymphocytes in size and shape, with scanty and basophilic cytoplasm, and uniform, dark, and generally round nuclei (15, 16).

In 1960 it became clear that oat-cell carcinoma and other lung carcinomas had a very different histogenesis but were histogenetically related with other carcinoids instead (17). Tracing of the cytological and biochemical properties of these tumours led to the cells of the APUD (amine precursor uptake and decarboxylation) system. APUD cells are NE cells capable of secreting a variety of polypeptide hormones, including catecholamines and 5-hydroxytryptamine (5-HT, serotonin) (18). In fact, 5-HT was first isolated in 1948 and by 1953 was confirmed to be the major hormone responsible for the carcinoid syndrome, characterised by flushing, diarrhoea, bronchoconstriction, and valvular heart disease (19).

The concept of atypical carcinoid (AC) having a worse prognosis than other carcinoids emerged in 1972 by Arrighi et al. with a histologically carcinoid variant organised like a gland, with large polymorphic nucleated cells (20). In 1977 a study reported an intermediate polygonal large-cell variant of the oat-cell carcinoma showing decreased responsiveness to therapy (21). It was then logical to think that carcinoids and oat-cell carcinomas were part of a spectrum of cells where (well-differentiated) typical carcinoids (TC) are at one end, and typical small-cell (oat-cell) carcinoma in the other end of the spectrum. The atypical or intermediate forms were the link between the typical forms (22, 23, 24, 25).

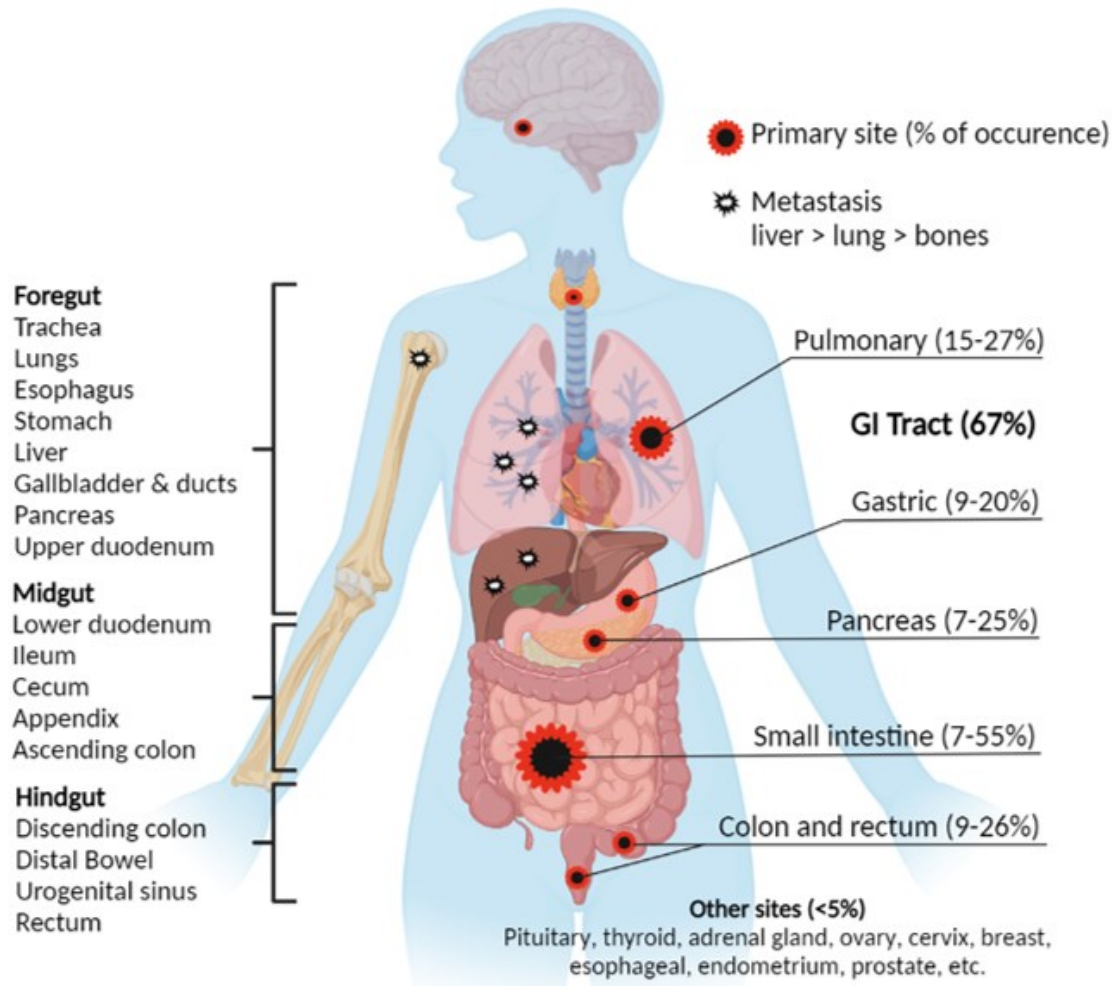
In the last century, several schemes for NEN classification were considered, including classifying them based on their APUD properties, morphologic pattern (26) and silver staining affinity (27), and based on their embryotic origin (1963) (**Figure 1**): foregut, (thymus, oesophagus, lung, stomach, duodenum, biliary, pancreas), midgut (appendix, ileum, cecum, ascending colon), and hindgut (distal bowel and rectum) (28). Site-specific classification is still used however restrictive because clinical behaviour of two NEN arising at the same embryogenic site can vary considerably. Taken together with histological characteristics, NEN started to be divided in typical (well-differentiated) and atypical (poorly differentiated) carcinoids of specific tissue. Thus, a universal consensus for nomenclature of NEN was missing, and with growing knowledge sowed greater confusion.

Table 1 *List of Bioproducts Secreted by Gastrointestinal and Pancreatic Neuroendocrine Cells and Respective Tumour Types*

Tumour type	Cell of origin	Tissue site	Secreted products
Non-functional pNEN	Precursor cell or omnipotent stem cell	Pancreas	None defined
Colorectal NEN	L cells, EC	Colon-rectum	5-HT, glucagon-like peptide-1, YY, Neuropeptide Y
ECLoma (type I-III)	Enterochromaffin-like (ECL)	Gastric fundus	Histamine
Gastrinoma	G cells	Gastric antrum and duodenum, pancreas	Gastrin
	N cell	Jejunum and ileum	Neurotensin 1
Small bowel carcinoid	EC	Entire GI tract	5-HT, substance P
	Beta	Pancreatic islets	Amylin
	M cells	Small intestine	Motilin
	S cell	Duodenum and jejunum	Secretin
Small intestinal NEN	Enterochromaffin (EC)	Entire GI tract	Serotonin, substance P, guanylin, melatonin
Ghrelinoma	Ghrelin cells (Gr)	Oxyntic glands, pyloric glands, small intestine	Ghrelin
CCKoma	I cells	Lining of the duodenum	Cholecystokinin (CCK)
GIPoma	K cells	Small intestine	Gastric inhibitory polypeptide (GIP)
Glucagonoma	Alpha	Pancreatic islets	Glucagon
Insulinoma	Beta	Pancreatic islets	Insulin
Somatostatinoma	Delta	Stomach, intestine and the pancreatic islets	Somatostatin

Figure 1

Schematic distribution of primary NEN in the human body and common sites of metastasis



Note. Left: classification based on embryotic origin. Right: % of occurrence. Created with BioRender.com.

Classification: World Health Organisation

Cancer diagnosis relies on a classification system that is standardised and accepted internationally, providing consistency in patient treatments and allowing cancer workers in all parts of the world to compare their findings. To this aim, the World Health Organisation (WHO) in collaboration with pathologists from 13 countries published in 1980 its first classification system for NEN in the *Histological Typing of Endocrine Tumours* book. In the explanatory notes, the Authors recognise the existence of several cells related to the DNES scattered throughout the body, especially the GI tract, which have been shown to produce a specific hormone and metabolise amine precursors. They have also suggested, in agreement with the state of knowledge of that time, that these cells could all belong to the APUD cell system. Accordingly, in this issue, the term carcinoid was used to describe all tumours of the DNES excluding endocrine tumours of the pancreas, thyroid and paragangliomas (29).

Carcinoids were further divided based on their functional state, i.e., their ability to produce and secrete bioproducts, and based on major cell type: argentaffinoma or the “classical” carcinoid, arising from EC-cells were typically found in the midgut and associated with the production of 5-HT; gastrinomas from gastrin-producing cells; other unspecified carcinoids, which classification was not an easy task and included carcinoids arising at any organ (29). The 1980 WHO classification was rapidly considered ambiguous as carcinoid terminology was applied differently among pathologists and clinicians. Pathologists considered carcinoids all tumours with NE differentiation, whereas for clinicians only functioning tumours presenting carcinoid syndrome were termed carcinoid. Moreover, given the degree of heterogeneity that these tumours retained, it was becoming evident that carcinoids arising at different sites and atypical forms could no longer belong to the carcinoid category.

A more inclusive and uniform terminology was necessary and by 1995 the term “neuroendocrine tumour” (NET) was proposed to replace “carcinoid” (30). Tumours were subdivided based on their site of origin, histology, invasiveness, presence of metastasis and hormonal activity. This nomenclature suited all NET, arising at any site, and was soon put into practice within the 2000 WHO classification system, which identified three major histologic groups: well-differentiated endocrine tumour with benign or uncertain behaviour, well-differentiated endocrine carcinoma with low-grade malignant behaviour and poorly differentiated endocrine carcinoma with high-grade malignant behaviour (31). Several issues have arisen with this classification as there were a high number of clinicopathologic variables to be assessed to correctly identify tumour category; many of them evaluable only after resection. Another issue that was probably addressed only recently, is the grey zone that divide well-differentiated tumour with high grade malignancy from well-differentiated carcinoma. In the 2000 classification system, they would all belong to the latter, precluding further prognostic stratification in patients with well-differentiated tumours and distant metastasis.

In an attempt to address these issues, the European Neuroendocrine Tumor Society (ENETS) proposed a site-specific staging system based on the well-known tumour-node-metastasis (TNM) template that could aid the prognostic stratification of GEP NET (32). Stage I included T1 NET with limited growth, stage II comprised T2 or T3 larger or more invasive tumours with no metastasis, stage III included tumours invading the surrounding structures (IIIA) or with regional node metastasis (IIIB) and stage IV, tumours presenting distant

metastasis. **Table 2** shows exemplary TNM classification and staging proposal for pancreatic NEN (33, 34). In that venue, they also proposed a generic grading system suitable for all digestive NEN based on the mitotic count and proliferation index (Ki67), which was later adopted by the 2010 WHO classification: well (G1 and G2) and poorly differentiated tumours (G3) were replaced by NET (G1 and G2) and neuroendocrine carcinoma (NEC, G3) (35) (**Table 3**). Several studies demonstrated not only that stage and grade were complementary, but that the cut-points used to separate low/high grade malignancies were predictive and prognostically significant, as high-grade malignancies often associated with decreased survival (36, 37, 38).

Table 2 ENETS Staging and TNM classification proposal for Pancreatic NEN

Stage	T	Primary Tumour	N	Regional lymph Node metastasis	M	Distant Metastasis
I	T1	Limited to the pancreas and with <2 cm	N0	No	M0	No
IIa	T2	Limited to the pancreas and with 2-4 cm	N0	No	M0	No
IIb	T3	Limited to the pancreas and with >4 cm or invading duodenum or bile duct	N0	No	M0	No
IIIa	T4	Invasiveness to adjacent organs	N0	No	M0	No
IIIb	Any		N1	Yes	M0	No
IV	Any		N1	Yes	M1	Yes

Table 3 ENETS 2006/2007 Grading Proposal Endorsed by the WHO 2010 Classification

Grade	Mitotic count (per 10 HPF)	Ki-67 (%)
Grade 1 (low)	<2	≤2
Grade 2 (intermediate)	2–20	3–20
Grade 3 (high)	>20	≥20

Note: HPF= high power fields.

It was only in the 5th edition of the WHO classification of tumours that NEN arising at a specific organ started to be described within that organ's chapter, containing detailed description for each functioning or non-function NEN subtype (39). In this edition, NEN arising in any part of the body have been subdivided in NET and NEC. Within the NET group a grade 3 (G3) category, defined as having a mitotic rate >20 per 2 mm² or Ki67 >20%, was added to support stratification of those well-differentiated tumours with high grade malignancies (**Table 4**). NEC, on the other hand, is considered high-grade by definition and may be subdivided in small/large-cell type. NET and NEC may be further

distinguished based on molecular differences as MEN1, DAXX and ATRX mutations usually occur in NET, whereas TP53 or RB1 mutations in NEC.

Table 4 WHO GEP-NEN classification

GEP-NEN (WHO 2019)		
Terminology	Criteria:	
	Mitotic counts per 2 mm ²	Ki-67 index
NET, grade 1 (G1)	<2	<3%
NET, grade 2 (G2)	2–20	3–20%
NET, grade 3 (G3)	>20	>20%
NEC (small or large cell)	>20	>20%
MiNEN		

Note. MiNEN: mixed NE with non-NE neoplasm

NE pulmonary lesions, almost as a separate entity, followed similar but different nomenclature. In the second edition of The World Health Organisation Histological Typing of Lung Tumours (1982) small-cell carcinoma was divided into oat-cell carcinoma, an intermediate cell type and combined oat-carcinomas with other major types, whereas carcinoid tumours (typical and atypical) included lesions arising from EC cells (40). The 1999 WHO classification included large cell neuroendocrine carcinoma (LCNEC) as one of the major NET categories and refined the criteria for TC/AC identification based on the mitotic count and presence of necrosis. Four major groups were characterised by increasing aggressiveness: low-grade TC, AC having an intermediate differentiation and worse prognosis; LCNEC and small-cell carcinoma (SCLC) (41, 42), both high-grade malignancies.

In the 2004 WHO-IARC (International Agency for Research on Cancer) revision for lung and thymus NET the term “carcinoid” was reinforced and referred almost exclusively to pulmonary NEN. The already described morphological lung NEN categories remained the same (TC, AC, LCNEC, SCLC), whereas criteria for classification included mitotic count, presence/absence of necrosis, tumour mass and morphology (43). TC and AC have carcinoid morphology, resemble other carcinoids found in other organs and are more often found in younger patients. TC, as the less aggressive carcinoid was characterised as having less than 2 mitoses per 2 mm² (10 HPF) and lacking necrosis; AC with 2-10 mitoses per 2 mm² (10 HPF) OR presence of necrosis. The main criterion for separating carcinoid forms from LCNEC and SCLC was a mitotic count of 11 or more mitoses per 2 mm², with an average

of 70-80 per 2 mm². Whereas, LCNEC vs SCLC detection is much trickier and included a set of cytologic parameters that could aid the identification of a non-small cell carcinoma such as large cell size, abundant cytoplasm, frequent nucleoli, among others.

In 2015 the 4th edition of the WHO classification of tumours of the lung, pleura, thymus, and heart included a few changes from the previous 2004 edition, however it did not follow the uniform NEN classification system applied to other organs (44). NEN were grouped under one major NET category and the role of Ki-67 was marginal to separate NEC from TC and AC. Due to conflicting data at the time, the use of Ki-67 marker to separate TC from AC was not recommended, whereas methods for counting mitoses were considered the key criteria for separating them from each other and from NEC. Terminology and criteria for classification of lung NEN remained largely unchanged in 2021 with the latest edition for lung NEN classification (**Table 5**). Ki-67 evaluation is still marginal, however, a rate of 30% is considered the upper limit for lung carcinoids. Therefore, although a NET grade 3 category does not exist in lung NEN grading, it is becoming increasingly evident that high-proliferative carcinoids do exist and need further consideration. The current proposal is to classify these carcinoids as “LCNEC with morphologic features of carcinoid tumor” (45).

Table 5 Lung NEN classification

Terminology	Mitotic counts per 2 mm ²
Typical carcinoid (TC)	<2
Atypical carcinoid (AC)	2–10 (or necrosis)
SCLC and LCNEC (NEC)	>10
Combined NEC and NSCLC	

Recently, the 2022 WHO Classification of Tumours Editorial Board have implemented new classification principles in the 5th edition of the WHO Classification of Endocrine Tumors, now called Classification of Endocrine and Neuroendocrine Tumors (46). It is an important change as all NEN belong to the NEN category and within this book site-specific NEN are described. The universal nomenclature based on cell differentiation and grading has been maintained from the latest expert consensus meeting held in 2018. Whilst paragangliomas represent the neuronal type NEN, NET and NEC characterise well/poorly differentiated epithelial neoplasms. NET may be graded in G1, G2 or G3 depending on proliferation status, whereas NEC are high grade by definition and may be further subdivided in small/large cell type (**Table 6**). Further, prognostic stratification by this grading system in three tiers has

been proved effective and reliable not only in the GI tract but also in the respiratory system (46).

Table 6 *The 2022 WHO/IARC universal taxonomy for epithelial NE neoplasia*

Tumour category definition	Neuroendocrine neoplasia (NEN)	
Tumour family/class definition	Well-differentiated NEN	Poorly differentiated NEN
Tumour type definition	NET	NEC
Tumour subtype definition	Variable depending on site	Large cell NEC or small cell NEC
Tumour grade definition	G1, G2, G3	High grade (by definition)

Note. Adapted from " Overview of the 2022 WHO Classification of Neuroendocrine Neoplasms" by Rindi G. et. al, Copyright © 2022, The Author(s), under exclusive licence to Springer Science Business Media, LLC, part of Springer Nature.

Epidemiology

As mentioned above, the nature of NEN is very complex: they belong to a very heterogenous group of malignancies, with often confusing histology and nomenclature. Not only that, NEN are very rare, accounting for only 0.5-1.0% of all newly diagnosed malignancies. They often follow an indolent course, though 10-30% are highly proliferative and may present resistance to therapy, characterised by rapid disease progression. Epidemiological studies in such a wide category of malignancies need considerable and accurate population-based registries, as well as a long longitudinal follow up (47, 48). Few countries have epidemiological data on NEN, and many available studies regard specific centres with a small cohort, or are site-specific, usually GEP- or lung NEN given their higher frequencies. The most used population-based registry regarding NEN belong to the American National Cancer Institute's Surveillance, Epidemiology, and End Results (SEER) Program, which is a comprehensive cohort initiated in 1973 annually updated (49).

Incidence

Incidence refers to newly diagnosed individuals in a population over a specified time interval. The most recent epidemiological NEN study utilised data from the National Cancer Registry and Analysis Service (NCRAS) of England, and evaluated demographic, clinical, and prognostic features from 1995 to 2018 (50). According to this study, the annual age-adjusted incidence of NEN has increased from 2.5 in 1995 to 8.8/100,000 inhabitants in

2018. The increase in incidence was reported in NEN arising at any site, stage and grade (50, 51). Other studies report similar trends and are shown in Table 7 (50, 51, 52, 53). The largest increase was reported in the lung followed by small intestine (50, 51) (**Figure 2**). Whilst the incidence of all malignant neoplasms has remained mostly stable, NEN incidence has steadily risen in the last decades (**Figure 3**) probably due to a number of factors such as greater awareness and improved diagnostic/imaging tools, not to mention the constant effort put into classification, grading and staging systems of these neoplasia over the years (50).

Prevalence

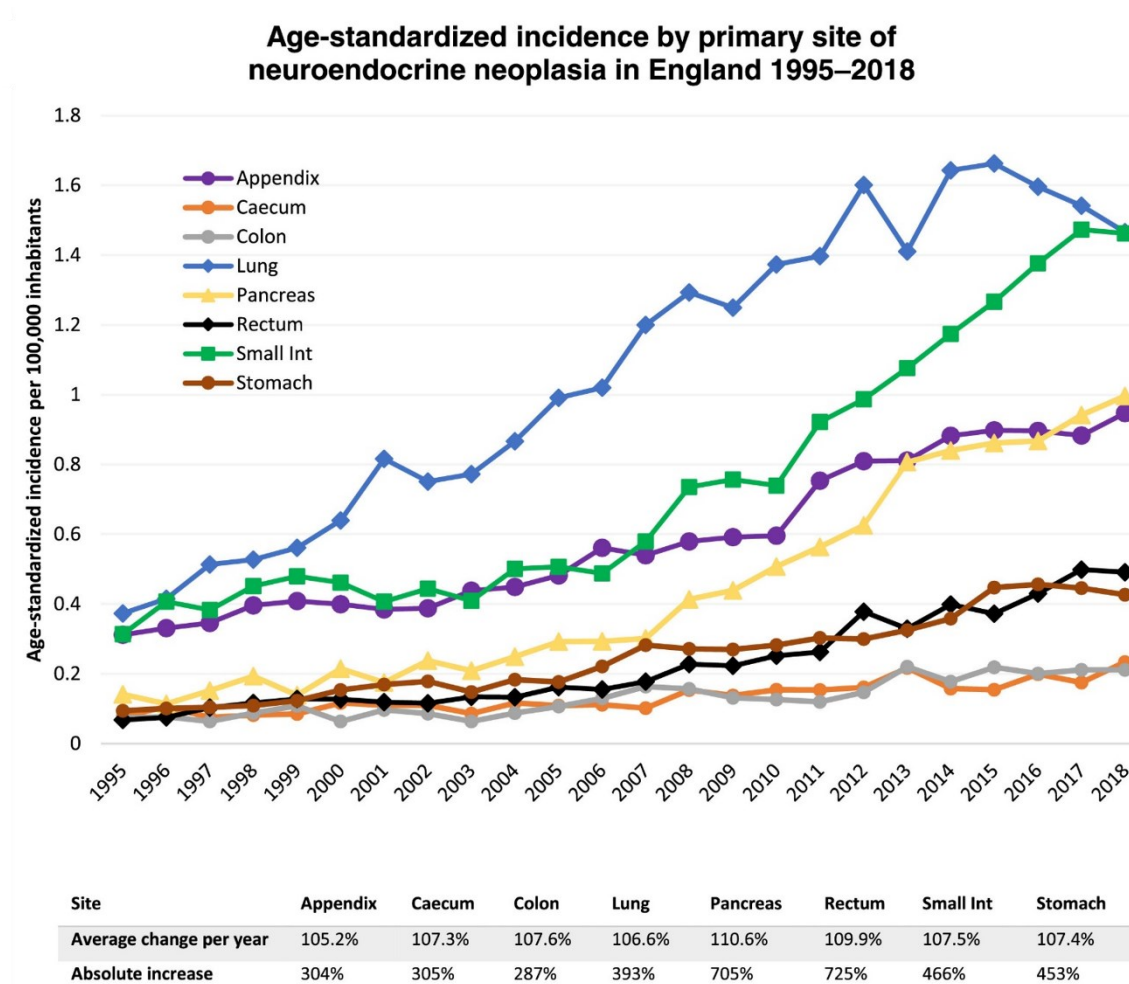
The overall prevalence of NEN has also increased in the last decades, however, values may vary considerably among studies due to the way they are reported. Prevalence is the proportion of affected individuals in a population at a specified point in time or over a specified period, usually 10 or 20 years. Some Authors report in %, some in counts out of 100, others in number of cases per 100.000 inhabitants. A 29-year limited-duration prevalence for NEN was estimated from incidence over the American SEER 9 registry (1972 to 2004) as 35/100,000 or 103,312 alive patients (54). Differently, Dasari et. al reported a 20-year limited-duration prevalence increase from 0.006% in 1993 to 0.048% in 2012, corresponding to 700% (51).

Survival

Survival may be reported as time (years or months) that patients survive a disease since first diagnosis or as % of patients alive after diagnosis in a determined period of time, usually 5 or 10 years. All-NEN survival statistics should be considered lightly because it can vary considerably depending on the population, tumour grade, site of origin and presence of metastatic disease. Moreover, a study conducted with the Ontario Cancer Registry reported that other factors such as male sex, low-income and rural living associated with worse survival (55). In fact, early diagnosis is essential in determining survival, whereas low-income and rural living might relate to the scarce access to healthcare services. Dasari et. al Localised NET had better median OS vs. regional NET (10.2 years) and distant NET (12 months). Among graded NEN, G1 had the highest median OS (16.2 years), G2 8.3 years, G3 and NEC had the worst OS of 10 months (51).

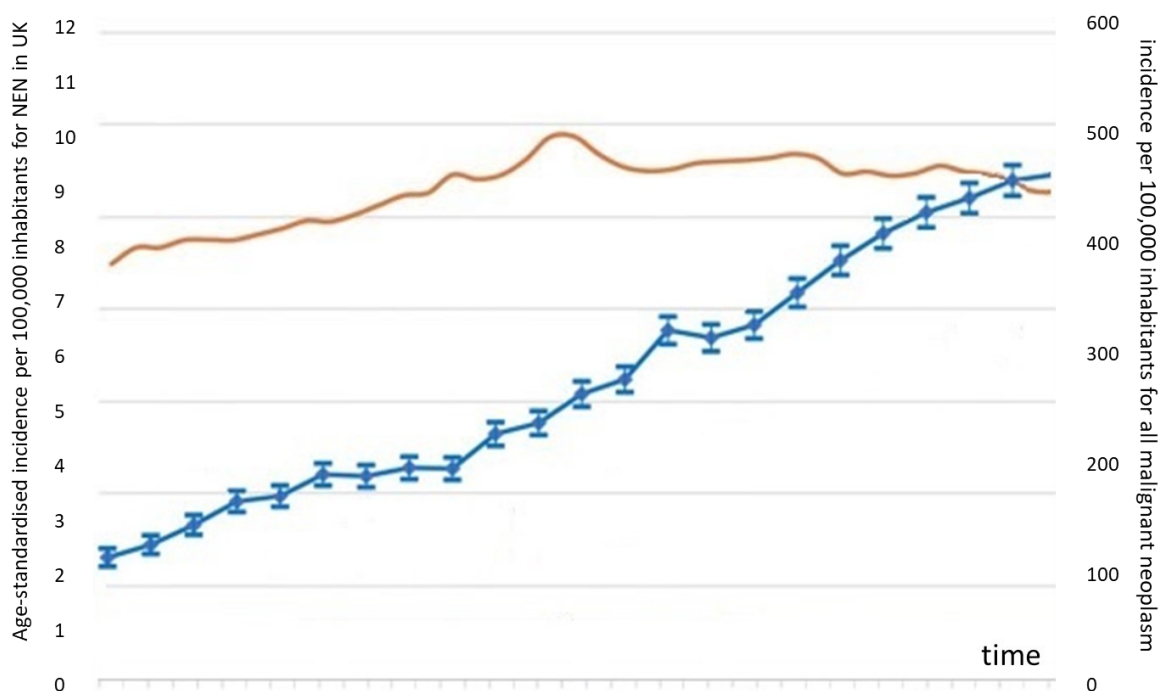
Figure 2

NEN incidence by primary site in England from 1995 to 2018



Note. Age standardized incidence of 40,534 NEN at main sites from 1995–2018 in England with average percentage change per year and absolute rise. Data source: NCRAS. From "Incidence of neuroendocrine neoplasia in England 1995–2018: A retrospective, population-based study" by White B. et. al, 2022, *The Lancet Regional Health – Europe*, Volume 23. Copyright 1969, Elsevier.

Further, the Authors calculated separately the median OS among registries in order to evaluate if there were changes in the survival rates of NEN. Patients diagnosed between 2005-2008 and 2009-2012 had 17.1 and 21.3% lower risk of death vs. patients diagnosed between 2000-2004, indicating an improvement in survival over the years. In fact, nine years before, Yao et. al had reported a much lower median OS over the same American SEER registry: 75 months for all-NEN, 124 and 64 months for patients bearing G1 and G2 tumours, respectively, 10 months for G3 NET and NEC (56). In England White et. al calculated 5-year survival rate for NET and NEC by type of NEN. Appendix had the best survival rate: 92% for NET and 65% for NEC. Rectal NET presented one of the highest rates (90%),

Figure 3*NEN incidence trend from in England 1995 to 2018 vs. all malignant neoplasia*

Note. Age standardized incidence of 63,949 neuroendocrine neoplasia from 1995–2018 in England. 95% confidence interval displayed (blue) and incidence for all malignancies (yellow). Data source: NCRAS. Adapted from "Incidence of neuroendocrine neoplasia in England 1995–2018: A retrospective, population-based study" by White B. et. al, 2022, The Lancet Regional Health – Europe, Volume 23. Copyright 1969, Elsevier.

Table 7 *NEN reported incidence among studies*

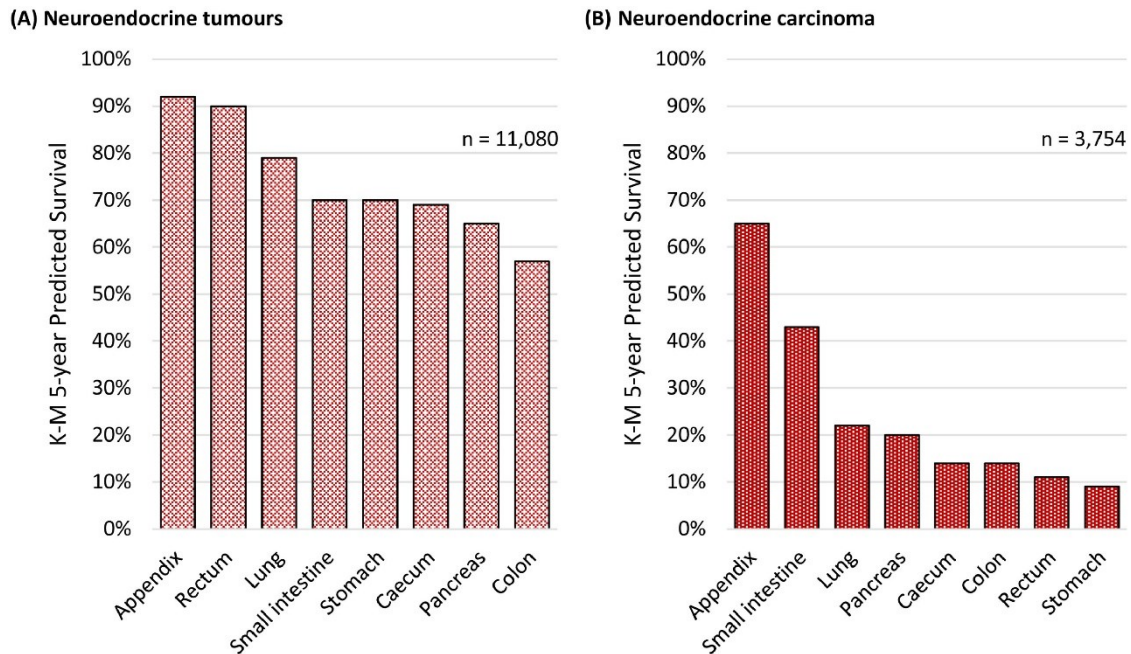
Country	Cohort (n)	Year range	Incidence/100.000 inhabitants		Reference
USA	64.971	1973 2012	1.09	6.98	Dasari et. al 2017
United Kingdom	63.949	1995 2018	2.5	8.8	White et. al 2022
Norway	2.030	1993 2004	2.35	4.06	Hauso et. al 2008
Ontario, Canada	5.619	1994 2009	2.48	5.86	Hallet et. al 2014

however rectal NEC has one of the worst rates (11%). Lung NET presented a good 5-year survival rate of >75%, however lung NEC survival did not reach 25% (50) (**Figure 4**). White et. al also reported an improvement in NEN survival rates over the years, especially in NEN of the small intestine, colon and pancreas (**Figure 5**). The smallest improvement was reported in NEN of the appendix, lung and rectum (50).

Mortality

Many Authors choose to estimate and report only survival rates, although mortality is strictly associated with it. Mortality may be reported as hazard ratio, often used as measure to

Figure 4
NET and NEC 5-year survival by primary site

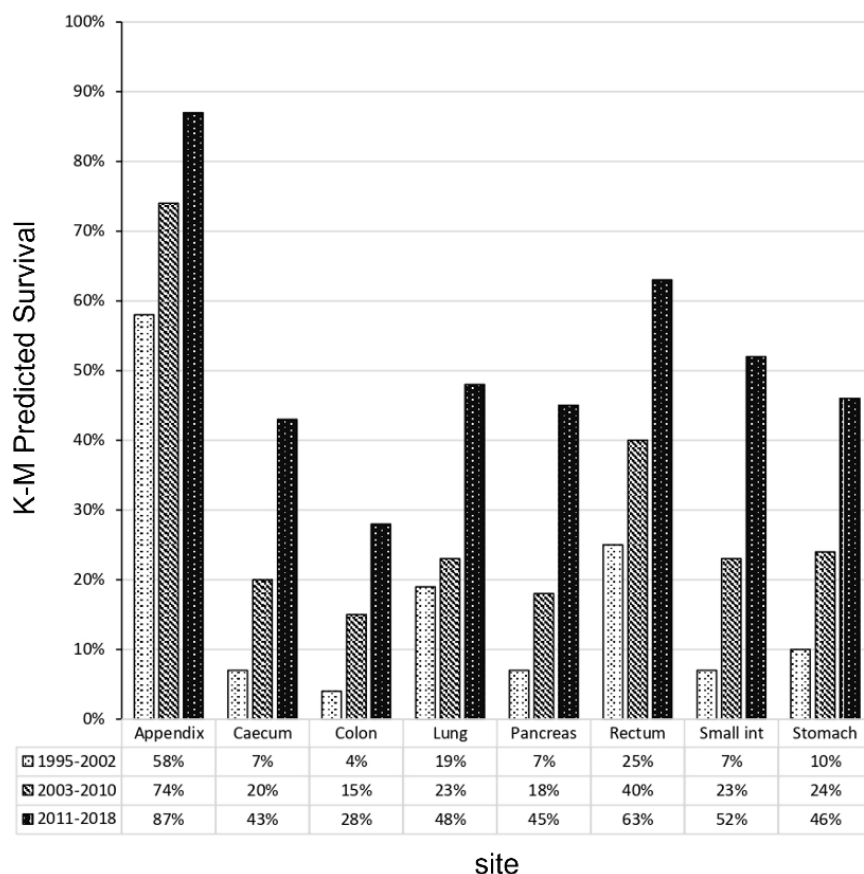


Note. Kaplan–Meier predicted 5–year survival of (A) 11,080 neuroendocrine tumours and (B) 3,754 neuroendocrine carcinomas between 2012 and 2018 in England. Source data: NCRAS. Adapted from "Incidence of neuroendocrine neoplasia in England 1995–2018: A retrospective, population-based study" by White B. et. al, 2022, *The Lancet Regional Health – Europe*, Volume 23. Copyright 1969, Elsevier.

survival, or standardised mortality rates (SMR) which is the ratio of observed deaths in the studied cohort to expected deaths in the general population over the same period. In a study based on the UK population between 2013 and 2015, cell morphology, stage, sex, age and low-income associated with mortality. Specifically, Genus et. al reported 5233 observed deaths over 1442.6 expected deaths, meaning an increased mortality of 3.6-fold for all malignant NEN diagnosed in that period (57). Notwithstanding the increased incidence trends, survival rates are increasing as well probably due to greater awareness, availability of treatment and improved therapies. Unfortunately, NEN are often difficult to characterise, and mortality is still high, especially for some NEN type which are still orphan of an effective therapy. They can be silent for many years and mimic various other disorders. This often translate in significant delays in diagnosis.

Figure 5

NEN predicted 5-year survival of 40,534 neuroendocrine tumours by site over time from 1995–2018 in England.



Note. Kaplan-Meier predicted 5-year survival of 40,534 neuroendocrine tumours by site over time from “Incidence and survival of neuroendocrine neoplasia in England 1995–2018: A retrospective, population-based study” by White B. et. al, 2022, The Lancet Regional Health – Europe, Volume 23. Copyright 1969, Elsevier.

Different population-based studies have reported presence of metastatic disease at first diagnosis in proportions ranging from 20-70% (58, 59, 60). Interestingly, a recent study reported a mean delay of 52 months between symptoms identification and diagnosis and that patients bearing NEN see an average of six different healthcare providers before receiving an accurate diagnosis (61). For these reasons, early diagnosis of NEN through non-invasive routine procedures would help increase survival rates, reduce morbidity and mortality.

Risk factors

Because of the nature of NEN, literature regarding NEN risk factors is scarce, mostly conducted in the USA and Europe in case-control studies. They are a family of very different and rare neoplasms, suffering of the lack of funding and reference standards for so long. Despite the heterogeneity regarding this argument in the literature, some risk factors have

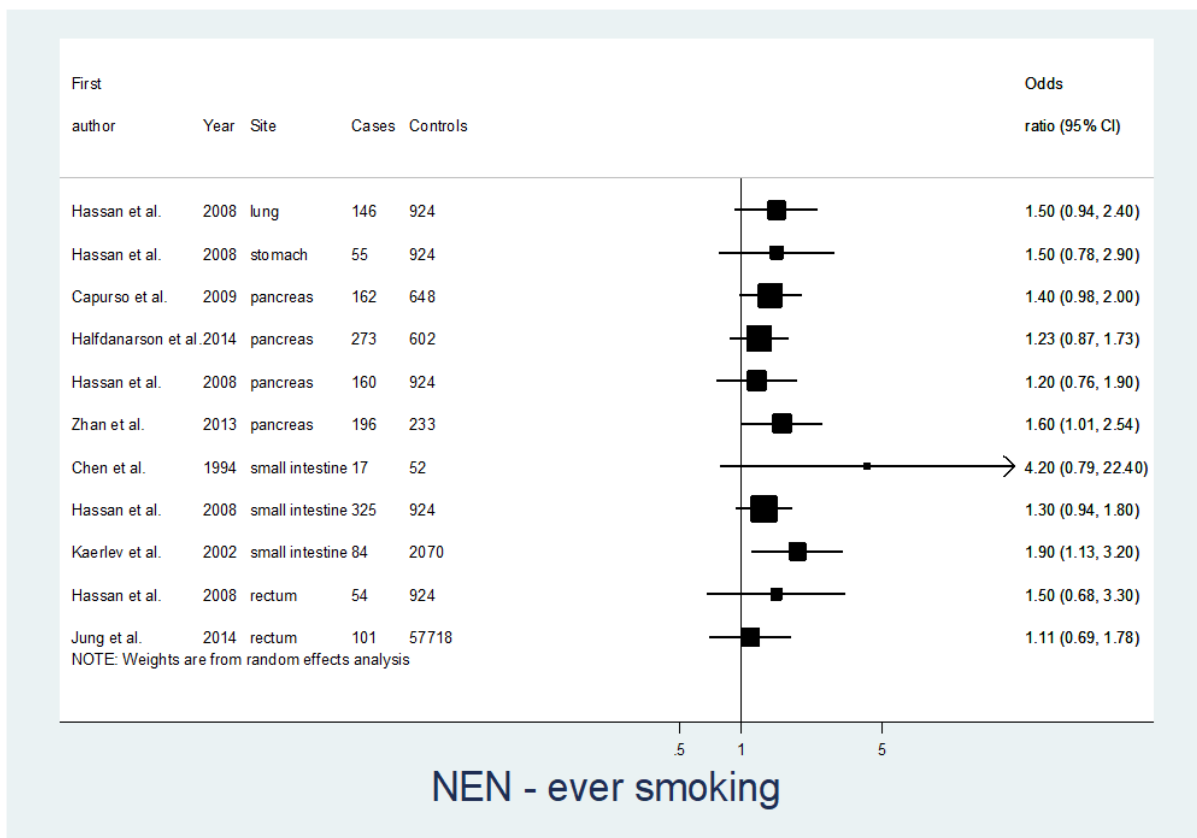
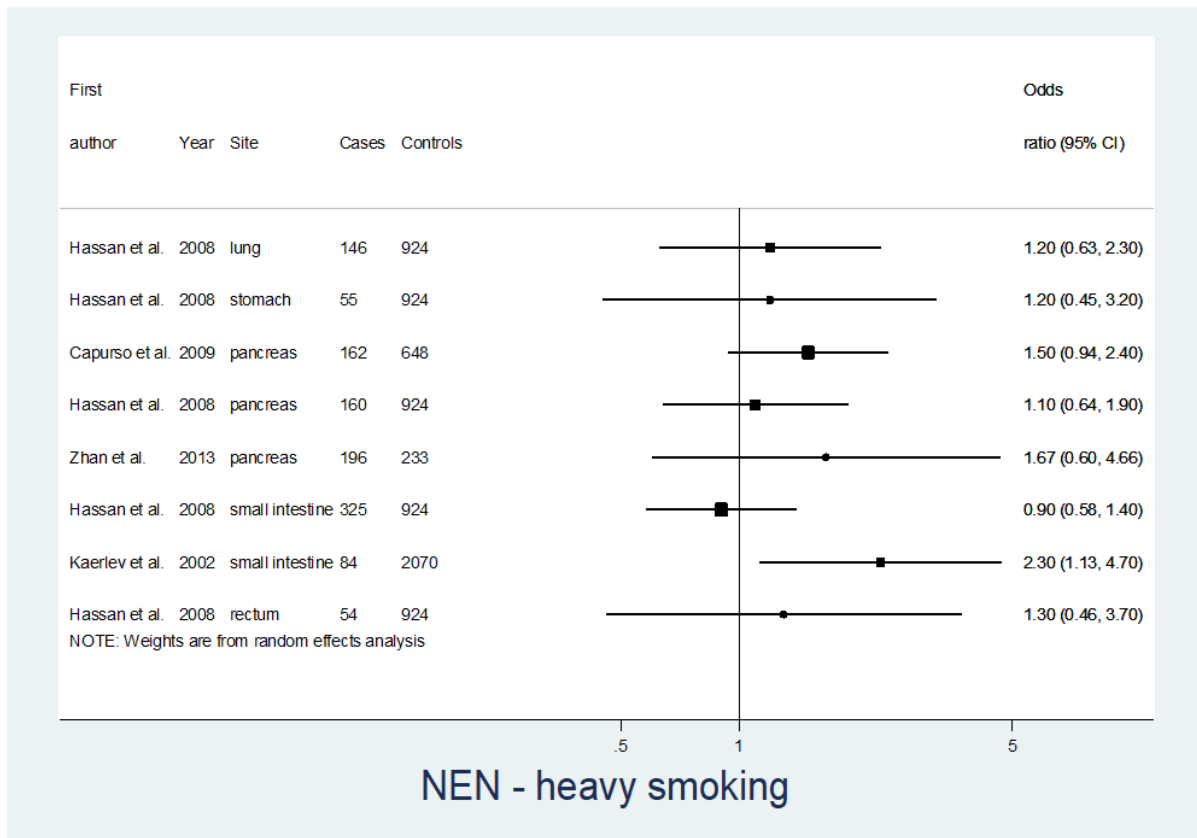
been reported to augment the risk of NEN. A recent meta-analysis reviewed 24 publications that included epidemiological studies investigating NEN potential risk factors, including eight cohort studies, 15 case-control, one nested case-control and one cross-sectional (62). Family history of malignancy, tobacco smoking, alcohol consumption, and abnormal metabolic states such as diabetes and obesity were recurrently reported at NEN of various anatomical sites. Family history of cancer seems to be the most relevant risk factor for NEN occurring in any site, followed by BMI and diabetes. Tobacco smoking and alcohol consumption increased the risk in some site specific NEN including pancreas (both smoking and drinking), lung and small intestine (only drinking) (**Figure 6**).

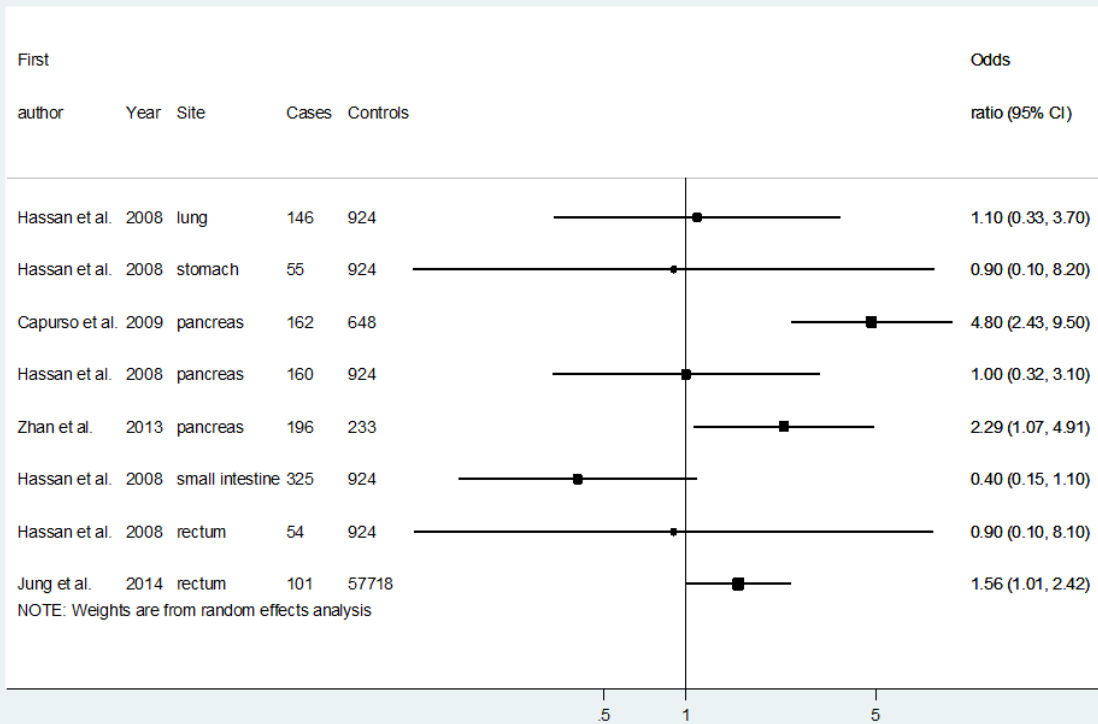
NEN are usually sporadic, however, there are hereditary conditions that may increase the risk of developing the disease, including multiple endocrine neoplasia type I (MEN1), MEN2, MEN4 (63), von Hippel-Lindau disease (64), neurofibromatosis type I (65) and tuberous sclerosis (66). MEN1 is autosomal dominantly inherited syndrome that occurs due to a germline mutation the Menin gene, a tumour suppressor which role include regulation of telomerase activity. Likewise, MEN2 is an autosomal dominantly inherited syndrome caused by germline mutations in the RET gene, which can be further subdivided in MEN2A and MEN2B. RET encodes for a tyrosine kinase receptor involved in cell differentiation, growth, migration and survival. MEN4 occurs due to mutations in the CDKN1B gene, which encodes for p27kip1 protein. p27 plays a key role as a tumour suppressor of the cell cycle. p27 loss of function lead to cell cycle dysregulation and tumorigenic processes (63).

Biomarkers Landscape

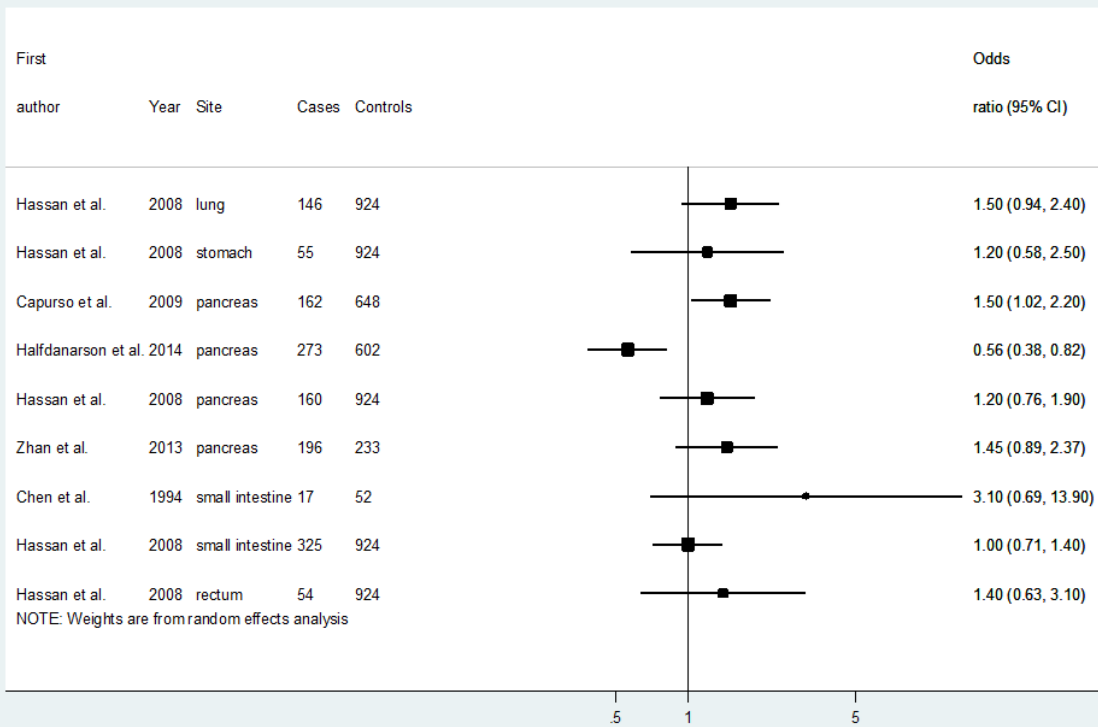
NEN are epithelial neoplasms with neuroendocrine differentiation capable of producing and secreting a variety of hormones and active peptides/amines that can influence the clinical course of the disease. Many of these bioactive compounds could serve as a prognostic/predictive biomarker. There are specific and non-specific biomarkers to NEN. Specific are produced and secreted by functioning NEN, whereas non-specific by potentially all NEN. Even though functioning or non-functioning NEN may be silent for many years before circulating biomarker is discovered, biomarkers for functioning NEN are helpful serum indicator of neoplasia activity (**Table 1**).

Figure 6
NEN Risk factors at a glance from a systematic review

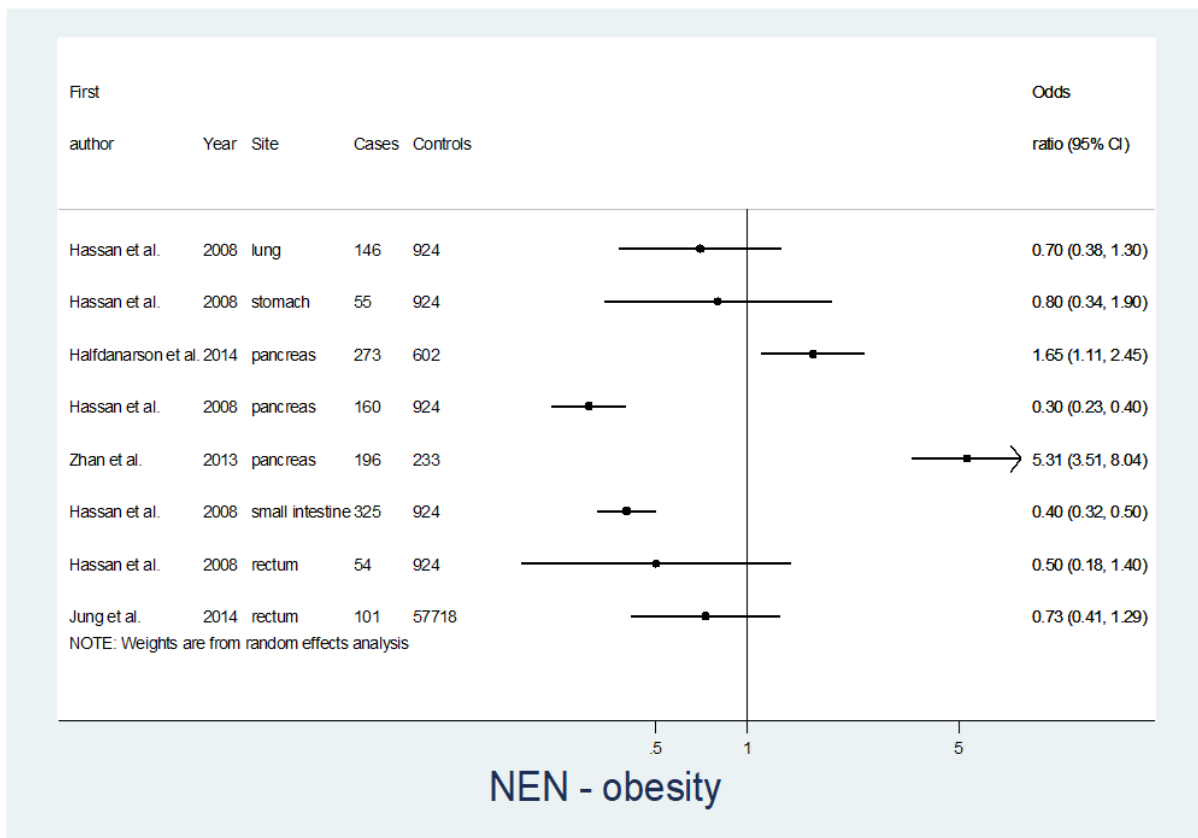
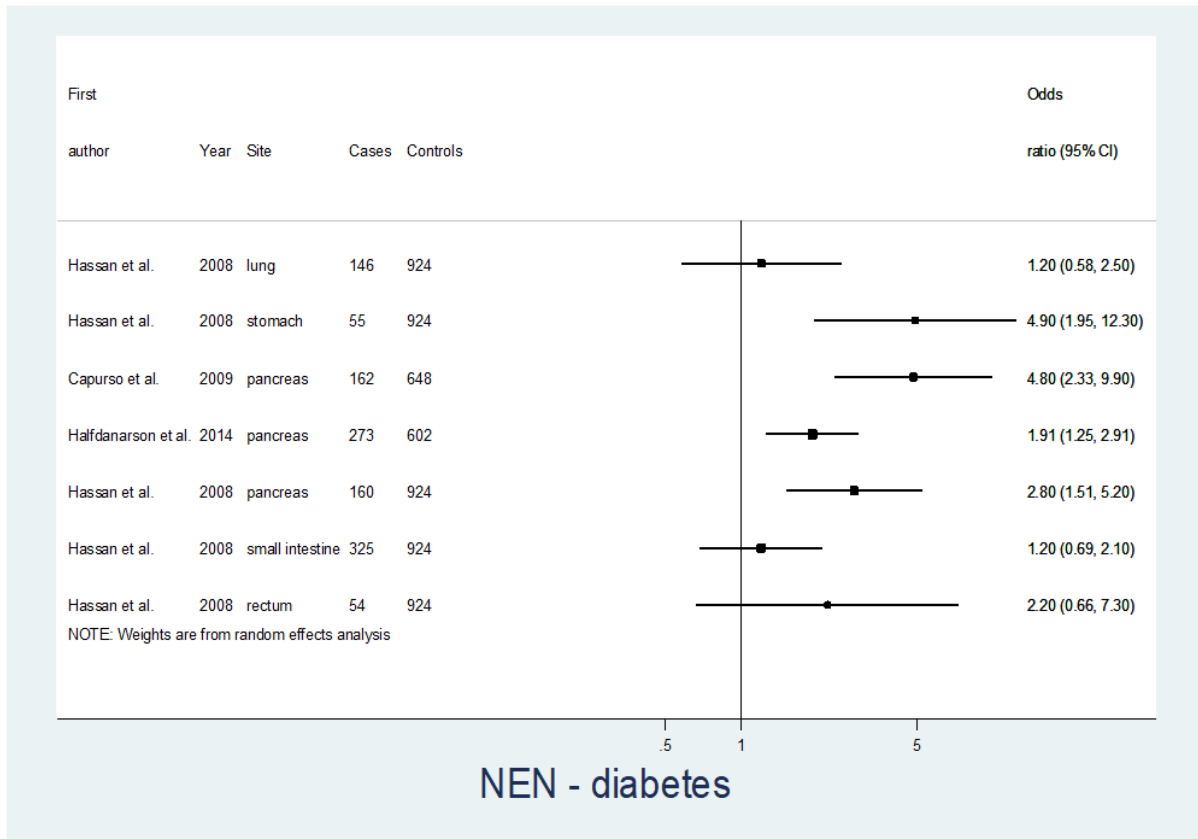




NEN - heavy drinking



NEN - ever alcohol



Note. Graphical description of various risk factors for NEN from “Risk factors for neuroendocrine neoplasms: a systematic review and meta-analysis” by Leoncini E. et. al, 2016, *Annals of Oncology*, Volume 27. Copyright © 2016, Elsevier.

However, functioning NETs with distinct clinical syndromes are a minority (67). Nonspecific biomarkers, on the other hand, lack of specificity due to expression by normal tissues or other pathological processes. To date, most of the biomarkers used in NENs are non-specific. For this reason, their assessment is recommended as an additional indicator rather than for screening purposes.

Non-specific biomarkers

Commonly expressed markers are insulinoma-associated protein 1 (INSM1), synaptophysin, and chromogranin, especially CgA (68).

INSM1

INSM1 is a zinc-finger transcription factor involved in the development of NE differentiation in several tissues (69, 70). It can potentially identify all NEN, with high sensitivity and specificity. However, it has been reported to in other non-NEN.

Synaptophysin

Synaptophysin is an integral membrane glycoprotein found in presynaptic vesicles of neurons and of the adrenal medulla. It is highly sensitive for NEN but likewise ISNM1 also expressed in some non-NEC (68).

Chromogranin A

Chromogranin A (CgA) belong to the granin family, which encode for precursors of several molecules. CgA is a 49-kDa glycoprotein secreted by neurons and NE cells, precursor of pancreastatin, catestatin, and vasostatins I and II. CgA is routinely assayed to help diagnosis and tumour follow-up, especially in carcinoid tumours (67). Unfortunately, CgA levels may be increased duo to several pathological processes nonrelated to NEN that often hamper its use as biomarker for NEN. Nonetheless, CgA measurement is still used in the clinical practice and have proven to be of great value in certain situations including metastatic disease to the liver, or when combined with other screening techniques, especially imaging based on somatostatin receptors (71).

Neuron-Specific Enolase

Neuron-Specific Enolase (NSE) may be found in neurons and NE cells, however, only 30-50% of NEN actually secrete NSE. As CgA, NSE levels are often increased in other non-NEN tumours such as thyroid cancer and prostate carcinoma and therefore should be used for diagnostic purposes. However, NSE levels can be a good prognostic tool since in the presence of diagnosed tumours, NSE overexpression is associated with poorly differentiated tumours and is often indicative of a small cell type (71).

Immune and vascular factors

Several studies have attempted to identify immunological and vascular factors as predictive and diagnostic circulating NEN biomarkers such as IL-8, IL-2, vascular endothelial growth factor, among others. As many other potential biomarkers, they have little discriminatory potential for NEN diagnosis. Two molecules have been reported as potentially useful, however, information about them is not enough to ascertain their effectiveness (67). First, paraneoplastic MA2 antibodies have been reported as small intestine NEN biomarker for both clinical diagnosis and risk of recurrence, having a sensitivity and specificity superior to CgA for the risk of recurrence. Second, increased serum levels of angiopoietin 2 have been reported in NETs (67), however there is no robust evidence to sustain its use in routine practice.

Specific biomarkers

Pancreatic Polypeptide

Pancreatic polypeptide (PP) is a hormone with unknown function is hardly recommended in the clinical practice. Several factors may increase its levels, including physical activity. However, because it is mostly secreted by pancreatic cells (F cells), high levels of PP in presence of diagnosed tumour could be an indicator of pancreatic NEN, and decreased PP after treatment is considered a useful prognostic biomarker (71).

Serotonin

5-HT is produced and secreted by EC cell, especially in the small intestine, to regulate GI motility. Because serotonin is fully metabolised by the liver, circulating high levels of this

monoamine are responsible for carcinoid syndrome symptoms and are predictive of liver metastasis. 5-Hydroxyindoleacetic acid (5-HIAA) is the main metabolite of 5-HT and can be measured both in the plasma and urine. Several studies report that in patients bearing midgut NET, 5-HIAA levels assessment should be considered not only for metastatic disease identification but also for predicting carcinoid heart disease and risk of a carcinoid crisis during anaesthesia (71).

Insulin

Insulin is an anabolic hormone secreted by beta cells of the pancreatic islets which function is to regulate the metabolism of the main types of macronutrients by promoting glucose absorption from the blood into the liver, fat and skeletal muscle cells. Insulin-secreting pancreatic NETs (pNETs) are also called insulinomas and are diagnosed based on the overproduction of insulin (hyperinsulinism) which should be diagnosed during confirmed hypoglycaemia through Whipple's triad assessment: signs of hypoglycaemia, simultaneously low glucose plasma levels and glucose homeostasis restored after correction of the hypoglycaemia. Several studies have reported 100% sensitivity in the detection of insulinomas after 72-hour of controlled fasting, with most patients fulfilling Whipple's triad in the first 48 hours (71).

Glucagon

Just like insulinoma, glucagonoma is the name given to glucagon-secreting NETs. Diagnosis should be assessed during fasting and values of more than 10-20 times above the upper cut-off is a clear indication of disease (71).

Bradykinin and the tachykinins

Bradykinin and tachykinins are peptides able to induce a few symptoms of carcinoid syndrome in midgut NET such as vasodilation, skin flushing and intestinal contraction. The use of this biomarker adds little value as a diagnostic tool alone. The assessment of multiple tachykinins values has showed a sensitivity of 70% in midgut NETs presenting carcinoid syndrome (67), however, recent reports are lacking.

Vasoactive intestinal peptide

Vasoactive intestinal peptide (VIP) is a neuropeptide able to stimulate the contraction of the enteric smooth muscle cells, the secretion of exocrine pancreas and inhibition of gastric acid secretion. High levels of VIP cause severe diarrhoea, resulting in acidosis and hypokalaemia which is often observed in pNET patients (67).

Gastrin

Gastrin is a peptide hormone responsible for gastric acid secretion. High levels of gastrin may cause the Zollinger–Ellison syndrome, a disorder that results in the excessive secretion of gastrin, possibly leading to peptic ulcers in the stomach and intestine. Gastrinomas often localise in the pancreas or duodenum and are characterised by hypersecretion of gastrin. For diagnosis purposes gastrin should be evaluable alone or in combination with secretin test during fasting state (67).

Somatostatin

Somatostatin (sst) is a neuropeptide produced mainly in the central nervous system and in the GI tract. Among its many functions, sst has an overall inhibition effect over the body. Somatostatinomas often originate in the duodenum or pancreas where it inhibits pancreatic and GI hormones production. Patient bearing sst-producing NETs can present multisecretory insufficiency. Sst levels assessment may be a good diagnostic tool when its use is restricted to NEN of the pancreas and duodenum with symptoms of steatorrhea, cholelithiasis and diabetes mellitus are present (67).

RNAs

More recently, as a result of the “omics” era, several new potentially predictive/prognostic biomarkers have been identified, including microRNA (miRNA) and long non-coding RNA (lncRNA). There is a growing body of studies reporting that the RNA landscape is altered in NEN. miRNA dysregulation is an accepted hallmark of cancer. As of today, it is known that there are groups of miRNAs that not only correlate with clinical pathophysiological features such as staging, progression, prognosis, among others, but also that are specific to a specific malignancy site. For instance, some authors have reported that upregulation of

miRNA-7 and miRNA-375 are generic markers for NE cell differentiation, whereas site-specific NEN such as pNET, lung NEN or small intestine NEN are characterised by different and more specific miRNA profiling, almost unique to their tumour site (72). Several miRNAs have been recognised as potentially biomarkers with high sensitivity and specificity for specific NEN. Notwithstanding its recent discovery, lncRNAs have been extensively studied in recent years (73). Among pathological lncRNAs' functions, modulation of the chromatin, gene expression regulation, and epithelial-to-mesenchymal transition may lead to tumour development, progression, cell survival and tumorigenesis (74). lncRNAs have been evaluated in different anatomical NEN sites and just like miRNAs, lncRNAs expression correlated with NE differentiation and tumour characteristics which could indicate a possible role for these molecules as biomarkers and/or therapeutic targets in NENs (75). The list of miRNAs and lncRNAs involved in tumour malignancy, as well as in the development and progression of NENs is already large and continues to grow.

Genomic biomarkers

Genomic landscape often differs according with the anatomical site of origin, differentiation, response to therapy, among others. NEN originating in the pancreas may present a different genomic profile respect to lung NEN. Next Generation Sequencing (NGS) has turned the tables in the field of biology as DNA sequencing has become an easy and affordable technique. In the last decades, several studies have reported oncogenic drive mutations in different malignancies, including NEN (76, 77, 78, 79, 80, 81). Knowledge of the genomic profile and mutational signatures of a given malignancy may help diagnosis and management of the disease, including the choice of therapy, metastasis detection and tumour recurrence. In the era of high throughput sequencing, several mutational profiles have been reported in recent years. Furthermore, dividing cells normally release cell-free DNA (cfDNA) fragments into the blood stream. Likewise, tumour cells release circulating tumour DNA (ctDNA) fragments into the circulation, which may be extracted and sequenced. CtDNA analysis is also called liquid biopsy. Several studies have attempted to find unique molecular signatures in specific malignancies by sequencing DNA derived from both solid and liquid fractions of a tumour. Once a mutational match is found, liquid biopsy may be used as a diagnostic/prognostic biomarker, giving important information regarding the location of the malignancy, its tumour burden and patient stratification. Giving that many NEN are difficult to identify, that metastasis is often present when patients are first diagnosed and that liquid biopsy is a much less invasive procedure, liquid biopsy strategies

applied to NEN could be key in their early identification, consequently providing a real-time monitoring tool that would aid the clinical management of this disease and reduce its burden. Just like for ctDNA, it is possible to identify circulating tumour transcripts (ctRNA) into the blood stream. Matched transcriptomes derived from solid and liquid biopsies could allow the identification of a unique transcriptional profile for a given malignancy. In fact, transcriptome-based assessment has already proven its efficacy in discriminating some types of NEN as well as identify the presence metastatic disease (82, 83).

NETest

NETest is a PCR-based 51-marker that analyse NET-specific gene transcripts from liquid biopsy showing high sensitivity (85–98%) and specificity (93–97%). The 51 transcripts were identified (**Table 8**) through computational analysis of 3 microarray datasets including 15 tissue NEN samples, 7 NEN liquid biopsies and 363 adenocarcinomas. The candidate gene signature was then tested in 130 blood samples and validated in two independent cohorts of 115 and 72 NENs (84). However, a case-control study performed in 140 GEP-NETs and 113 healthy volunteers, has reported much lower specificity of 56%, which is still greater than testing for CgA alone, but could preclude the use of this test for screening purposes (85). NETest is the most validated NET-specific biomarkers test applied to liquid biopsy. It shows important diagnostic features and are a promising tool for NEN management. The test has proven greater efficacy when compared to assessment of CgA levels in the identification of GEP-NENs, lung-NENs, paragangliomas and pheochromocytomas (86), not only in NEN diagnosis, but also in the identification of residual disease after surgery, in monitoring therapeutical efficacy and progression (86, 87).

Table 8 List of NETest 51 marker genes

ID	Gene name
AKAP8L	A kinase (PRKA) anchor protein 8-like
APLP2	amyloid beta (A4) precursor-like protein 2
ARAF	v-raf murine sarcoma 3611 viral oncogene homolog
ARHGEF40	Rho guanine nucleotide exchange factor (GEF) 40
ATP6V1H	ATPase, H ⁺ transporting, lysosomal 50/57 kDa, V1 subunit H
BNIP3L	BCL2/adenovirus E1B 19kDa interacting protein 3-like
BRAF	v-raf murine sarcoma viral oncogene homolog B1
C21orf7	chromosome 21 open reading frame 7
CD59	CD59 molecule, complement regulatory protein
COMMD9	COMM domain containing 9
CTGF	connective tissue growth factor

ENPP4	ectonucleotide pyrophosphatase/phosphodiesterase 4 (putative function)
FAM131A	family with sequence similarity 131, member A
FZD7	frizzled homolog 7 (Drosophila)
GLT8D1	glycosyltransferase 8 domain containing 1
HDAC9	histone deacetylase 9
HSF2	heat shock transcription factor 2
KRAS	v-Ki-ras2 Kirsten rat sarcoma viral oncogene homolog
LEO1	replicative senescence down-regulated leo1-like protein
MKI67	antigen identified by monoclonal antibody Ki-67
MORF4L2	mortalin factor 4 like 2
NAP1L1	nucleosome assembly protein 1-like 1
NOL3	nucleolar protein 3 (apoptosis repressor with CARD domain)
NUDT3	nudix (nucleoside diphosphatase linked moiety X)-type motif 3
OAZ2	ornithine decarboxylase antizyme 2
PANK2	pantothenate kinase 2
PHF21A	PHD finger protein 21A
PKD1	polycystic kidney disease 1 (autosomal dominant)
PLD3	phospholipase D family, member 3
PNMA2	paraneoplastic antigen MA2
PQBP1	polyglutamine binding protein 1
RAF1	v-raf-1 murine leukemia viral oncogene homolog 1
RNF41	ring finger protein 41
RSF1	remodelling and spacing factor 1
RTN2	reticulon 2
SLC18A1	solute carrier family 18 (vesicular monoamine), member 1
SLC18A2	solute carrier family 18 (vesicular monoamine), member 2
SMARCD3	SWI/SNF related, matrix associated, actin dependent regulator of chromatin, subfamily d, member 3
SPATA7	spermatogenesis associated 7
SSTR1	somatostatin receptor 1
SSTR3	somatostatin receptor 3
SSTR4	somatostatin receptor 4
SSTR5	somatostatin receptor 5
TECPR2	tectonin beta-propeller repeat containing 2
TPH1	tryptophan hydroxylase 1
TRMT112	tRNA methyltransferase 11-2 homolog (S. cerevisiae); similar to CG12975
VPS13C	vacuolar protein sorting 13 homolog C (S. cerevisiae)
WDFY3	WD repeat and FYVE domain containing 3
ZFHX3	zinc finger homeobox 3; hypothetical LOC100132068
ZXDC	ZXD family zinc finger C
ZZZ3	zinc finger, ZZ-type containing 3

Immune Response Biomarkers

Immunotherapy has dramatically changed the course of several cancer subtypes, including melanoma, lung cancer, and kidney cancer. Because there is little information regarding

effective immune markers for NEN, the benefits of this treatment are still meagre. To date, the most studied biomarkers for immunotherapy response are based on the programmed cell death protein 1/ligand 1 (PD-1/PD-L1) or on markers of microsatellite instability and mismatch repair deficiency. Several clinical trials have been and are being conducted. Two immunotherapeutic agents have been approved by the Food and Drug Administration (FDA) for the treatment of Merkel cell melanoma (88) and SCLC (89), for instance, however in general, response rates of immunotherapy in NEN are not that promising. Therefore, finding effective biomarkers and targets for immunotherapy remain a challenging task.

Neuroendocrine Neoplasms of the Lung

Bronchopulmonary NEN (BP-NEN) arise from pulmonary NE cells (PNEC) sparsely distributed among epithelial cells in 1:2500 ratio (90). First described in 1954, these are the first cells to differentiate in the pulmonary epithelium during development until they reach a peak in neonatal period, remaining throughout life as a viable cell population (91). PNECs may exist both as solitary cells and as neuroepithelial bodies, which are innervated cluster of PNECs. The former is distributed in the bronchopulmonary tree, whereas neuroepithelial bodies occur exclusively within intrapulmonary airways (92). The precise physiological function of PNECs is not entirely known. However, an overexpression of PNECs and their secretion products are associated with several lung diseases (93). It has been hypothesised that PNECs respond to environmental stimuli given by aerosolised particles, functioning as dual neurosensory and endocrine cells (94). Bioproducts secreted by PNECs include serotonin, calcitonin gene-related peptide (CGRP), and bombesin (GRP).

BP-NEN represent ~30% of all NENs and ~20% of all lung cancers (95), comprising a heterogeneous population of tumours arising from PNECs (17). Bronchial carcinoid (BC) account for ~2% of lung primary tumours (with typical to atypical ratio of 10:1), LCNEC ~3%, and SCLC account for ~15%. NECs (LCNEC and SCLC) tend to grow fast and are more frequently found in smoking individuals (96); BCs are slow growing NETs mostly occurring in never-smoking persons (97). Whereas decreased cigarette smoking is probably responsible for the decreased incidence of SCLC in the last few years, BC incidence has increased probably as a result of several factors including improved radiographic technology, histological diagnostic tools, as well as to the remarkable efforts in lung cancer screening programs worldwide.

NECs and BCs malignancy differences could be explained based on the extent of molecular alterations found in those lesions (98). In fact, NECs are often affected by chromosomal alterations including deletions of chromosome 3p, whereas MEN1 mutations are typically found in BCs. A recent published study by whole-exome sequencing has brought light into the genetic landscape of BP-NEN and several altered genes have been identified in which TERT, RB1, MEN1 correlated with poorer prognosis and KMT2D with longer survival. Whilst alterations in PI3K/AKT/mTOR pathway were more frequent in NECs than BCs, which could represent a potential therapeutic target in malignant BP-NEN (99, 100).

Bronchial Carcinoids

Typical and atypical bronchial carcinoids (TC and AC) are well-differentiated NEN of low and intermediate malignant potential, respectively, accounting for 0.5-2.5% of primary lung neoplasms (101). Notwithstanding their low- or intermediate malignancy grade, BC are capable of regional lymph node or distant metastasis, which affects prognosis. In fact, TCs and ACs metastasise in 5-20% and 30-40%, respectively (97). As a result, delayed diagnosis increases metastatic disease probability with many patients presenting recurrent disease or metastases to the liver or bone (**Figure 1**) (54, 102). Even though there are important clinical and histological differences between ACs and TCs, little is known about the factors affecting their prognosis. To date, studies focused on differential genetic and molecular patterns of BCs are scarce. As a result, accurate predictive markers are still lacking (103) and prognostic markers able to give accurate information regarding the current landscape of the tumour such as residual disease, treatment response or recurrence are under intensive investigation (104, 105).

Diagnosis & Management

Depending on the location of primary tumour, tumour stage and clinical presentation, the diagnosis of BCs may require several diagnostic procedures (clinical, biochemical, radiological, nuclear medicine or endoscopic procedures). Early-stage disease is often treated with surgical resection, which, unfortunately, is not always feasible in the presence of metastatic disease (106). As mentioned above, genetic and molecular profiling of BP-NEN studies are scarce and biomarkers that may constitute therapeutic targets and have a predictive/prognostic value in the management of this disease are missing. The WHO

recommends for the assessment of the immunohistochemical markers CgA, synaptophysin and CD56 biomarkers to confirm lung NET (107).

Clinical Presentation

There is no difference in gender distribution, ACs and TCs occur equally in male and female, nor age (108). In general, BCs tend to be asymptomatic, and diagnosis often occur accidentally during imaging procedures. Symptomatic BC entangle directly the broncho-pulmonary tree consisting in non-specific tumour-related respiratory symptoms such as cough, bronchitis, obstructive pneumonia, atelectasis and wheezing (109). however even in the presence of symptoms diagnosis is often delayed and/or incidental. Approximately 80% of BC are located in the central airways, whereas ~20% are peripheral and consist of mainly ACs (110, 111). Unlike GEP-NETs, carcinoid syndrome is very unusual in lung NET. A recent study reported that 7.6% of patients bearing BC have carcinoid syndrome at diagnosis (112). Also, functioning BCs are rare but do exist in aggressive carcinoid variants, which have been associated with Cushing's syndrome and acromegaly (113, 114).

Imaging procedures

As mentioned previously, BC diagnosis often occur accidentally during imaging procedures, all of which also play a key role in identifying tumour extent and staging (115). Approximately 75% of BC pulmonary nodules are detected with X-ray, whilst smaller lesions may be identified with computed tomography (CT). TCs usually present smooth edges, are central-located lesions with infrequent nodal involvement, however none of these radiological features are specific enough to differentiate TCs from ACs (116). Magnetic resonance imaging (MRI) may help detect bone or liver metastases (117). Several imaging techniques have been developed based on the overexpression of somatostatin receptors (SSTR) in NETs, including somatostatin receptor scintigraphy (SRS) and positron emission tomography (PET) that use radiolabelled sst analogues (SSA) to identify SSTR-expressing tumours (e.g., ^{68}Ga -DOTATATE, ^{68}G -DOTA-Octreotide) (118). SSTR-based imaging techniques *per se* are very dynamic and constantly improving as scientists continue to research newer SSA with higher affinity for SSTR and ways to reduce radiation dose. SSTR-based imaging also provides an estimation of receptor density, providing important information for treatment selection. Further, integration of different imaging procedures

such as PET/CT scan have been introduced and reported to increase diagnostic capacity (119).

Given BC preferred central location, bronchoscopy technique is recommended to obtain preoperative biopsies. In the presence of accessible peripheral carcinoid transthoracic biopsy could be preferred. Endobronchial endoscopic ultrasonography (bronchoscopy + ultrasonography) is usually recommended when there is suspicion of lymph node mediastinal involvement and to exclude lymph node metastasis before surgery. In special cases when biopsy is not possible, surgery may be indicated upfront in cases of localised and resectable BC (120). The ENETS released a detailed guidelines for the diagnosis and management of TCs and ACs, in which they recommend the use of imaging techniques, histopathologic evaluation, assessment of genetic alteration and biochemical secretions (**Figure 7**) (121).

Treatment approaches

Surgery is the gold standard treatment for localised disease with the goal of total resection of the primary tumour whilst conserving as much as functional lung tissue as possible. Tumour debulking with a tumour-free resection margin is associated with good prognosis. The 5-year survival rates for resected TCs and ACs have been reported as 90% and 70%, respectively (121). The ENETS guidelines recommend lobectomy/segmentectomy and sampling of a minimum of 6 lymph nodes with lung parenchyma conservative surgery (122). **Adjuvant therapy** should be considered for ACs with positive lymph nodes and high proliferative index, whereas adjuvant therapy is not indicated for TCs given their excellent prognosis. For those indolent lesions, the ENETS consider **watchful waiting** approach, however, SSA have been reported to stabilise tumour progression in 30–70% of patients with well-differentiated NETs. SSA are also indicated for functional NETs, symptomatic BC and in SSTR positive status on the PET scan (122). Different trials have assessed SSA effect in NEN (PROMID, CLARINET, RADIANT 2 and 4). More recently, the randomised SPINET trial assessed SSA effect in patients with BC. Results were promising, especially for TC. Reported progression-free survival (PFS) was 21.9 months with SSA lanreotide against 13.9 months of the placebo arm, whereas AC bearing patients had an inferior increase in the progression-free survival (PFS) of 13.8 vs. 11 months of the placebo group. Treatment for metastatic or unresectable BC aims preventing disease progression by controlling

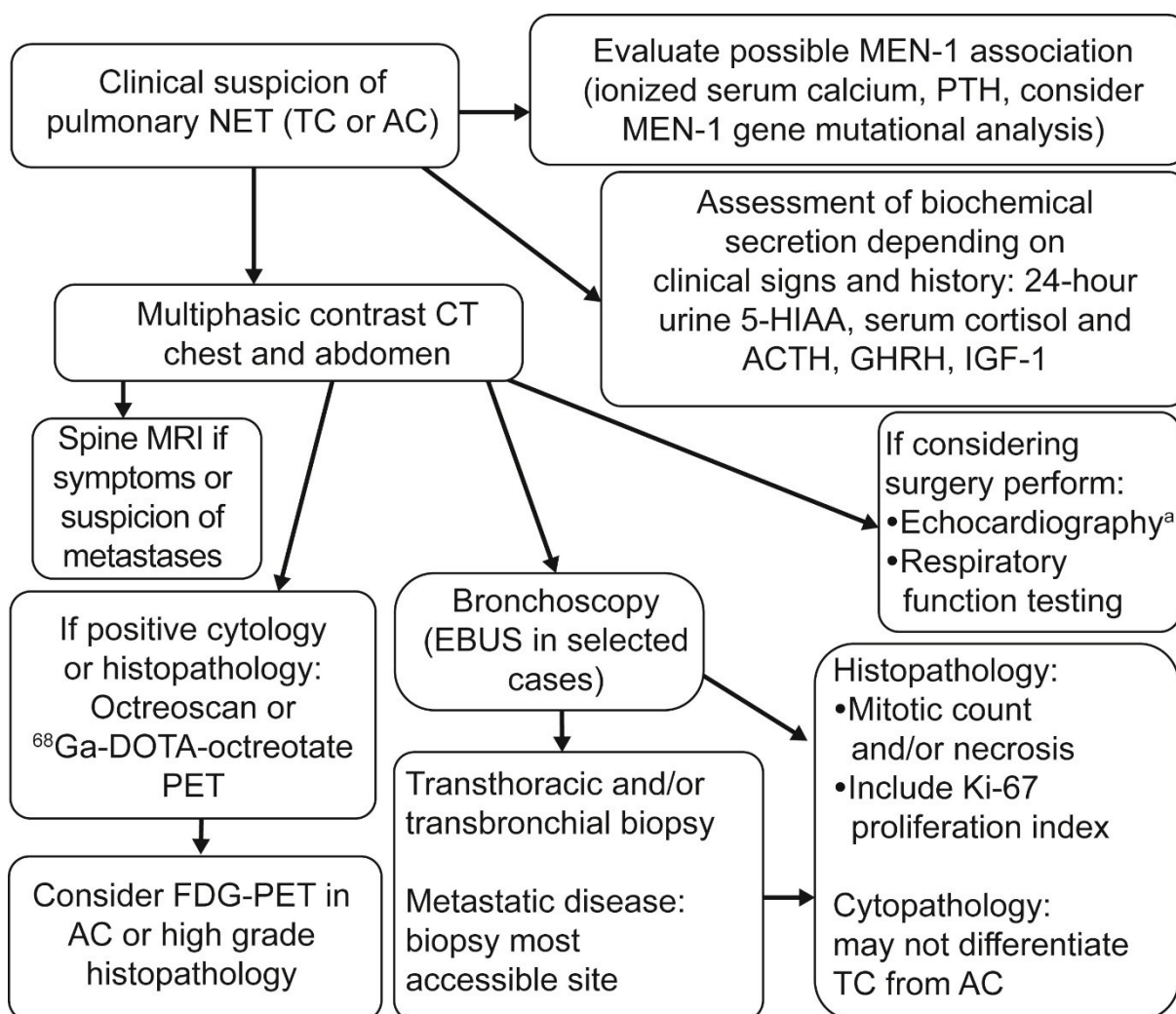
hormonal activity, extending the OS and maintaining the quality of life. Advanced disease usually has to be evaluated from a multidisciplinary angle in reference centres; given BC low incidence not all centres have the expertise to deal with challenging BC.

It is known that PI3K/AKT/mTOR pathway is often found impaired in NENs and will be discussed further on. In recent years, new therapeutic options for metastatic NENs have arisen (123, 124, 125). *In vitro* and *in vivo* studies have demonstrated that **target therapies** directed against growth factor receptors and mammalian target of rapamycin (mTOR) could be useful in reducing cell viability and improving PFS (126, 127, 128). Studies have indicated everolimus (eve), the mTOR inhibitor, as a potential anti-tumour agent in aggressive BC and, in fact, RADIANT-4 clinical trial demonstrated its efficacy in the treatment of these rare tumours. Eve was approved by the U.S. Food and Drug Administration (FDA) on 2016 for the treatment of adult patients with progressive, well-differentiated non-functional GEP-NETs or lung NETs with unresectable, locally advanced, or metastatic disease (129). However, a number of patients do not benefit from eve treatment likely due to the development of primary or acquired resistance to this drug (130, 131, 132).

Peptide Receptor Radionuclide Therapy (PRRT) such as ^{177}Lu -DOTATATE is indicated for patients with advanced, progressive, and SSTR-positive tumours. PRRT delivers radiation to cells by using SSA conjugated with a therapeutic radionuclide (e.g., Lutetium177, Yttrium-90) (133). There are limited prospective studies on PRRT's efficacy in BCs. However, ^{177}Lu -Dotatate has showed significant efficacy in several retrospective studies and one prospective, the NETTER-1 trial which included locally advanced or stage IV midgut NETs. However, ^{177}Lu -Dotatate did not improve significantly median OS vs. high-dose long-acting SSA octreotide (134).

Chemotherapy is usually not recommended in advanced BC due to its limited efficacy in these lesions, however several cytotoxic chemotherapeutic agents have been employed in the past (e.g., doxorubicin, carboplatin, cisplatin, temozolomide, among others). High malignancy BC in which no adjuvant treatment has been effective, platinum-based or a combination of chemotherapeutic agents could be indicated (100, 133).

Figure 7
ENETS guidelines for TCs and ACs.



Note. Diagnostic evaluation/work-up recommendations according to the European Neuroendocrine Tumor Society guidelines for typical carcinoids (TCs) and atypical carcinoids (ACs). From " Neuroendocrine Tumors of the Lung: Current Challenges and Advances in the Diagnosis and Management of Well-Differentiated Disease" by Hendifar A. E. et. al, 2017, Journal of Thoracic Oncology, Volume 12, issue 3. Available under the Creative Commons CC-BY-NC-ND, Elsevier. NET, neuroendocrine tumor; MEN-1, multiple endocrine neoplasia type 1; PTH, parathyroid hormone; CT, computed tomography; 5-HIAA, 5-hydroxyindoleacetic acid; ACTH, adrenocorticotropic hormone; GHRH, growth hormone-releasing hormone; IGF-1, insulin growth factor 1; MRI, magnetic resonance imaging; EBUS, endobronchial ultrasonography; PET, positron emission tomography; FDG-PET, fludeoxyglucose F 18 positron emission tomography.

Immunotherapy may possibly represent the future of solid cancer treatment, however there is still little information. Two trials are currently assessing the role of PD-1 inhibitors monotherapy, spartalizumab and pembrolizumab in lung NETs patients. More studies are necessary to evaluate the real efficacy of immunotherapy in BCs as monotherapy or in combination with other treatment approaches.

Signalling Pathways

Cell-cycle

The cell cycle is a series of events that cells go through as they grow and divide. It is regulated by a series of proteins, including cyclins and cyclin-dependent kinases (CDKs). There are four types of cyclins (A, B, D, and E) that bind to specific CDKs to form cyclin/CDK complexes. These complexes promote cell cycle progression, with cyclin D expression increasing in the G1 phase and decreasing in the M phase, while cyclin E, A, and B expression peak in the G1/S, G2, and G2/M phases, respectively. In addition to their roles in the cell cycle, these proteins have also been implicated in cancer. Overexpression of cyclin D1 has been observed in several types of cancer, including breast, ovarian, and lung cancer. In fact, high levels of cyclin D1 have been associated with a worse prognosis in some types of cancer (135, 136). Targeting these proteins has shown promising results. For example, the mTOR inhibitor everolimus has been shown to reduce cyclin D1 expression in certain types of cancer cells and has been approved for the treatment of neuroendocrine tumours, including BC (137, 138).

PI3K/Akt/mTOR

The phosphoinositide 3-kinase (PI3K)-Akt/mTOR pathway (**Figure 8**) is key in regulating several cellular processes such as survival, proliferation, metabolism, angiogenesis, and cell motility. In fact, it is found commonly activated in several human cancers (139). Under physiological conditions, it regulates important metabolic processes in response to growth factors, cytokines and insulin. Once the PI3K/Akt/mTOR pathway is impaired, cancer cells reprogram the regulation of the metabolism so as to support the new demands of the aberrant cancerous cells. For this reason, it has been extensively studied as potential biomarker and target for treatment in several human cancers, including NEN. As a result, mTOR inhibitors such as everolimus have proven efficacy in the treatment of several tumours, including NEN (RADIANT-3 and RADIANT-4 clinical trials) (140, 141).

mTOR is a serine–threonine protein kinase that forms part of two complexes as a catalytic subunit (142). Activation of mTOR occurs via phosphorylation from upstream signalling. Phosphatidylinositol 3-kinase (PI3K) may be activated by tyrosine kinases receptor, G-coupled receptors, or Ras proteins. PI3K is the key upstream regulator of mTOR, acting

through phosphorylation of Akt by converting phosphatidylinositol-4,5-diphosphate (PIP2) to phosphatidylinositol-3,4,5-triphosphate (PIP3). Akt regulates mTORC1, among other downstream proteins, promoting protein synthesis, lipid, nucleotide, and glucose metabolism and protein turnover (142, 143). Once activated, mTORC1 triggers different effectors, including 4EBP1 (eIF4E Binding Protein) and S6K1 (p70S6 Kinase 1), which enhance cell proliferation, survival, and angiogenesis by regulation of Cyclin D1, Bcl-2, Bcl-xL, hypoxia-inducible factor-1 (HIF-1) and VEGF. Negative regulation of mTOR occurs through the tumour suppressor proteins phosphatase and tensin homolog (PTEN) and tuberous sclerosis complex 1 (TSC1) and 2 (TSC2). When Akt is activated, it phosphorylates TSC2, inhibiting it and thereby promoting mTOR activation (144), setting in motion a series of events that stimulate tumorigenesis including increased protein synthesis, cell growth, proliferation, and angiogenesis. Whilst mTORC2 function is not completely established, it is believed to regulate survival and metabolism through signalling originated from different factors, acting as an upstream Akt regulator, increasing its activity (145).

Rapamycin (and other rapalogs) is an allosteric inhibitor of mTOR. It forms a complex with the FK-binding protein 12 (FKBP12) which then binds directly to mTORC1, affecting cell cycle progression, survival, angiogenesis, and metabolism (146). Several rapalogs have been developed in last decades, including everolimus.

As previously mentioned, the PI3K/Akt/mTOR pathway is found impaired in several human cancer, including NENs. There are different players involved in the regulation of PI3K/mTOR signalling that can lead to uncontrolled cell growth, survival, etc. Mutations in one of these players may constitutively activate PI3K/mTOR signalling. Different mutations have been described in NEN patients including somatic mutations in the PI3K gene, loss of function of the tumour suppressors PTEN and TSC2, as well as overexpression of upstream tyrosine kinase receptors.

TGF- β

The transforming growth factor beta (TGF- β) pathway plays a crucial role in various physiological processes, including cell proliferation, differentiation, and apoptosis. Dysregulation of the TGF- β pathway has been linked to various diseases, including cancer (147), fibrosis (148), and autoimmune disorders (149). TGF- β is a multifunctional cytokine

that is produced by many cell types and is involved in a wide range of biological processes (150). It is activated by the binding of TGF- β to a complex of receptors on the surface of target cells, which leads to the activation of downstream signalling pathways (**Figure 8**). One of the key functions of the TGF- β pathway is its role in cell proliferation. In normal physiological conditions, TGF- β acts as a suppressor of cell proliferation (151), but in certain pathological conditions it can activate and promote cell growth and survival (152). In fact, TGF- β has been shown to play a role in the development and progression of various types of cancer, including breast, lung, and colorectal cancer, whereas its inhibition has been shown to reduce the growth and progression of cancer (153).

TGF- β may elicit the activation of different pathways that have been described as canonical and non-canonical pathways, which then modulate gene expression and cellular behaviour (147, 150) (**Figure 8**). The canonical pathway, also known as the Smad pathway, is activated by the binding of TGF- β to the type I (TGF β RI) and type II (TGF β RII) receptors on the cell surface. This leads to the phosphorylation and activation of the Smad proteins, which then translocate to the nucleus and modulate gene expression. The canonical pathway has been reported to be involved in many pathophysiological processes, including cell proliferation, differentiation, and apoptosis (150, 154). The non-canonical pathway, on the other hand, leads to the activation of various signalling pathways, including the MAPK pathway, the PI3K-Akt pathway, and the Rho-associated protein kinase (ROCK) pathway. The non-canonical pathway has been reported to be involved in processes such as cell migration, extracellular matrix remodelling and epithelial-mesenchymal transition (EMT) (154, 155).

EMT is a process by which epithelial cells, which are typically polarized and attached to a basement membrane, undergo a series of changes to become mesenchymal cells, which have a fibroblastic and migratory phenotype (156). EMT is important in various pathophysiological processes, including embryonic development, tissue repair, and cancer metastasis. In cancer, EMT can allow tumour cells to become more invasive and migrate to other tissues, leading to the formation of distant metastases (156). TGF- β has been shown to promote EMT by downregulating the expression of epithelial markers, such as E-cadherin, and upregulating the expression of mesenchymal markers, such as vimentin and N-cadherin. TGF- β can promote EMT through the activation of the non-canonical pathway, which leads to the activation of various signalling pathways, including the PI3K/Akt/mTOR pathway (157). TGF- β inhibition has been shown to hinder the metastatic potential of cancer cells.

Hence, understanding the role of TGF- β in EMT and its role in disease is therefore of great importance in the fields of biology and medicine. Given the diverse functions elicited by TGF- β , targeting its pathways has been a promising therapeutic strategy (158, 159, 160, 161). There are currently several drugs, including monoclonal antibodies and small molecule inhibitors that have shown promising results in preclinical and clinical studies, but further research is needed to fully understand their mechanisms of action and potential side effects.

PI3K/mTOR & TGF- β Crosstalk

There is evidence of crosstalk between the PI3K/Akt/mTOR pathway and TGF- β pathway in cancer, with both pathways influencing each other's activity (157, 162, 163, 164). In cancer cells, the PI3K/Akt/mTOR pathway and TGF- β cooperate to control EMT, cell migration, metastasis, and cell differentiation (157, 165). The PI3K/Akt/mTOR pathway plays an important role in the modulation of TGF- β -induced activation of various EMT responses, and inhibition of PI3K/Akt/mTOR by pharmacological inhibitors has been reported to abolish TGF- β -induced EMT and cell migration (165). Also, TGF- β has been reported to induce the phosphorylation of Akt in a Smad-independent manner, resulting in the activation of PI3K/Akt/mTOR signalling (157). TGF β RI may play an important role in the crosstalk between the two pathways since its inhibition has been reported to prevent Akt phosphorylation by TGF- β (162). Moreover, effectors of Akt, including P70S6K, the 4E-BP1, and mTOR, were found to be activated in a Smad-independent manner by TGF- β (157).

Understanding the crosstalk between the PI3K/mTOR pathway and TGF- β pathway in cancer and how it is regulated has the potential to lead to the development of new therapeutic strategies for the treatment of cancer, including NEN. Further research into these pathways may also provide insights into the mechanisms of cancer progression and may lead to the identification of new biomarkers for the diagnosis and prognosis of cancer.

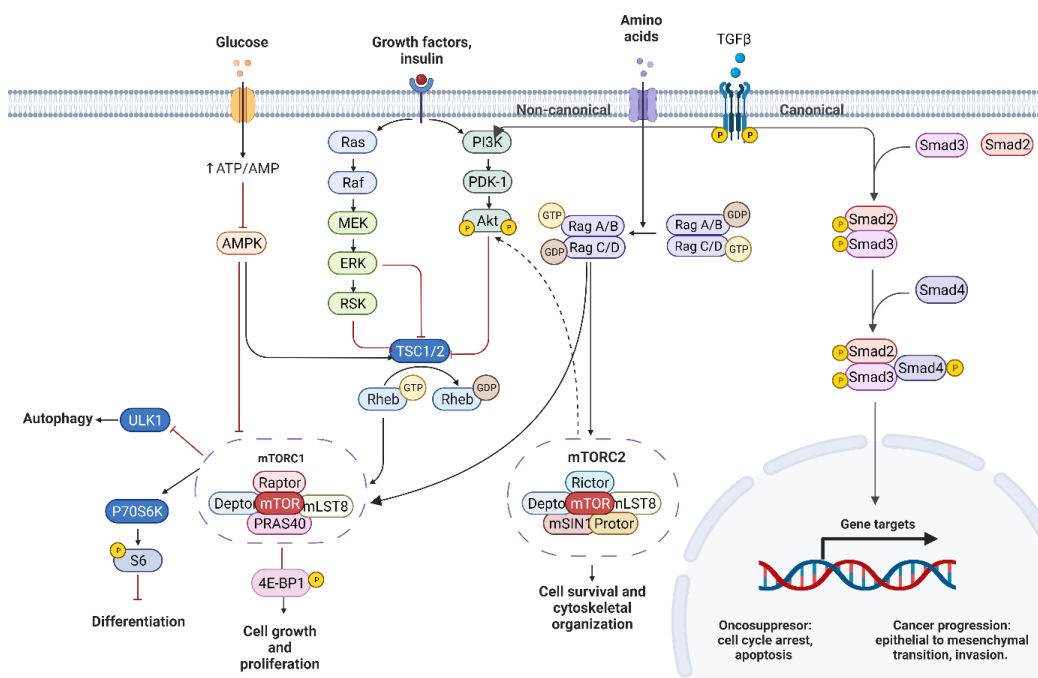
AIMS

Previous studies and clinical trials have reported that the mTOR inhibitor everolimus may reduce malignancy features and improve the PFS in patients with progressive lung or GI neuroendocrine tumours (126, 140, 166). However, TBC have shown reduced sensibility to mTOR inhibitors respect to ABC (126), notwithstanding its less aggressive behaviour. It is

not uncommon for cancer cells that are more aggressive or have a higher degree of malignancy to be more resistant to treatment than less aggressive cancer cells. This can be due to a variety of factors, such as the presence of genetic mutations that allow the cancer cells to evade the effects of treatment or the ability of the cancer cells to repair DNA damage caused by treatment. In the case of BC, it is not fully understood why TBC (which are generally less aggressive and have a better prognosis) may be more resistant to treatment than ABC (which tend to be more aggressive and have a worse prognosis). Further research is needed to understand the underlying mechanisms that contribute to the differential sensitivity of these two types of lung NET to treatment.

It is possible that the crosstalk between the TGF- β and the PI3K/Akt/mTOR pathway may contribute to the differential sensitivity of BC to treatment. TGF- β has been shown to activate the mTOR pathway and induce EMT in other types of cancer, and it is possible that a similar process may occur in BC. Understanding the mechanisms underlying this crosstalk may help to identify new therapeutic targets for the treatment of particularly malignant BC that are resistant to treatment. This information could potentially be used to develop new treatment strategies or to identify which patients are likely to benefit from treatment with mTOR inhibitors or other combined therapies.

Figure 8
Simplified depiction of the PI3K/Akt/mTOR and TGF- β pathways crosstalk.



Note. Created with BioRender.com.

MATERIALS & METHODS

Drugs & Reagents

Dinaciclib and TGF- β were purchased from Selleckchem (TX, USA) and Preprotech (Rocky Hill, NJ, USA), respectively. IGF-1 (insulin-like growth factor 1), Paclitaxel, Chloroquine, TGF- β 's inhibitors GW788388 and LY2109761 were purchased from Sigma Aldrich (Milan, Italy). Everolimus was provided by Novartis Pharma (Basel, Switzerland). RIPA buffer and Protease and Phosphatase Inhibitor Cocktail were from Thermo Fisher Scientific (Milan, Italy). The list of antibodies used are shown in **Table 9** List of primary antibodies. Cell media was from (Euroclone, Milano, IT). All other reagents, if not otherwise specified were purchased from Sigma (Milan, Italy).

Cell culture

Cell lines were purchased from the American Type Culture Collection (Manassas, VA, USA). The TBC-derived NCI-H727 was cultured and maintained in RPMI 1640 medium supplemented with 10% of foetal bovine serum (FBS), whereas the ABC-derived NCI-H720 cell line was cultured and maintained in DMEM-F12 supplemented with 0.005 mg/ml insulin, 0.01 mg/ml transferrin, 30nM sodium selenite, 10 nM hydrocortisone, 10 nM beta-oestradiol, final concentration of 4.5mM L-glutamine (for final conc. of 4.5 mM) and 5% FBS. Both cell lines were routinely tested for mycoplasma contamination by PCR. Cell doubling time was applied to estimate cell population growth.

Cell viability

Cell viability was assessed with the CellTiter Glo® Luminescent Cell Viability Assay from Promega and luminescence was measured with the EnVision™ 2104 Multilabel Reader (Perkin-Elmer). The CellTiter-Glo® Luminescent Cell Viability Assay is a homogeneous method to determine the number of viable cells in culture based on quantitation of the ATP present, which signals the presence of metabolically active cells and is directly proportional to the cells number present in the culture. The Assay relies on the properties of a proprietary thermostable luciferase (Ultra-Glo™ Recombinant Luciferase), which generates a stable “glow-type” luminescent signal after a specific reaction, as shown in Figure 18, with a consequent light emission. This assay is a homogeneous method to determine the number of

viable cells in culture and is based on ATP quantitation present in the well. ATP is considered as a signal of metabolically active cells and can therefore represent a good indicator for viability assessment. The assay relies on the properties of a proprietary thermostable luciferase that, in presence of its substrates, generates a stable “glow-type” luminescent signal. Light emission can be measured with a luminometer, and, in this setting, it is directly proportional to the amount of ATP inside the well and, therefore, to viable cells. The detailed process is indicated in figure 8. This assay was used to analyse variation in cell viability in both the second and the third part of the study.

Briefly, NCI-H727 and NCI-H720 were seeded at 3 and 5×10^4 cells/well, respectively, in 96-well black plates in complete medium. Cells were synchronized by overnight incubation in 0% FBS medium. The day after, cells were treated with TGF-B, eve, GW788388, LY2109761, IGF-1 and paclitaxel, alone or combined. After 24- or 48-hours cell viability assay was assessed adding substrate solution directly to cell culture plates. Results are expressed as mean value \pm standard error of the mean (S.E.M) percent RLU vs. untreated control cells in three replicates.

Caspase activation

Caspase 3/7 activity was performed by using Caspase-Glo 3/7 assay (Promega, Milano, IT) according to the manufacturer’s instructions. Luminescence was measured with the EnVision™ 2104 Multilabel Reader Multilabel Counter (Perkin-Elmer) and expressed as relative light units (RLU). The Caspase-Glo® 3/7 Assay is a homogeneous, luminescent assay that measures caspase-3 and -7 activities. These members of the cysteine aspartic acid-specific protease (caspase) family play key effector roles in apoptosis in mammalian cells. The Caspase-Glo® 3/7 Assay relies on the properties of a proprietary thermostable luciferase (Ultra-Glo™ Recombinant Luciferase), which is formulated to generate a stable “glow-type” luminescent signal, after cell lysis and caspase cleavage of the substrate, Figure 19; luminescence is proportional to the amount of caspase activity present. Caspase activation was evaluated by using the Caspase-Glo 3/7 assay (Promega, Milano, Italy) according to the manufacturer’s instructions, as previously described (167). Luminescent signal was measured with the EnVision™ 2104 Multilabel Reader and expressed as RLU. Results are expressed as mean value \pm S.E.M percent RLU vs. untreated control cells in six replicates.

Briefly, cells were seeded and treated as previously described for the CellTiter-Glo® Luminescent Cell Viability Assay. Results are expressed as mean value \pm SEM percent RLU vs. control cells in three replicates.

Migration capacity assay

Wound healing technique was performed to analyse the capacity of cell lines to migrate. NCI-H727 cells were plated in 12-well plates at 3×10^5 cell/well density. When confluence was reached, cells were serum starved for 1 hour. A wound was made in the centre of each well using a 100 μ l sterile pipette tip. Cells were rinsed with PBS to remove detached cells and then treated with serum-free medium supplemented with corresponding treatments (eve, TGF-B, IGF-1, paclitaxel, GW788388, LY2109761). Images were taken as random triplicates per well at baseline and after 24 hours of incubation with each of the treatments. The healing of each wound was then analysed and calculated as the area recovered by cells due to migration compared to baseline image using ImageJ software (168). Experiments were performed at least four times.

Protein isolation

For protein isolation from human frozen tissues, lysates were obtained by using Tissue Raptor (Qiagen, Hilden, Germany), according to the manufacturer's instructions. Protein derived from line cell cultures were obtained after seeding in 12-well plates of NCI-H727 and NCI-H720 cells at 3×10^5 and 5×10^5 cells/well, respectively. Human cell lines and human tissues were lysed in RIPA buffer (Thermo Fisher Scientific, Waltham, MA, USA) with 1X Halt™ Protease and Phosphatase Inhibitor Cocktail according with manufactures protocols, kept in ice for 30 minutes, then sonicated and centrifuged at 13,000 rpm for 30 minutes at 4°C. The supernatant was then transferred to a new tube and protein concentration was measured by the BCA Protein Assay kit (Thermo Fisher Scientific). The BCA assay is based on the colorimetric reaction between bicinchoninic acid and copper ions (Cu^+) from the copper sulphate which is reduced by the binding of proteins present in the sample. The change of colour from green to purple is proportional to the amount of protein present, followed by reading at a wavelength of 562 nm at the Envision 2104 Multilabel Spectrophotometer (Perkin Elmer, Monza, Italy).

Western blot analysis

Protein levels were analysed by western blot (WB). NEN cells were seeded at 3×10^5 (NCI-H727) and 5×10^5 (NCI-H720) cells/well, respectively and serum starved for 24 hours after 70% confluence was reached. Cells were then treated with same compounds as previously described. Total protein collected from fresh tissue were lysed and quantified. Total protein obtained from cell line was lysed after 24- and 48 hours or time-coursed at 0, 3, 6, 9, 12, 18, 24, 36 hours of treatment to access cell cycle proteins. 30ug of protein were prepared with laemmli buffer (62,5 mM Tris-HCl (pH 6.8), 25% glycerol, 2.1% sodium dodecyl sulphate, 0.01% bromophenol blue, DTT) in 1:1 ratio, boiled at 90°C for 5 minutes and loaded in 12 or 15% acrylamide gel. Proteins were separated by SDS-PAGE and transferred to a nitrocellulose membrane (Millipore, Darmstadt, Germany). Membranes were blocked for an hour with 5% non-fat milk dissolved in Tris-buffer saline and 0.05% Tween 20 (TTBS). Membranes were then incubated in agitation with primary antibodies (**Table 9**) overnight in 4°C chamber. The next day, membranes were washed 3 times with TTBS and incubated with horseradish peroxidase-conjugated goat anti-rabbit or mouse IgG secondary antibody at half the concentration of primary antibody for 1 hour. Membranes were again washed 3 times with TTBS and binding of antibodies was revealed by enhanced chemiluminescence using the Azure c300 (Azure Biosystems, Dublin, CA, USA). Analyses were carried out using densitometric analysis with ImageJ software (168) and relative protein expression was normalised against housekeeping protein GAPDH.

Table 9 List of primary antibodies

Primary Ab	Reference	Molecular Weight (kDa)	Source	Concentration
Caspase 3	Cell Signaling #9662	35	Rabbit	1:1000
TGF- β	Cell Signaling #3709	12, 45-60	Rabbit	1:500
TGF β RI	Cell Signaling #3712	52	Rabbit	1:1000
TGF β RII	Cell Signaling #11888	70-80	Rabbit	1:1000
SMAD2/3	Cell Signaling #8685	52, 60	Rabbit	1:1000
SMAD4	Cell Signaling #38454	70	Rabbit	1:1000
SMAD6	Invitrogen MA5-15687	53	Mouse	1:1000
N-cadherin	Cell Signaling #14215	140	Mouse	1:1000
E-cadherin	abcam ab1416	110	Mouse	1:1000
Cyclin D1	abcam ab74646	33	Mouse	1:1000
Cyclin E1	Cell Signaling #4129	48-56	Mouse	1:1000
CDK4	abcam ab3112	34	Mouse	1:1000
CDK2	Cell Signaling #2546	33	Rabbit	1:1000
LC3	abcam ab48394	15	Rabbit	1:1000
GAPDH	Cell Signaling #8884	37	Rabbit	1:1000

Statistical analysis

All analyses were assessed using GraphPad Prism 6.01 (GraphPad Software, La Jolla, CA, USA). Cell viability, caspase activation, migration quantification and western blot analyses were analysed by one-way ANOVA followed by Bonferroni's post-hoc test. Cell cycle proteins before and after treatment conditions were analysed by calculating the differences between the area under the curve (AUC) of each condition using the following equation: $z = \frac{|AUC_1 - AUC_2|}{\sqrt{SE_{AUC1}^2 + SE_{AUC2}^2}}$. The two-tailed p-value was calculated with the following Microsoft Excel function $p = 2x(1 - DISTRIB.NORM.ST(z))$. All data were obtained from at least three independent experiments from different cellular passages and expressed as mean \pm SEM. p-values smaller than 0.05 were considered statistically significant and represented as $p \leq 0.05$ (*), $p \leq 0.01$ (**), $p \leq 0.001$ (***) , $p \leq 0.0001$ (****).

RESULTS

TBC vs. ABC cell-cycle protein profile

Previous studies by Gagliano et. al reported that two mTOR inhibitors, including eve, influenced cell-cycle progression by inducing a delay in the G1 phase only in the ABC cell line NCI-H720. The Authors also report that both inhibitors decreased cyclin D1 expression especially in the ABC cell line. However, the measurement was performed at a single time point and did not include other cell-cycle proteins that could allow further characterisation of resistant BC. To understand if there were differences in the expression of cell-cycle proteins in TBC vs. ABC and evaluate eve effects, the levels of cyclin D1, cyclin E, CDK4 and CDK2 were assessed by WB. Protein levels were evaluated after 24h hour starvation at baseline and after treatment with eve at 0, 3, 6, 9, 12, 18, 24, 36h. As shown in **Figure 9** cell-cycle proteins are differentially expressed in BC cells. Precisely, cyclin D1 is expressed almost 2-fold more in TBC vs. ABC ($p=0,0004$), whereas CDK4 is >3-fold more expressed in ABC ($p=0,026$). Moreover, the effect of eve on reducing cyclin D1 expression in the TBC cell line NCI-H727 was relatively moderate compared to the effect observed in ABC cells, whereas cyclin E expression was reduced by treatment with eve only in the ABC cell line (AUCs comparison in **Table 10**, **Figure 10** and **Figure 11**).

Increased expression of the canonical TGF- β signalling in typical carcinoids

Total proteins were extracted and analysed by WB from tissue samples of 4 TBC and 3 ABC. GAPDH was used as loading control. The levels of almost all the analysed proteins were found to be higher in TBC compared to ABC (**Figure 12**). The mean differences (\pm S.E.M.) between TBC and ABC were as follow: TGF- β ($135,5 \pm 30,30$, $p=0.003$), TGF β RI ($22,49 \pm 3,020$, $p=0.0003$), TGF β RII ($40,57 \pm 15,34$, $p=0.01$), SMAD 2/3 ($310,4 \pm 54,31$, $p=0.0006$), SMAD 4 ($87,92 \pm 16,99$, $p=0.003$) and SMAD 6 ($35,61 \pm 48,59$, $p=\text{non-significant (ns)}$).

TGF- β increases cell malignancy features in typical carcinoids

In order to further explore the differences found in the TGF- β /Smad signalling, BC cells were treated with eve and/or TGF- β and cell viability, caspase activation, apoptosis, and cell migration were assessed. IGF-1 and paclitaxel (pac) were used as positive and negative control, respectively.

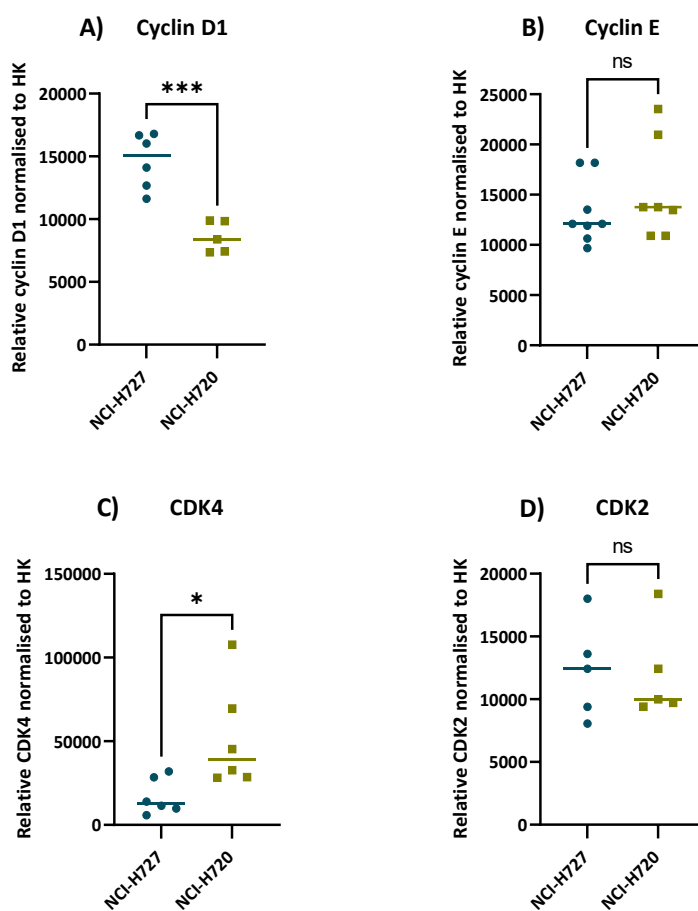
Cell migration was assessed through the wound healing assay as previously described. Cells were treated with eve and/or TGF- β , whereas IGF-1 and paclitaxel pac were used as positive and negative control to migration, respectively (**Figure 13A**). As shown in **Figure 13B**, eve treatment had no significant effect in TBC cell migration. On the other hand, TGF- β increased cell migration in TBC by 40% vs. untreated cells ($p=0.002$), whereas combined treatment with eve abrogated TGF- β effect by 27,85% vs. untreated cells ($p=0.002$) and by 68,36% vs. TGF- β treatment alone ($p= <0,0001$). Moreover, combined treatment of TGF- β and pac significantly increased migration by >50% vs. pac treatment alone ($p=0.03$) (**Figure 13C**), indicating that TGF- β was responsible for the observed increased migration in these cells, whereas combination with IGF-1 had no further effect vs. IGF-1 treatment alone.

EMT marker N-cadherin is more expressed in typical carcinoids

One of the primary ways in which TGF- β contribute to disease is through their involvement in EMT. EMT is a process that occurs during development and tissue repair in which cells of epithelial origin lose their cell-cell adhesions and become more mesenchymal in nature. During EMT, TGF- β can stimulate the expression of N-cadherin and other mesenchymal markers, leading to the acquisition of a more mesenchymal phenotype by epithelial cells. In fact, N-cadherin has been shown to promote the migration and invasion of cancer cells and

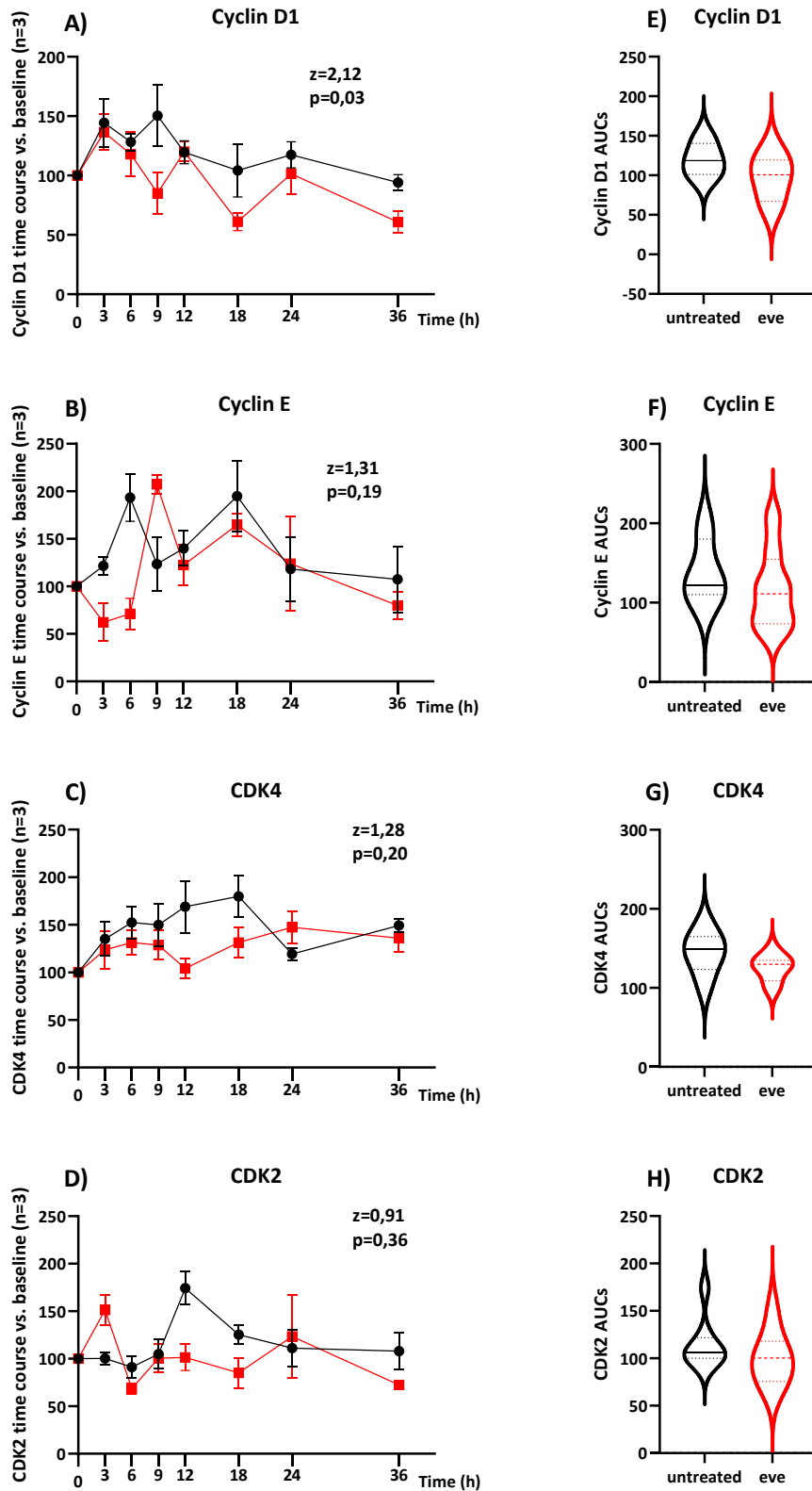
to be associated with a poor prognosis in several types of cancer. Therefore, we assessed the levels of E- and N-cadherin in TBC and ABC derived from fresh tissue and cell lines (**Figure 14**). Interestingly, N-cadherin expression was higher in NCI-H727 vs. NCI-H720 cells ($p=0.009$), whereas there were no significant differences in BC derived from fresh tissue samples. Treatment with eve, TGF- β and the combination of both further increased N-cadherin expression in the TBC NCI-H727 cell line but not in NCI-H720 (**Figure 14E/G** and **Figure 15**) by 45 (0.05), 137 ($p<0,0001$) and 79% ($p=0,002$), respectively. On the contrary, eve treatment increased the epithelial marker E-cadherin in the ABC cell line NCI-H720 by 80% vs. control ($p=0.004$) whereas combined treatment with TGF- β increased N-cadherin marker by 33% vs. control ($p=0.02$) (**Figure 14F/G** and **Figure 15**).

Figure 9
Cell-cycle proteins profile in TBC vs. ABC at baseline



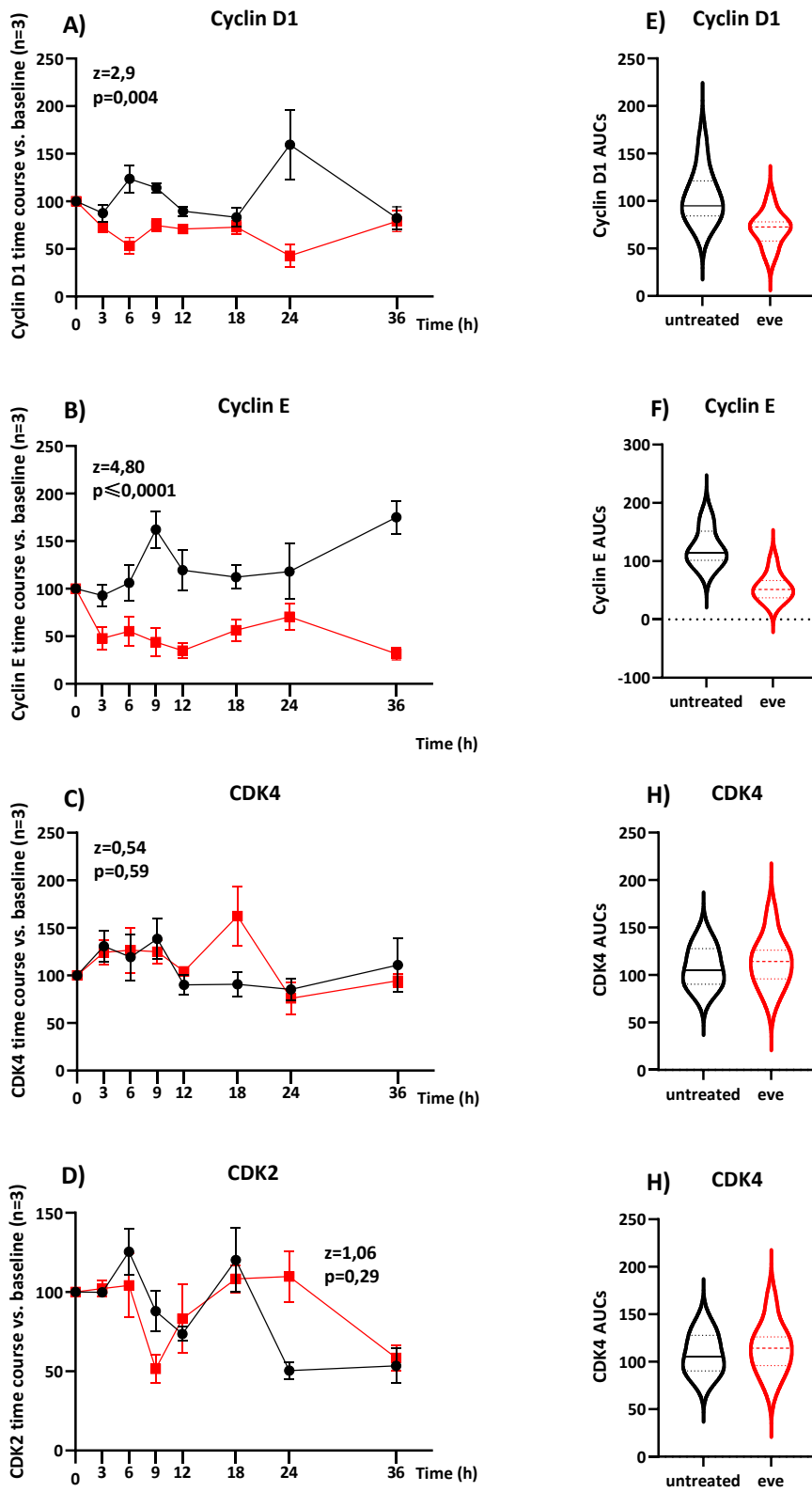
Note. WB quantification for cyclin D1, CDK4, cyclin E and CDK2 protein expression in BC cell lines. HK=housekeeping GAPH.

Figure 10
Time course of cell cycle proteins in NCI-H727 cells



Note. A-D) Time course of Cyclin D1, Cyclin E, Cdk4, Cdk2 protein expression levels in TBC cell line treated with 100 nM eve (RED) or untreated (BLACK) over a time frame of 36h. Values are shown \pm SEM from at least 2 independent experiments. E-H) Violin plots of the global differences of the expression profile in untreated (BLACK) vs. eve treated (RED) cells. in NCI-H727.

Figure 11
Time course of cell cycle proteins in NCI-H720 cells



Note. A-D) Time course of Cyclin D1, Cyclin E, Cdk4, Cdk2 protein expression levels in ABC cell line treated with 100 nM eve (RED) or untreated (BLACK) over a time frame of 36h. Values are shown \pm SEM from at least 2 independent

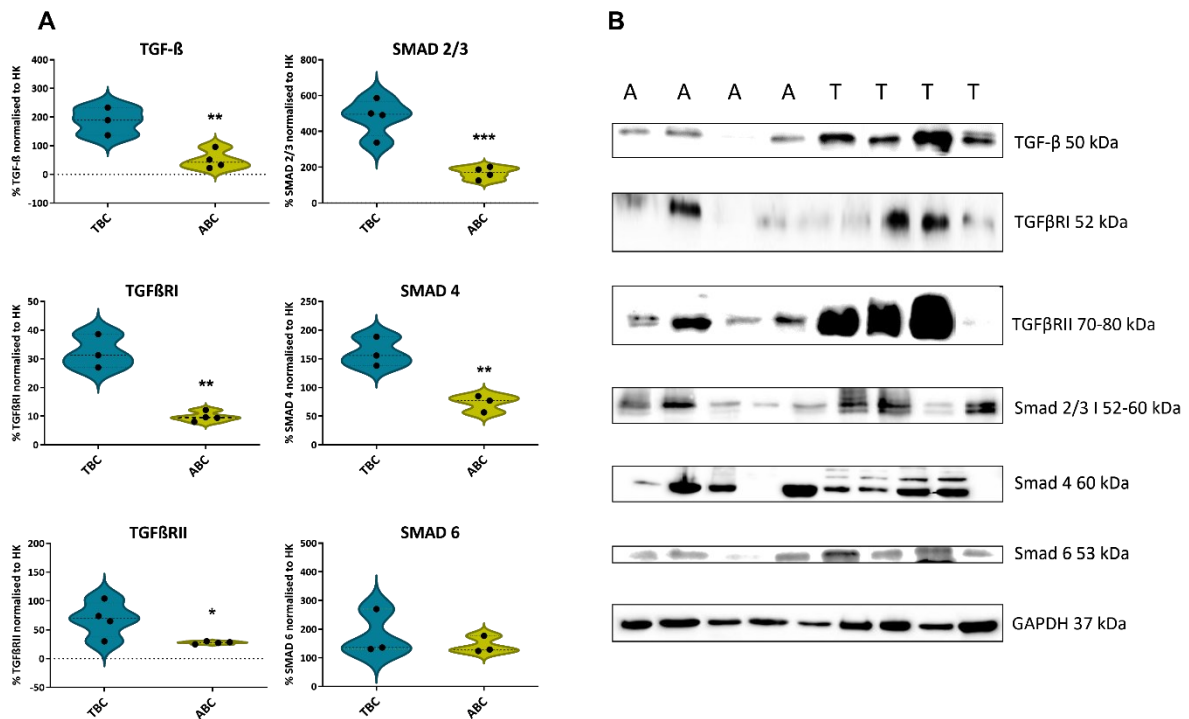
experiments. E-H) Violin plots of the global differences of the expression profile in untreated (**BLACK**) vs. eve treated (**RED**) cells. in NCI-H720.

Table 10 Area under the curve of time course of cell cycle proteins in TBC and ABC cell lines

NCI-H727	AUC 1		AUC 2		z	p-value
	Untreated	eve	Untreated	eve		
Cyclin D1	4204	3353	4204	3353	2,12	0,03
Cyclin E	4225	3625	4225	3625	0,91	0,36
CDK4	5271	4699	5271	4699	1,28	0,20
CDK2	4361	3982	4361	3982	0,91	0,36
NCI-H720						
Cyclin D1	3959	2368	3959	2368	2,89	0,004
Cyclin E	4557	1909	4557	1909	4,80	≤ 0,0001
CDK4	3698	3971	3698	3971	0,54	0,59
CDK2	2917	3287	2917	3287	1,06	0,29

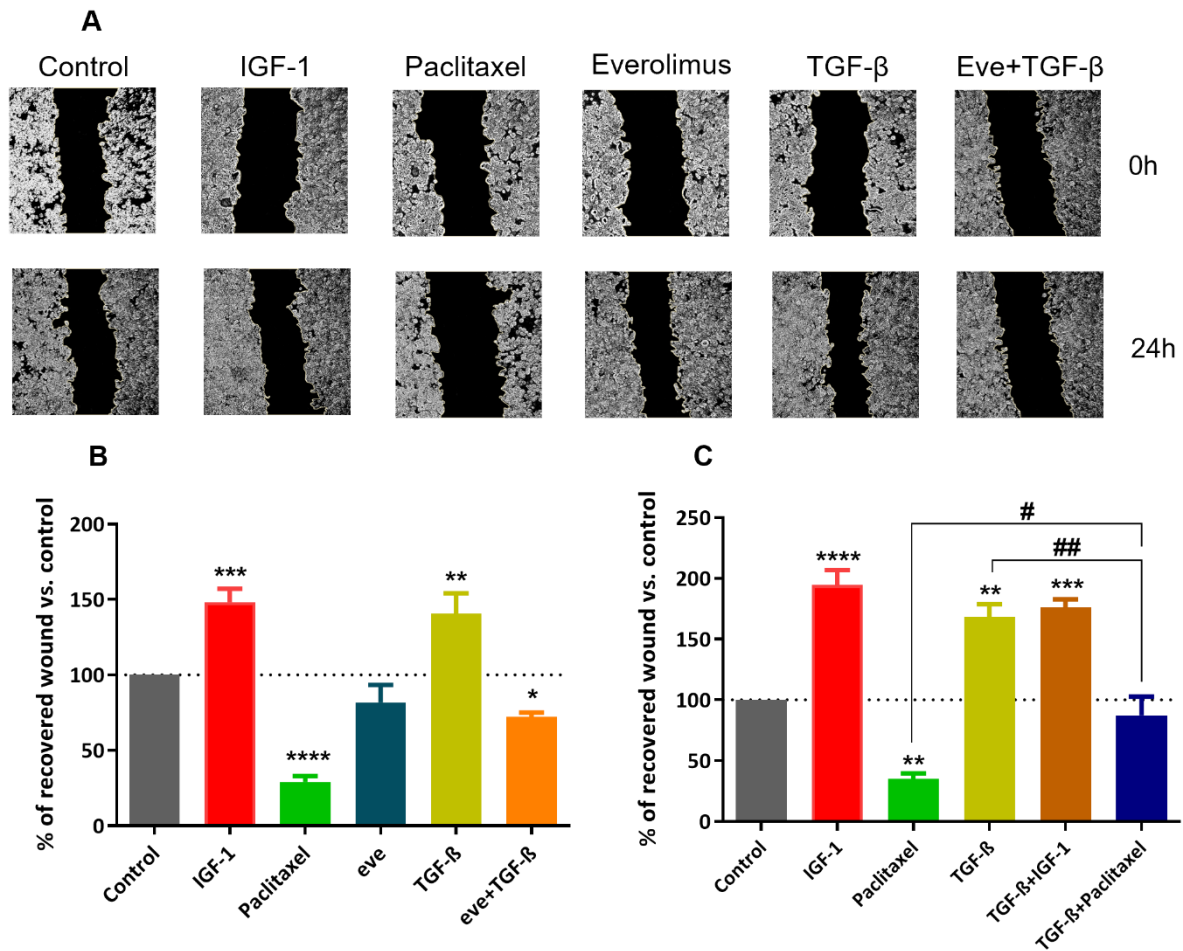
Figure 12

Basal levels of TGF- β pathway's proteins in bronchial carcinoids fresh tissue.



Note. A) Western blot quantification with ImageJ. Y-axis shows % of total basal protein normalised to HK=housekeeping (GAPDH). B) Exemplary WBs; A=atypical carcinoid; T=typical carcinoid.

Figure 13
TGF- β -induced migration in atypical carcinoids.



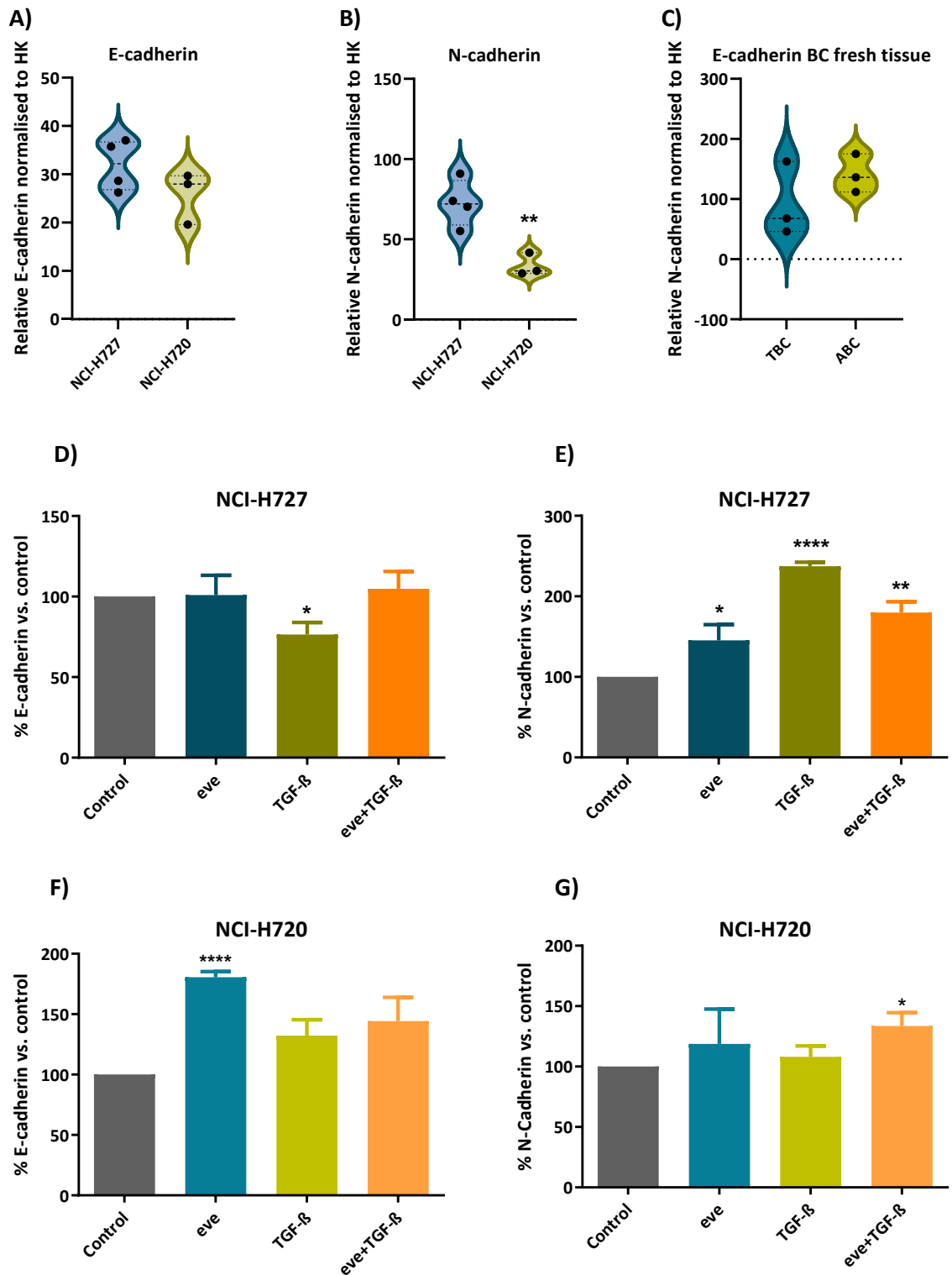
Note. A) Cell migration (scratch wound healing assay). Representative images are shown from at least three independent experiments. The black area (=wound area) was quantified with ImageJ at baseline and after 24h. B) and C) % of wound recovery vs. untreated control cells. TGF- β increased cell migration vs. control cells and in combination with negative migration control paclitaxel. Data are expressed as the mean \pm S.E.M. percent of specific assay vs. untreated control cells.

Cell viability, caspase activation and apoptosis were next assessed to verify if TBC and ABC cell lines presented different functional responses to treatment with eve and/or TGF- β . Though eve had little effect in the viability of the TBC cell line (\sim 7% reduction vs. control, $p=0.05$), it decreased the cell viability of ABC cells by \sim 20% ($p=0.01$) (**Figure 16A and D**). TGF- β , in contrast, increased the activation of caspase 3/7 in the TBC cell line by \sim 15% vs. untreated control cells ($p=0.002$) (**Figure 16B and E**), but not in ABC cells. Interestingly, caspase activation in TBC cells was not accompanied by apoptosis as cell viability was not modified by TGF- β (**Figure 16C**), indicating that caspase might be playing a non-canonical role in this setting. In fact, the levels of the caspase 3 protein were higher in TBC vs. ABC, although this difference was only statistically significant when the analysis was done on BC cell lines ($28,49\% \pm 9,225$, $p=0.03$) and not on fresh tissue (**Figure 16G/H**).

Inhibition of mTOR and TGF- β signalling reduce TBC malignancy features

To understand if the concomitant inhibition of mTOR and TGF- β signalling could be of interest in the treatment of resistant BC, the TBC cell line was treated with eve alone or combined with LY2109761 and GW788388, both inhibitors of TGF- β receptor I and II, and cell migration (**Figure 17A/B**), cell viability (**Figure 17C**) and apoptosis (**Figure 17E**) were evaluated. LY2109761 is a dual inhibitor of TGF β RI/II with K_i of 38 nM and 300 nM, respectively, and it has been studied as a potential treatment for various diseases, including cancer, fibrosis, and autoimmune disorders. GW788388 is potent and selective inhibitor of TGF β RI with K_i of 18 nM, but also inhibits activin type II receptor. It has been shown to inhibit the growth of cancer cells and reduce fibrosis in animal models. As shown in **Figure 17**, GW788388 treatment alone increased cell migration by >40% vs. control ($p < 0,0001$) and cell viability by ~29% ($p = 0.003$) which is a strong indicator that GW788388 is not suitable for the purpose of ameliorating advanced BC disease. However, both inhibitors significantly reduced cell migration in combination with eve without causing any significant impact on cell viability: GW788388 by 31% ($p = 0,0084$) and LY2109761 by 24% ($p = 0,0009$). Even more interesting is the combination of both inhibitors with eve which caused a reduction in cell migration of >40% vs. control ($p < 0,0001$) accompanied by cell viability reduction of ~28% vs. control ($p = 0,006$) and ~24% more apoptosis vs. eve treatment alone ($p = 0.04$).

Figure 14
E- and N-cadherins expression in bronchial carcinoids

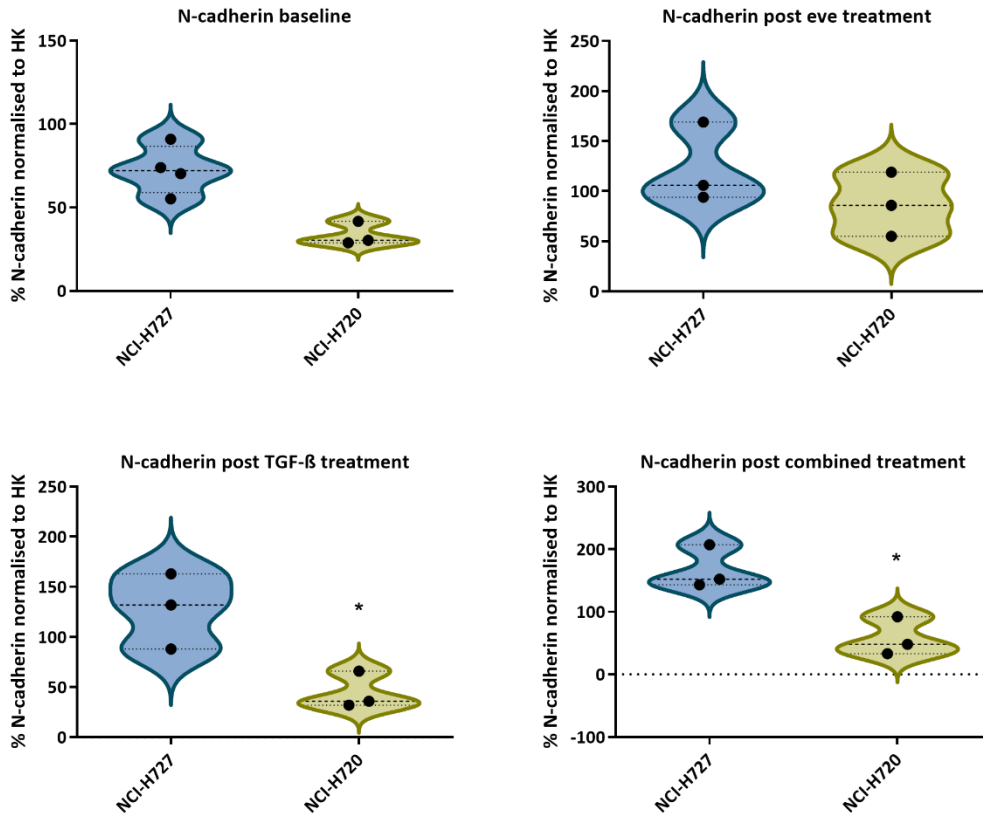


Note. A-C) E- and N-cadherin expression profile in NCI-H727 (A), NCI-H720 (B) and BC fresh tissues (C, only E-cadherin). D-E) Changes in E- and N-cadherin expression after treatment with everolimus (eve) and TGF- β alone or combined in TBC cell line NCI-H727 vs. untreated control cells. Protein expression is shown as % mean \pm SEM. F-G) Same as D-E for ABC cell line NCI-H720.

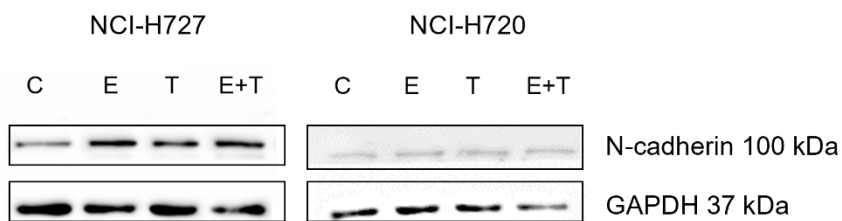
Figure 15

N-cadherin expression in BC cell lines after treatment with everolimus and/or TGF- β

A)



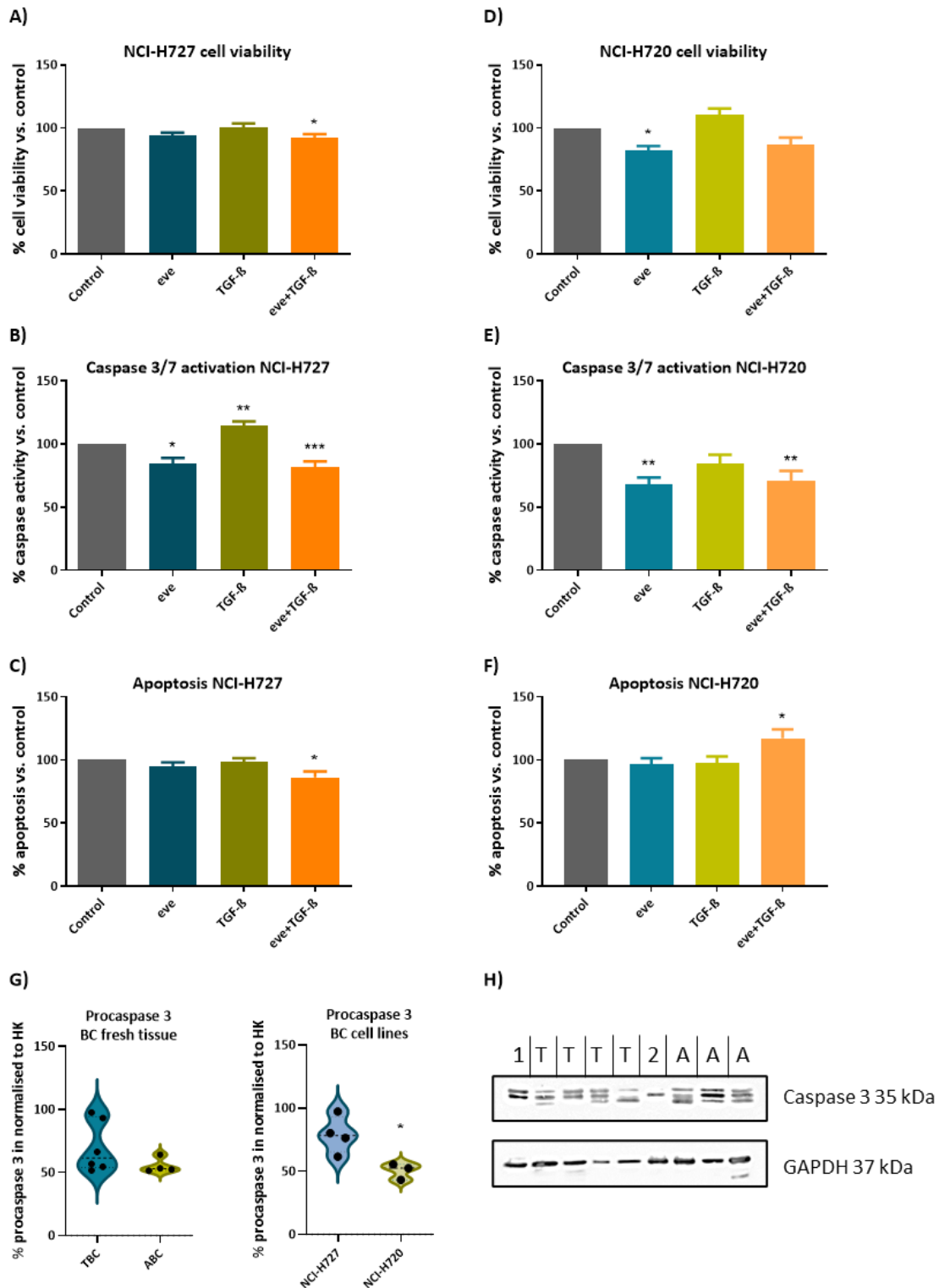
B)



Note. A) N-cadherin protein expression in NCI-H727 vs. NCI-H720 before and after treatment with everolimus, TGF- β and combination of both. B) Exemplary Western blot of N-cadherin expression in bronchial carcinoid cell lines; HK=housekeeping GAPDH.

Figure 16

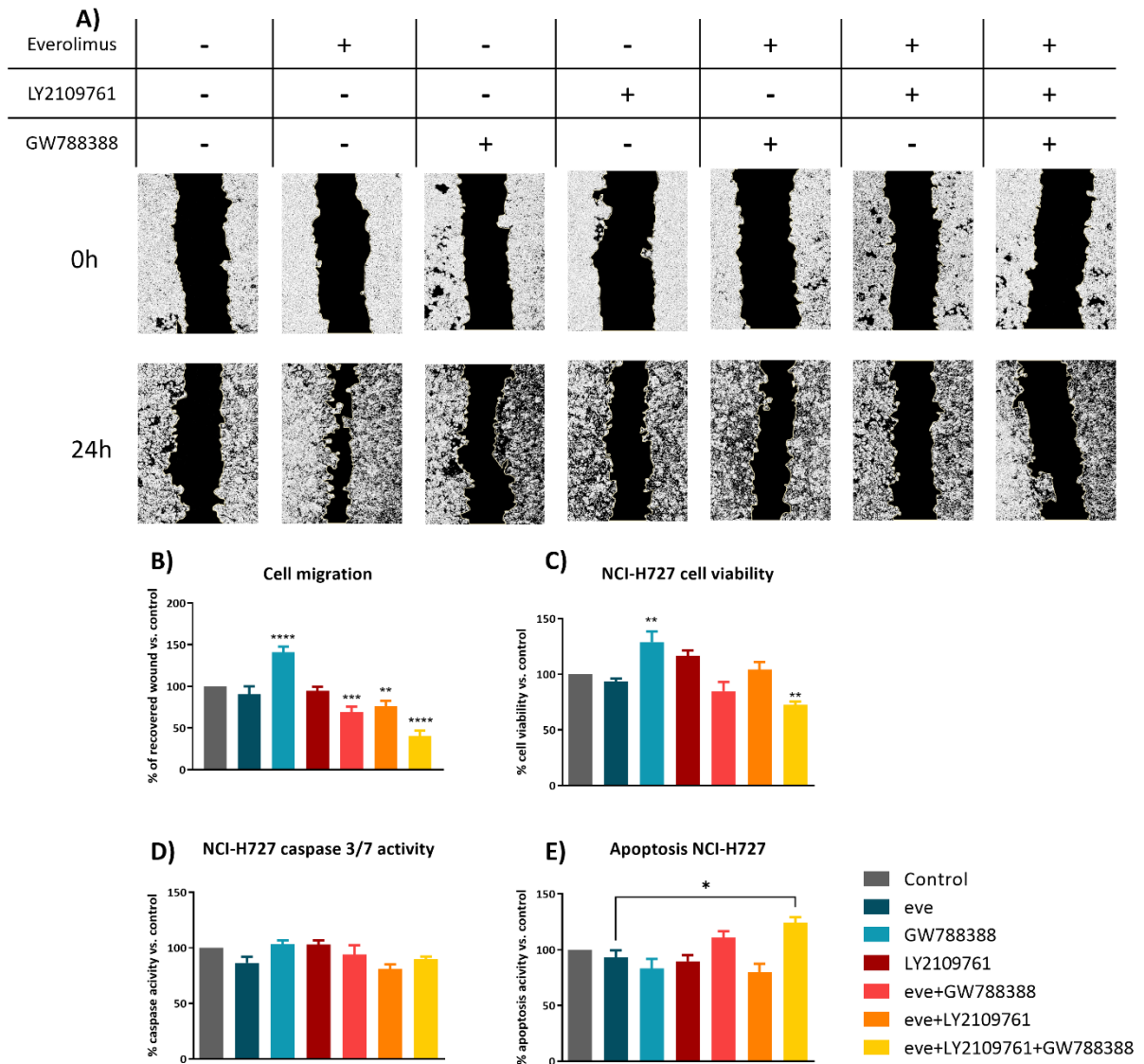
TBC and ABC functional responses to treatment and Caspase 3 expression



Note. A-C) Cell viability (A), caspase 3/7 activation (B) and apoptosis measured as ratio of caspase activation over cell viability (C) in the TBC cell line NCI-H727. D-F) Same as A-C in the ABC cell line NCI-H720. Data are expressed as the mean \pm S.E.M. percent of specific assay vs. untreated control cells. G) Procaspase 3 expression in bronchial carcinoids derived from fresh tissue (left) and bronchial carcinoids cell lines (right). H) Total proteins were isolated from NCI-H727, NCI-H720 cells and fresh tissue and western blot analysis for procaspase 3 protein expression was performed. HK=housekeeping GAPDH; 1= lane for NCI-H727, T=typical carcinoids, 2= lane for NCI-H720, A= atypical carcinoids.

Figure 17

PI3K/mTOR and TGF- β pathway inhibition reduce malignancy features in typical carcinoids



Note. NCI-H727 Cells were treated with TGF- β receptors inhibitors LY2109761 and GW788388 alone or combined with everolimus. A) Cell migration (scratch wound healing assay). Representative images are shown from three independent experiments. The black area (=wound area) was quantified with ImageJ at baseline and after 24h. B) Quantification of the recovered area of the wound vs. control. C) Percentage of cell viability vs. untreated control cells. D) Percentage of caspase activity vs. untreated control cells and E) percentage of apoptosis calculated as the ratio of caspase activity over cell viability. Data are expressed as the mean \pm S.E.M. percent of specific assay vs. untreated control cells.

CONCLUSIONS

Bronchial Carcinoids are a rare type of NET which often follow an indolent course, meaning they grow slowly and may not cause symptoms for many years. However, in advanced disease, BC can be very aggressive and difficult to treat. Resistant BC are a significant clinical problem because they are often associated with a poor prognosis and limited treatment options. Advanced disease in BC refers to BC that has spread beyond the primary site, meaning tumour debulking is unlikely. Treatment options for advanced BC may include chemotherapy, radiation therapy, targeted therapy, and surgery. Notwithstanding an overall improvement in the survival rates of NEN, lung NEN had one of the smallest improvements, probably due the fact that an adequate therapy is still missing (50).

TBC tends to have a more favourable prognosis and is typically treated with surgery, while ABC may require additional treatments such as chemotherapy or radiation. Despite the generally less aggressive nature of TBC compared to ABC, some studies have found that TBC cells are more resistant to treatment, including the mTOR inhibitor eve. Understanding the molecular mechanisms underlying resistance in BC is crucial for the development of targeted therapies that can effectively treat these tumours. Therefore, chapter one of the present assay aimed to identify if there were different expression profiles in BC that could explain the distinct functional responses found in these carcinoids. Resistance to treatment can be caused by various factors, including the overexpression of proteins that promote cell growth and survival, such as cyclins and CDKs, and the activation of signalling pathways that are able to drive tumour progression, such as the TGF- β /Smad and the PI3K/mTOR pathway. In this setting, we have evaluated different proteins and signalling pathways that are involved in the growth and proliferation of cancer cells.

It is well established that cyclin D1 is often overexpressed in various types of tumours, including breast, ovarian, and colorectal cancers (135, 169, 170, 171). This overexpression can contribute to the development of cancer by promoting cell cycle progression and inhibiting cell death. The levels of cyclin D1, cyclin E, CDK4 and CDK2 were assessed by WB after treatment with eve at different time points. The protein levels were quantified and the resulting AUCs were calculated to determine if there were differences between the typical and atypical carcinoid cell lines in terms of protein levels and response to eve treatment. In our study, TBC cells expressed higher basal levels of cyclin D1 and were less sensitive to the effects of eve treatment compared to ABC cells, which express higher levels

of CDK4. Results on cyclin D1 overexpression are in line with previous report regarding cyclin D1 overexpression and aberrant Rb pathway in TBC cells (172). The fact that TBC cells have higher levels of cyclin D1 may be relevant in terms of the resistant phenotype that has been observed in these cells, which could potentially benefit from targeted therapies that are tailored to the specific molecular characteristics of each type of carcinoid (i.e., CDK inhibitors such as dinaciclib).

Previous studies have also reported a possible crosstalk between TGF- β signalling and the PI3K/mTOR pathway in cancer progression (165, 173). Preliminary studies have reported a differential TGF- β signalling in BC cells lines. Therefore, we continued the analysis by verifying if TBC and ABC from fresh tissue presented similar differences. We have found that the canonical TGF- β /Smad pathway is much more expressed in TBC than ABC, making this pathway an interest target for advanced BC. TGF- β regulates several cellular processes, including cell growth, differentiation, and apoptosis. The TGF- β /Smad is a signalling pathway that is activated by TGF- β and involves the phosphorylation and activation of transcription factors called Smads. TGF- β can stimulate the expression of mesenchymal markers, such as N-cadherin, and lead to the acquisition of a more mesenchymal phenotype by epithelial cells through EMT. N-cadherin is a protein that is involved in cell-cell adhesion and is upregulated during EMT. High levels of N-cadherin have been associated with increased migration and invasion of cancer cells and a poor prognosis in several types of cancer. We have found that TBC cells have higher expression of proteins involved in the TGF- β /SMAD pathway, and treatment with TGF- β promotes the migration of TBC cells, an effect that is abrogated by treatment with eve. Moreover, TBC cells also present higher basal levels of N-cadherin, a known marker of EMT, which expression is further induced by TGF- β or combined treatment with eve. Interestingly, we have also found an overexpression of procaspase 3 in TBC vs. ABC, as well as a major caspase activation following TGF- β treatment in these cells, which could indicate a non-canonical role for caspase in TBC. In fact, in addition to their role in apoptosis, caspases have also been shown to play non-canonical roles in cancer, including the regulation of migration, invasion and metastasis (174).

Given the above results, TGF- β signalling could be participating in the resistant phenotype found in some TBC through activation of caspase 3 and induction of EMT. Therefore, we assessed the concomitant inhibition of the PI3K/mTOR and TGF- β pathways, which may be

a promising approach for increasing the PFS of patients with advanced BC. TBC cells were treated with eve alone or in combination with inhibitors of the TGF- β receptor I and II (LY2109761 and GW788388). We found that treatment with GW788388 alone increased cell migration and viability, indicating that it is not suitable for the treatment of these neoplasms. However, both LY2109761 and GW788388 significantly reduced cell migration in combination with eve, and the combination of both inhibitors with eve caused a further reduction in cell migration and in cell viability, which was also associated with increased apoptosis vs. eve treatment alone. These results suggest that the concomitant inhibition of the PI3K/mTOR and TGF- β pathways may be an effective strategy for reducing the malignancy of TBC cells in terms of invasiveness, thereby improving the prognosis and PFS of patients with advanced disease.

In summary, TBC are often slow-growing and may not cause any symptoms in the early stages. However, when they do spread, they can be difficult to treat, as they can spread to virtually any part of the body. Carcinoid tumours are usually treated with surgery to remove the tumour, but if the tumour is inoperable or resistant to treatment, it can be difficult to manage. Finding new treatments and management strategies for inoperable or treatment-resistant TBC is therefore of great importance. TBC and ABC differ in their expression of cell-cycle proteins and signalling pathways, with TBC exhibiting higher levels of certain proteins and a more pronounced response to TGF- β . These differences may contribute to the observed resistance of TBC to treatment with eve and suggest the need for alternative therapeutic approaches for this subtype of BC. Targeting simultaneously PI3K/mTOR and TGF- β pathways, as shown herein, could increase the PFS in patients with advanced typical carcinoids for whom there are no other treatment options.

CHAPTER 2

COMPOUND 5 MECHANISM OF ACTION

INTRODUCTION

Normal cells are in constant equilibrium between cell growth, differentiation, and programmed cell death (apoptosis). Many pathways are involved in maintaining such equilibrium and when the balance is disturbed, abnormal cellular accumulations may result (175). Tumour cells can acquire capabilities that allow them to grow under suboptimal conditions and escape from cell growth control and pro-apoptotic signals. Mutations in the pathway of apoptotic signal transduction may cause tumour development, metastatic progression, and resistance to cell death stimuli, giving tumour cells the ability to resist chemotherapy treatments (176). Two major intracellular caspase cascades (intrinsic and extrinsic) are responsible for the activation of apoptosis, which are tightly regulated by different factors, including pro- and anti-apoptotic Bcl-2 family members, inhibitors of apoptosis proteins (IAP), and several protein kinases (177). The mitochondrial cascade, also known as the intrinsic pathway of apoptosis, is initiated by release of cytochrome C (cytC) and other polypeptides from the mitochondrial intermembrane space. The extrinsic pathway includes signalling through death-receptor pathway and begins with specialised ligand binding on cell surface. Survival outcome is determined by the balance of interactions between pro-apoptotic and anti-apoptotic members of the Bcl-2 family. There is a complex crosstalk between extrinsic and intrinsic pathways, i.e., activators of one may sensitise activation of the other.

Cancer cell resistance to a variety of structurally and functionally distinct medical treatments is the primary cause of failure of chemotherapeutic approaches for most human tumours, especially endocrine-related cancers (178). Mechanisms for chemoresistance may be due to decrease of active drug concentration owing to activation of membrane transporters or detoxification mechanisms, defective drug–target interactions and several factors able to influence cellular response to pro-apoptotic stimuli. Intrinsic mechanisms occur independently of prior exposure to chemotherapeutic drugs and hamper the efficacy of

chemotherapy, which is a common phenomenon in endocrine-related cancers. Acquired chemoresistance, instead, is developed by cancers initially sensitive to chemotherapy, undergoing selection and overgrowth of drug-resistant cancer cell clones, frequently occurring in targeted-therapy. Overcoming drug resistance is therefore crucial to understand the mechanisms participating to the chemoresistance phenotype, in order to identify new strategies to defeat this ominous phenomenon that causes recurrence, cancer dissemination and death.

Magmas

Tim16, encoded by the gene *Magmas*, is an integral constituent of the TIM23 translocase complex located in the mitochondrial inner membrane (**Figure 18**). It is highly conserved and ubiquitously expressed in mammalian cells at different levels, suggesting an important role in cell viability (179). Tim16 drives proteins from the intermembrane space into the mitochondrial matrix by functionally interacting with Tim14, another protein participating in the TIM23 complex. *Magmas* is involved in the Granulocyte-Macrophage-Colony Stimulating Factor (GM-CSF) signal transduction, which in turn regulates *Magmas* mRNA levels. GM-CSF is one of many growth factors that affect survival, growth and differentiation of hematopoietic cells. The highest levels of *Magmas* mRNA were observed in heart, skeletal muscle, and pituitary gland. Surprisingly, many of the tissues with high *Magmas* mRNA levels are not believed to express GM-CSF receptor, suggesting that *Magmas* expression is influenced by transduction pathways other than those regulated by GM-CSF (180). Although its role in cell growth is still unclear, some studies have highlighted possible correlation between Tim16 overexpression and poor cancer prognosis (167, 181). Tim16 overexpression has been reported in prostate cancer independently from the number of mitochondria present (182). An increased expression of *Magmas* has also been associated as being part of a poor prognostic gene-expression signature in breast cancer (183). Its overexpression has also been associated to impaired reactive oxygen species (ROS) homeostasis by promoting cellular tolerance through: (i) enhancing antioxidant enzyme activity, which prevents induction of apoptosis, and (ii) enhancing the activity of electron transport chain complexes, causing reduced ROS production (184). In this settings, previous studies in our laboratory demonstrated that Tim16 was also overexpressed in pituitary adenomas (PA) and *Magmas* silencing was able to sensitise ACTH-secreting mouse PA cell line (AtT-20 D16v-F2 cells) to pro-apoptotic stimuli (167). Moreover, fluorescence

microscopy analysis confirmed that Magmas overexpression is confined to the mitochondria other notwithstanding mitochondrial proteins normal expression levels measured by real time chain reaction (qPCR) (167). Magmas silencing also determined a reduced rate of DNA synthesis, an accumulation in G0/G1 phase with concomitant decrease in S phase. Interestingly, Magmas-silenced cells displayed basal caspase 3/7 activity and DNA fragmentation levels similar to control cells, which both increased under pro-apoptotic stimuli, the hypothesis that Magmas may play a role in tumour development by protecting neoplastic cells from apoptosis and by promoting cell proliferation. These findings were also confirmed in rat GH/PRL-secreting PA cell lines. In fact, in this other study, Magmas overexpression was able to inhibit Staurosporine-induced apoptosis by hampering CytC release from mitochondria, influencing Bax and Bcl-2 modulation by pro-apoptotic stimuli (185). Moreover, Magmas overexpression promoted S-phase accumulation in rat cell lines with concomitant increase in cell proliferation, which was not associated with decreased basal apoptotic rate, indicating that the protective effects towards apoptosis occur only in the presence of pro-apoptotic stimuli (167). Together, these studies suggest that Magmas may be involved in promoting pituitary cell growth through the activation of survival pathways.

Magmas Inhibitor: Compound 5

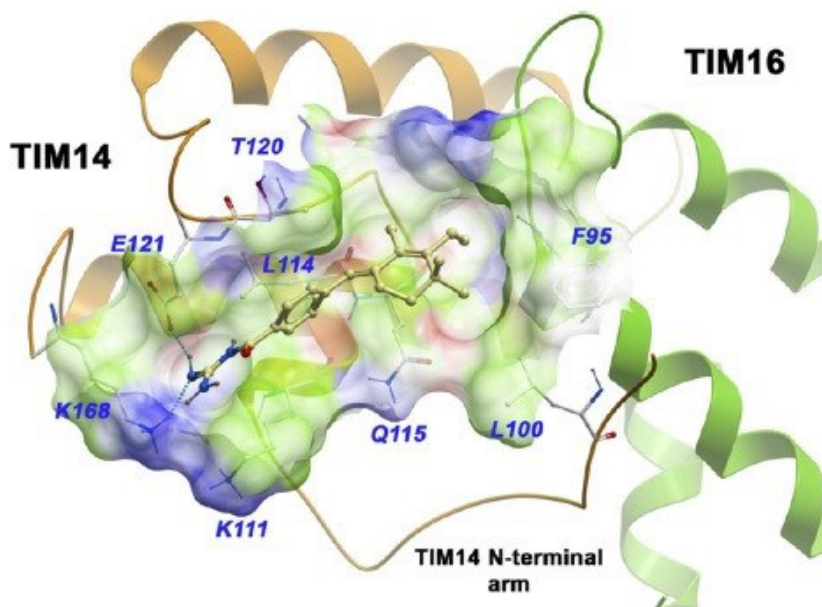
The evidence that Magmas protein, Tim16, could play a protective role towards pro-apoptotic stimuli prompted the search for chemical compounds that could effectively reduce Magmas function. In this setting, small molecules of Magmas inhibitors were synthesised and tested in *Saccharomyces cerevisiae* and mice (186), of which one resulted promising (

Figure 19). Starting from this inhibitor, six different compounds were synthesized and their ability to sensitize chemoresistant cells while lacking cytotoxic activity was tested. Among these, Compound 5 (**Figure 20**) was able to enhance the pro-apoptotic effects of Staurosporine on TT cell line, derived from a chemoresistant human medullary thyroid carcinoma (MTC), by reducing mitochondrial membrane potential (MMP) activation (187) while presenting almost noncytotoxic features (188).

Note. The TIM23 complex transports precursor proteins with positively charged presequences which are present in precursor forms of soluble matrix proteins (a), of inner membrane proteins with multiple (b) or single transmembrane domains (c); a group of inner membrane proteins contain an internal presequence-like element which together with the transmembrane domain serves as mitochondrial targeting signal (d). OM, outer membrane; IMS, intermembrane space; IM, inner membrane. From “The many faces of the mitochondrial TIM23 complex” by Mokranjac et. al 2022, (BBA) - Bioenergetics, Volume 1797, issue 6-7. Copyright 2010, Elsevier.

Figure 19

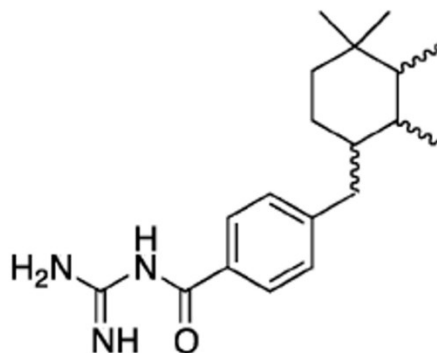
Model of Magmas inhibitor binding in the Tim14–Tim16 interface pocket



Note: The predicted Tim14–Tim16 binding pocket surface is colour coded according to protein binding properties (white: neutral surface; green: hydrophobic surface; red: hydrogen bonding acceptor potential; blue: hydrogen bond donor potential; brown: magmas inhibitor. From “Design, synthesis, and biological activity of novel Magmas inhibitors” by Jubinsky et. al 2011, Bioorganic & Medicinal Chemistry Letters, volume 21, issue 11. Copyright © 2011 Elsevier Ltd. All rights reserved.

Figure 20

Compound 5 chemical formula



Chemical formula: $C_{20}H_{31}N_3O$
Molecular weight: 329,48

MATERIALS & METHODS

Drugs and reagents

Compound 5, N-carbamidoyl-4-((3-ethyl-2,4,4-trimethylcyclohexyl)methyl)benzamide (**Figure 20**), was synthesized by the Department of Chemical and Pharmaceutical Sciences of the University of Ferrara (Italy). All other reagents, if not otherwise specified were purchased from Sigma (Milano, IT).

Cell culture

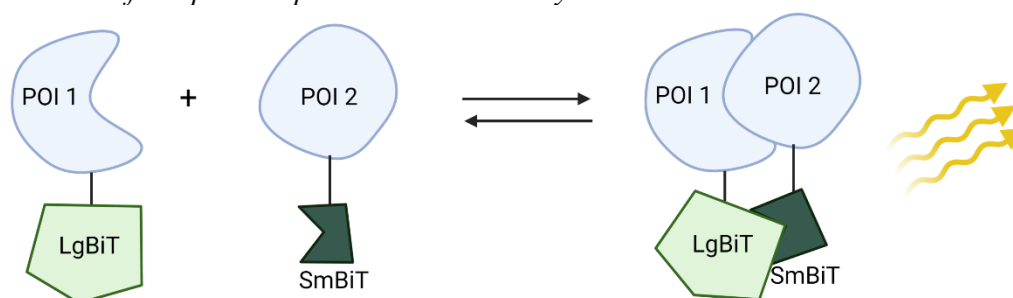
MCF7 cell line (ATCC® HTB-22™) was purchased from the ATCC® and grown in DMEM-High Glucose (Euroclone, Milano, Italy) supplemented with 10% FBS, 10 U/ml penicillin/streptomycin and maintained in a sterile incubator at 37°C with 5% CO₂.

NanoLuc® Binary Technology (NanoBiT)

NanoBiT is a luminescent assay from Promega based on structural complementation of two reporter system composed of a large bit (LgBiT) subunit and a small bit (SmBiT) subunit. These NanoBiTs are fused to proteins of interest (POI) in different C- and N-terminal configurations. In the event of protein-protein interaction in a kinetically favourable conformation, LgBiT and SmBiT interact to form a functional enzyme that oxidise Nano-Glo reagent containing furimazine substrate, generating a luminescent signal (**Figure 21**).

Figure 21

Overview of the protein:protein interaction system



Note. Proteins A and B are fused to LgBiT and SmBiT. Interaction of fusion partners leads to structural complementation of LgBiT with SmBiT, generating a functional enzyme capable of oxidising furimazine substrate. Created with BioRender.com.

Vectors, Plasmids & Primers

Plasmids containing Magmas and DNAJC19 genes are described in **Figure 22**. Tim16 and Tim14 full length coding sequences were received in pCMV6-Entry and pCMV6-AC-HA vectors, respectively (Origene: RC202828 and PS100004). Both Tim16 and 14 were amplified using ad hoc primers following standard cloning protocols to introduce genes of interest (GOI) into the NanoBiT vectors (**Figure 23**). Primers sequences used to amplify Tim16 and Tim14 proteins out of their vectors of origin, as well the primers used to sequence the resulting fusion gene, were designed with Primer3 software, and are represented in **Table 11**. From 5' to 3' primers included six random bases, six bases corresponding to unique restriction enzyme sequences found in the NanoBiT vectors, ATG start codon sequence for C- terminal NanoBiT tags, and TCA/TAA stop codons for N- terminal NanoBiT tags and 18-30 bases corresponding to the specific GOI. PCR products were purified on 1 % agarose gel and bands were extracted using the QIAquick Gel Extraction Kit (Qiagen) following the manufacturer's instruction. The amplified and purified GOI and NanoBiT vector were then digested with the same specific restriction enzyme (NheI or XhoI) to allow for the creation of sticky ends in both GOI sequence and vector, which were later ligated using T4 DNA Ligase (New England Biolabs, Ipswich. Massachusetts, USA) in a T4 DNA Ligase buffer from same kit and nuclease-free water for one hour at room temperature. To determine the optimal orientation of the fusion proteins eight possible combinations of expression constructs were tested.

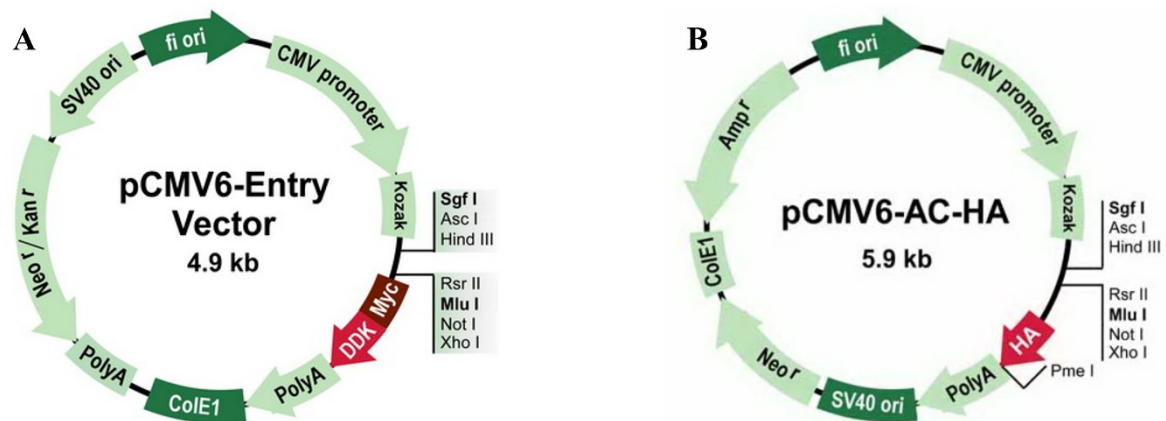
Table 11 Primers designed to fit the NanoBiT vectors

Primer ID	Sequence	RE
1) FW-TIM16-LgBiT/SmBiT C	5' CCTAAGGCTAGCATGGCCAAGTACCTGGCCCAG 3'	NheI
2) RV-TIM16-LgBiT/SmBiT C	5' CTTAGGCTCGAGCCCGTATGGGGCATCTGCC 3'	XhoI
3) FW-TIM16-LgBiT/SmBiT N	5' CCTAACCTCGAGCGGTGCCAAGTACCTGGCCCAG 3'	XhoI
4) RV-TIM16-LgBiT/SmBiT N	5' CCTAGGGCTAGCTCACGTATGGGGCATCTGCC 3'	NheI
5) FW-TIM14-LgBiT/SmBiT C	5' CCTAACGCTAGCATGGCCAGTACAGTGGTAGCAGTTG 3'	NheI
6) RV-TIM14-LgBiT/SmBiT C	5' CTTAGGCTCGAGCCTTTTTTAGCTTGACCTTCTAGTAAATCTTT 3'	XhoI
7) FW-TIM14-LgBiT/SmBiT N	5' CCTAACCTCGAGCGGTGCCAGTACAGTGGTAGCAGTTG 3'	XhoI

8) RV-TIM14-LgBiT/SmBiT N	5' CCTAGGGCTAGCTAAATTTTTAGCTTGACCTTCTAGTAAATCTTT 3'	NheI
9) NanoBiT FW	5' AAAGCCACCAGATCTGCTAGC 3'	-
10) NanoBiT RV	5' TCCACCTCCGCTCCCGCCACCACC 3'	-

Note. Primers were designed according with the manufacturer instructions. Bases are colour coded: red=random sequence, blue=specific restriction enzyme (RE) sequence, purple=start or stop codon, grey=included bases to allow in frame fusion of the protein of interest, black=Tim16, Tim14 or NanoBiT specific sequences.

Figure 22
Maps of the vectors containing the genes of interest

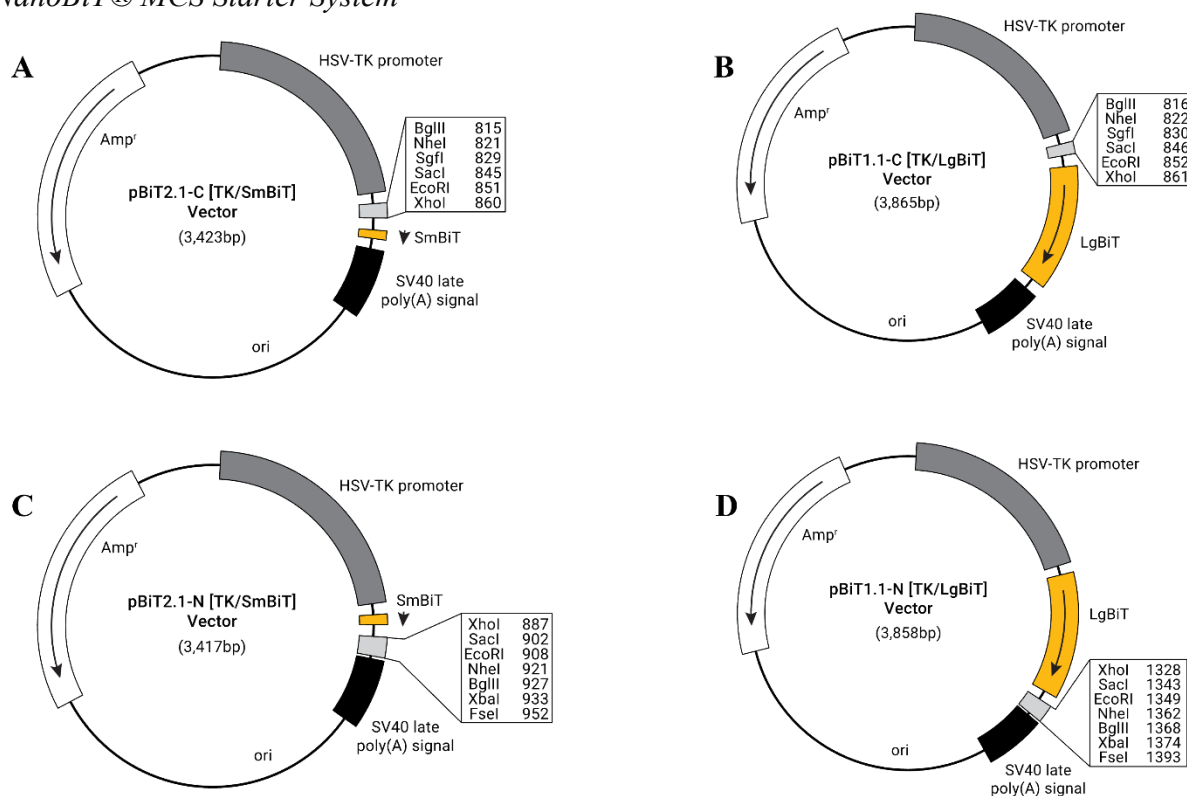


Note. A) plasmid RC202828 with Magmas and B) PS100004 with DNAJC19.

Transformation of DNA into *E. coli*

Plasmids were transformed into competent JM109 *E. coli* K strain. (Promega, Milano, IT). Briefly, 10 ng DNA were mixed with cells and incubated on ice for 30 minutes before being heat-shocked at 42°C for 45 seconds. Pre-heated 250 µl SOC media was added (2% tryptone, 0.5% yeast extract, 10 mM NaCl, 2.5 mM KCl, 10 mM MgCl₂, 10 mM MgSO₄ and 20 mM glucose; Sigma) and samples were shaken horizontally at 37°C for one hour before being centrifuged at maximum speed and resuspended in 50 µl SOC media. Cells were finally plated on antibiotic plates and incubated for 24 hours. Plates were made from LB-agar and 100 µg/ml ampicillin or 50 µg/ml kanamycin.

Figure 23
NanoBiT® MCS Starter System



Note. A) N-terminal LgBiT, B) C-terminal LgBiT, C) N-terminal SmBiT, D) N-terminal LgBiT.

Miraprep: purification of plasmid DNA

Colonies were picked from antibiotic-Luria Broth (LB)-Agar plates after 24 hours of incubation at 37°C, resuspended in 10 ml LB and incubated for 16 hours at 37°C with shaking at 225 rpm. The next day, the culture was processed via an altered miniprep protocol (189). Miraprep was performed using QIAprep Spin Miniprep Kit (QIAGEN, Milano, Italia) following the manufacturer's protocol except for one extra step: addition of 96% ethanol in an equal volume to supernatant after precipitation of proteins and chromosomal DNA in order to maximise binding of plasmid DNA to the column, consequently increasing DNA yield in the final elution. DNA concentration was quantified using the Invitrogen Qubit® 2.0 Fluorometer (Thermo Fisher, Waltham, Massachusetts, USA).

Sequencing

Purified DNA was sequenced by Sanger sequencing. Briefly two sequence reactions were performed for each sample in order to sequence both the sense and antisense strands of the

DNA. Each reaction contained 200ng of purified DNA, 1ul of forward/reverse primer (**Table 11**) at a concentration of 2.5 nM, 1ul of BigDye™ Terminator v3.1 Ready Reaction Mix (Thermofisher), and 2ul of 5X Sequencing Buffer from the same kit. The reactions were run on thw Applied Biosystems™ Veriti™ Thermal Cycler using a thermal cycling protocol of 96°C for 1 minute (1 cycle), 96°C for 10 seconds, 50°C for 50 seconds, and 60°C for 75 seconds (25 cycles), followed by a final hold at 4°C. The resulting sequences were then purified using the BigDye XTerminator™ Purification Kit and loaded onto the sequencer for analysis. The final cycle was a single hold at 4°C. The resulting sequences were analysed with the 3500 Dx Genetic Analyzer (Applied Biosystems).

Cell transfection & Plate reading

MCF7 and HeLa cells were seeded into 6-well plates at a density of 3.5×10^5 cell/ml in a 6-well plate. After 24 hours cells were transiently transfected with μg of each of the tagged vectors Tim16/Tim14-LgBiT/SmBiT using TransIT-LT1 transfection reagent (Mirus, Carlsbad, CA) according to the manufacturer's protocol. Briefly, DNA was added to serum-free media Opti-MEM and incubated at room temperature for five minutes. Lipofectamine reagent Mirus' TransIT® (Mirus Bio LLC, WI, USA) was added at a 3:1 ratio of TransIT-LT1 (μl) to DNA (μg) and incubated at room temperature for 30 minutes to facilitate formation of DNA-lipofectamine complexes. 100 μl were added dropwise to the 6-well plate and incubated at 37°C for 48 hours. Cells were co-transfected with the 8 possible combinations of Tim16 and Tim14 constructs in pairs to assess which pair of fusion protein produce the best response and with vector only. Forty-eight hours later, cells were detached with trypsin, counted, resuspended in phenol-red-free DMEM, plated on 96-well flat bottom plate with white walls at 5×10^4 cells/well density and treated with DMSO or 5 μM Compound 5 six hours after reseeding. 24 hours after Compound 5 treatment, Nano-Glo Live Cell Substrate dilution buffer (Promega) was equilibrated to room temperature and prepared 19 volumes to 1 volume Nano-Glo live cell substrate (Promega). 25 μl of solution were added per well and distributed by orbital shaking for two minutes. Luminescence was measured every two minutes for twenty cycles in the EnVision™ 2104 Multilabel Reader (Perkin-Elmer). Luminescence was measured in untreated co-transfected cells, mock transfected cells (vector only) and in co-transfected cells treated with Compound 5.

Table 12 Expression constructs that were created.

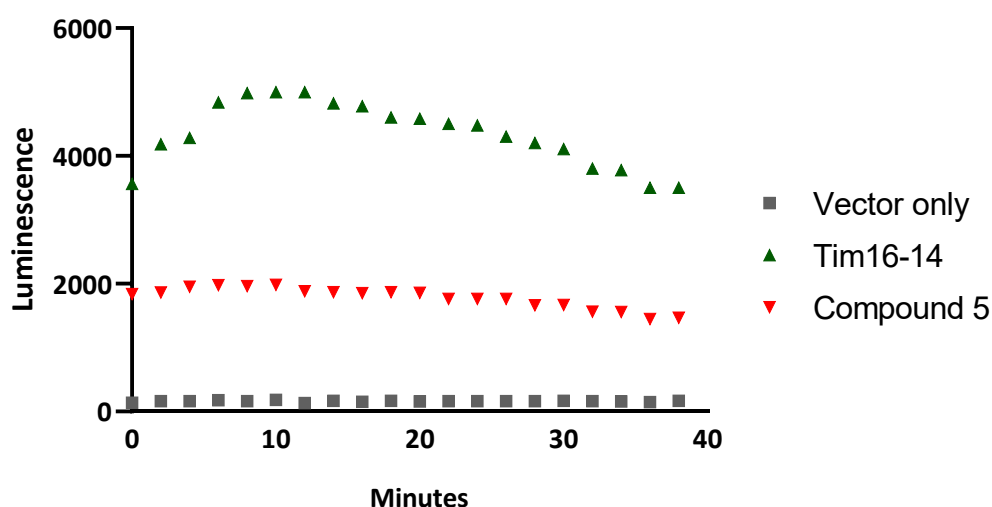
Tim16	TIM16-LgBiT LgBiT-TIM16 TIM16-SmBiT SmBiT-TIM16	Tim14	TIM14-LgBiT LgBiT-TIM14 TIM14-SmBiT SmBiT-TIM14
-------	--	-------	--

Note. Each POI is fused at either the N or C terminus with LgBiT and SmBiT. POI: protein of interest.

RESULTS

It is known that Tim16 forms a heterodimer with Tim14 and that there are inhibitors capable of interfering with such interaction. However, the mechanism of action of Compound 5 has never been tested in this context and its effect on Tim16-Tim14 binding is unknown. To examine whether Compound 5 altered the affinity of the Tim16-Tim14 binding, protein-protein interaction experiments were performed using the NanoBiT technology. The experiment was performed using MCF7 cells, treated with the inhibitor at 5 μ M for 24 hours post-transfection. Tim16 and Tim14 interaction was confirmed only when LgBiT-Tim16 and SmBiT-Tim14 were -C terminal tagged. Compound 5 significantly disrupted the physical interaction between Tim16 and Tim14 (**Figure 24**).

Figure 24
Effect of Compound 5 on Tim16-Tim14 interaction



Note. MCF7 cells were co-transfected with LgBiT-Tim16 and SmBiT-Tim14, both -C terminal tagged. Luminescence was measured in untreated cells, Compound 5-treated cells and mock-transfected (vector only).

CONCLUSIONS

Magmas is ubiquitously expressed in eukaryotic cells, which is involved at least in GM-CSF signal transduction, one of many growth factors that affect survival, growth, and differentiation of hematopoietic cells (180, 185). However, deregulation on expression levels of this gene has been linked to several tumour pathologies. It has been demonstrated that high levels of Magmas protect cells from apoptotic stimuli (167, 188). Previous studies in rat GH/PRL secreting pituitary adenoma cell line demonstrated that inhibition occurs by influencing Bax and Bcl-2 modulation, thus hampering CytC release from mitochondria. Magmas overexpression was also associated to increased cell proliferation. In addition, its protective effect towards apoptosis occurs only in presence of pro-apoptotic stimuli, whereas it does not influence spontaneous programmed cell death(185). Magmas encodes for Tim16, a member of TIM23 complex. Tim16 functionally forms a heterodimer with Tim14 to drive proteins from the intermembrane space into the mitochondrial matrix (190).

A chemical inhibitor of Tim16, named Compound 5, was synthesised and its ability to stimulate chemoresistant cells to apoptotic stimuli was evaluated. Previous studies on TT cell line established that Compound 5 alone did not affect cell viability, while it was able to enhance pro-apoptotic stimuli induced by Staurosporine (188). In the present study, we aimed to verify if Compound 5 acts through inhibition of Tim16-Tim14 interaction using the NanoBiT protein-protein interaction system. Tim16 and Tim14 interaction was confirmed only when LgBiT-Tim16 and SmBiT-Tim14 were -C terminal tagged, and Compound 5 significantly disrupted the physical interaction between Tim16 and Tim14.

Preliminary studies have shown that the ability of Compound to reduce Tim16 expression is enhanced by Compound 5 only in neoplastic cell lines but not in normal cell line. Altogether, these results indicate that Compound 5 does not affect cell viability, while it is capable of sensitising pro-apoptotic stimuli, probably by inhibiting Tim16 and preventing dimerization with Tim14 as shown herein.

CHAPTER 3

NGS IN THE PREOPERATIVE DIAGNOSIS OF INDETERMINATE THYROID NODULES

INTRODUCTION

Thyroid nodules

Thyroid nodules (TNs) are common entities frequently discovered during physical examination or, accidentally, during imaging procedures. The majority of TNs are benign and the clinical challenge is to accurately classify malignant nodules that need surgical attention from benign ones. The use of fine needle aspiration (FNA) biopsy, ultrasound guidance and The Bethesda System for Reporting Thyroid Cytopathology (TBSRTC) allow for accurate diagnosis in 60-80% of all nodules. TBSRTC is a standardised system used to report the results of FNA biopsy. It was first published in 1991 and has since been revised several times, with the most recent update published in 2017 (191). The Bethesda System is used to provide a consistent and standardised way of communicating the findings of a thyroid FNA to clinicians and patients. The Bethesda System divides thyroid FNA results into six categories:

- Negative for malignancy
- Benign follicular neoplasm
- Suspicious for a follicular neoplasm
- Suspicious for malignancy
- Malignant
- Cannot be classified

Each category is further divided into subcategories, which provide additional information about the findings of the FNA. For example, the "malignant" category is divided into subcategories such as papillary thyroid carcinoma (PTC) and follicular thyroid carcinoma (FTC).

Accurate distinction between benign nodules from cancer is extremely important for correct patient management. However, 10-20% of thyroid FNAs are not easily classified into benign or malignant categories and yield an indeterminate cytologic diagnosis defined as Atypia of Undetermined Significance (AUS) or Follicular Lesion of Undetermined Significance (FLUS), also known as Bethesda III category. AUS and FLUS describe FNA results that are not clearly benign or malignant but have cytological features that are not specific enough to classify them into one of the other categories. AUS is used to describe FNA results that show atypical cells, but the atypia is not sufficient to classify the sample as suspicious for a follicular neoplasm or suspicious for malignancy. AUS is considered a "grey zone" category, and it is often difficult to determine the clinical significance of AUS findings based on cytology alone. Additional studies, such as immunohistochemistry or molecular testing, may be needed to determine the significance of the atypia. FLUS is used to describe FNA results that show follicular cells, but the cytological features are not specific enough to classify the sample as benign or suspicious for a follicular neoplasm. Like AUS, FLUS is considered a "grey zone" category, and further evaluation may be needed to determine the clinical significance of the findings.

Each TBSRTC category has an implied cancer risk that helps clinical guidance, ranging from 0-3% for benign nodules to 100% for carcinomas. According to the BSRTC, the risk for malignancy for AUS/FLUS is 5-15%, whereas the risk for Bethesda IV category, Follicular Neoplasm (FN) or Suspicious for a Follicular Neoplasm (SFN), is 15-30%. Nevertheless, the real malignancy rate of Bethesda III and IV categories is difficult to ascertain and varies among laboratories because only a minority of patients undergo surgery and, therefore, histopathological analysis of the lesion is not available. Recommendations for both AUS/FLUS and FN/SFN are controversial and include repeating FNA after 6 months, thyroidectomy or clinical follow-up. Advancements in molecular biology allowed for the identification of genetic alterations associated with thyroid cancer (TC) that may assist clinical practice in the management of controversial FNAs.

Epidemiology

TNs are common findings in the general population, and their prevalence increases with age. According to a meta-analysis of epidemiological studies, the overall prevalence of TNs is

approximately 4-7% in the general population, but it can be as high as 50% in certain subgroups such as older individuals and individuals with a history of radiation exposure .

Thyroid nodules can be benign or malignant, and the risk of malignancy varies depending on various factors such as the patient's age, the size and location of the nodule, and the presence of other risk factors for thyroid cancer. The majority of thyroid nodules are benign, and the risk of malignancy is generally low. However, the risk of malignancy increases with the size of the nodule, and larger nodules are more likely to be malignant than smaller ones. The most common type of thyroid cancer is papillary thyroid cancer, which accounts for approximately 80% of all thyroid cancers. Papillary thyroid cancer is more common in women than in men and tends to occur in younger individuals. The incidence of papillary thyroid cancer has been increasing in recent years, although it is not clear why this is the case. Other types of thyroid cancer, such as follicular thyroid cancer and medullary thyroid cancer, are less common but tend to have a higher risk of recurrence and metastasis.

Risk factors for thyroid nodules and thyroid cancer include a family history of thyroid cancer, a personal history of radiation exposure, and certain genetic conditions such as multiple endocrine neoplasia type 2 (MEN2). Other risk factors for thyroid cancer include a history of goitre (enlargement of the thyroid gland) and a history of benign thyroid conditions such as thyroiditis or thyroid nodules.

Diagnosis & Management

The diagnosis and management of TN typically involves a combination of clinical evaluation, laboratory testing, and imaging studies. The first step in the evaluation of a TN is a thorough history and physical examination. The healthcare provider will ask about the patient's symptoms and medical history, including any family history of TC or other thyroid conditions. The provider will also perform a physical examination of the thyroid gland, looking for any signs of nodules or other abnormalities. If a thyroid nodule is detected during the physical examination, they may recommend further evaluation, including thyroid function tests and imaging studies. Thyroid function tests, such as thyroid-stimulating hormone (TSH) and thyroxine (T4) levels, can help to determine whether the thyroid gland is functioning normally. Imaging studies, such as ultrasound or thyroid scintigraphy, can be

used to visualize the thyroid gland and to identify the presence and location of thyroid nodules.

If the results of the initial evaluation suggest the possibility of a TN, the next step is typically the execution of a FNA biopsy. FNA is a procedure in which a thin needle is used to obtain a small sample of cells from the TN. The sample is then examined under a microscope to determine the nature of the nodule. FNA is generally considered to be a safe and reliable method for evaluating TNs, and it is often the most cost-effective way to determine whether a nodule is benign or malignant.

Depending on the results of the initial evaluation and the subsequent diagnostic testing. If the nodule is benign, the healthcare provider may recommend a follow-up visit to monitor the nodule for any changes. If the nodule is malignant or if there is a high risk of malignancy based on the results of the FNA, the healthcare provider may recommend surgery to remove the nodule or a portion of the thyroid gland. In some cases, radioactive iodine therapy may be recommended after surgery to destroy any remaining thyroid tissue and to reduce the risk of recurrence.

Molecular Testing

Molecular testing of FNA biopsy is a diagnostic approach that involves analysing the genetic makeup of TNs using molecular techniques such as polymerase chain reaction (PCR) and NGS, which can be used to identify genetic abnormalities that may be associated with an increased risk of malignancy. One of the main indications for FNA molecular testing is the evaluation of TNs that are classified as indeterminate by cytology, meaning that the results of the FNA are not clearly benign or malignant. FNA molecular testing can help to provide additional information about the nature of indeterminate nodules and guide the management of these cases. In fact, 67% of TC have one of common genetic alterations such as BRAF and RAS point mutations and RET/PTC, PAX8/PPAR γ , TK and ALK rearrangements. The predominant mutation in BRAF gene is represented by the V600E variant which is found in approximately 40% of papillary thyroid carcinomas (PTC). Molecular testing for this variant has shown to be a valuable tool to identify malignant nodules (high specificity) though it is not able to rule out cancer with enough certainty in most cases, showing <60% sensitivity.

RAS mutations and RET/PTC rearrangements, on their part, exhibit even lower sensitivity (4.2% and 15.3%, respectively).

Currently there are several commercially available genetic tests that can be used to evaluate TNs. These tests are typically performed on samples obtained by FNA biopsy and can be used to identify genetic abnormalities that may be associated with an increased risk of malignancy. With improving technology, NGS provides parallel high-throughput alternative to assess multiple targets of the genome. Different NGS platforms that use different technologies have been developed in the last decade. Bioinformatics is later used to analyse these sequences, mapping them to the human genome. Consequently, there are several potential uses of NGS from basic research to the clinical practice. As tumour cells accumulate somatically mutations, NGS allows for the identification of numerous genomic alterations simultaneously which may be further compared to normal tissue DNA or liquid biopsy for example, providing a picture of the tumour genetic landscape. NGS has improved both diagnosis and prognosis as many biomarkers have been identified through this technique, including biomarkers for drug response. It can be used to sequence whole genomes, exomes, transcriptomes or hot-spot genes for a specific disease from tissue DNA, liquid biopsy or single cell DNA. It depends on the set goals.

Some of the commercially available genetic tests for TNs include: Afirma Gene Expression Classifier (GEC), ThyroSeq v2, Thyroid FNA Analysis (TFA) and ThyGenX/ThyraMIR. The Afirma GEC is a gene expression test that uses microarray technology to analyse messenger RNA expression of 167 genes, optimized to recognize AUS/FLUS nodules presenting a benign expression profile. Multicentre prospective studies using the Afirma GEC have demonstrated that this test has finer potential to rule out cancer better than point mutation analyses, showing 90% sensitivity and 52% specificity(192). ThyroSeq (193) is an NGS-based test that analyses the DNA and RNA of TNs to identify genetic abnormalities that may be associated with an increased risk of malignancy. Several mutational panels that include genetic alterations identified in TC have been reported to aid the TC clinical management. Nikiforova et. al developed the ThyroSeq custom panel, designed to target 284 hotspot mutations in 12 genes (*BRAF*, *KRAS*, *HRAS*, *NRAS*, *RET*, *CTNNB1*, *PIK3CA*, *PTEN*, *TSHR*, *AKT1*, *TP53* and *GNAS*) that occur in TC. Following, version 2 of this targeted NGS panel (ThyroSeq v2 (193)) included point mutations in 13 genes and 42 types of gene fusions. In addition to the first mutational panel, ThyroSeq v2 included primers for detecting

the cytosine-to-thymine mutation 228 and 250 hotspots of the telomerase transcriptase (TERT) gene promoter, 38 types of RET fusion genes and other fusions found in TC. Few studies have assessed the performance of this multi-gene NGS assay which reports, for a prevalence of 26.9%, 90% sensitivity, 93% specificity, a positive predictive value (PPV) of 83% and a negative predictive value (NPV) of 96% in internal validation studies (194). Inasmuch as the population malignancy prevalence may alter test performance, it is important to validate within different patient population before accepting generalized use of ThyroSeq panels or other molecular approaches to all clinical practice. In fact, malignancy rates for indeterminate TNs are highly variable among different population, ranging from 5-40%. In these settings, Taye et. al analysed retrospectively 156 Bethesda III and IV TNs with the use of ThyroSeq v2 panel (195). The reported prevalence of malignancy in their population was 10-30%. Thyroseq v2 performance in this cohort exhibited high NPV value of >95%, 89% sensitivity, low PPV of 22%, and 43% specificity. Performance results in this study are consistent with a rule-out test. Moreover, the ability of ThyroSeq v2 to identify accurately malignant nodules in this study was inferior of that reported for GEC microarray-based assay (192). Another study by Livhits et. al compared test performance of both GEC and ThyroSeq v2. This study analysed 149 Bethesda III and IV nodules that were randomly assigned to GEC or Thyroseq v2 assay (192). Malignancy prevalence in their study was 13.9% and both assays performed 100% sensitivity and NPV. On the contrary, GEC reported a specificity of 52% and 38% PPV in conformity with other validation studies, whereas ThyroSeq v2 displayed higher specificity (60%) and PPV (57%). Interestingly, Authors explain the fact surgery was performed in only 53 nodules, 30 tested with GEC and 23 with ThyroSeq v2 and hence, histopathological analysis confirmation was not available for all negative samples. Therefore, some patients with a negative molecular test could represent a false negative, resulting in decreased sensitivity and NPV.

AIMS

Considering ThyroSeq knowledge, the aim of this study was to validate and apply a custom multi-gene NGS panel designed for TC diagnosis and verify if such panel may be used to correctly stratify PTC and follicular thyroid carcinomas (FTC) in the grey zone of the indetermined thyroid nodules.

MATERIALS & METHODS

Study Cohort

From January 2007 to June 2018, at the Section of Endocrinology of the University of Ferrara, 14686 nodules from 11996 patients underwent FNA biopsy. Among these, 1212 nodules were classified as indeterminate cytology and 268 were suspicious for neoplasm, which fall into Bethesda III and IV categories after recent TBSRTC reports. Of the 1480 nodules classified as AUS/FLUS or FN/SFN, 464 patients underwent surgery and histopathological confirmation of the lesion was available. The study consisted of 72 FNAs yielding AUS/FLUS, FN/SFN or adenomas cytological analysis. Samples were randomly selected using R software, considering ThyroSeq v2 performance statistics and our Centre malignancy rates. In summary, 39 benign nodules, 22 PTC and 11 FTC from 72 patients were retrospectively analysed to assess the performance of our Centre custom multi-gene test.

DNA extraction from cytology samples

Whenever FNA biopsy is requested, samples are obtained using a syringe with a 22-gauge needle passed three to four times. Material from the needle is prepared for cytology, whereas needle washing in normal saline, if requested, is sent for molecular analysis at the laboratory of Endocrinology of the University of Ferrara. Samples are centrifuged, pellet resuspended in new physiological solution and stored at -20°C FNA bank.

For this study, when FNA sample was available at the FNA bank, genomic DNA was extracted using the QIamp micro kit (Qiagen, Germantown, MD, USA) following the manufacturer's protocol. For those specimens that did not arrive in the same way at the laboratory of Endocrinology, cytology slides were kindly provided by the Section of Pathology of the University of Ferrara and DNA was extracted using the FFPE QIamp kit (Qiagen, Germantown, MD, USA). Briefly, slides were scraped and FFPE material was resuspended in buffer and proteinase K. The mixture was then vortexed and incubated overnight at 58°C for complete lysis. The next day samples were treated according to the manufacturer's instructions.

Multi-gene NGS panel design

The custom primers were design using the Ion AmpliSeq Designer tool from ThermoFisher Scientific. The NGS panel designed contained primers for the amplification of 188 genomic

Table 13 *NGS panel*

Gene ID	Region	Chromosome	Start	End
NRAS	Exons 1, 2 and 3	chr1	115259357	115259512
			115259357	115259512
			115259357	115259512
PI3KCA	Exon 9 and 20	chr3	178928212	178928371
			178948011	178948170
TERT	Exons	chr5		
BRAF	Exon 15	chr7	140453075	140453194
RET	Exons 8, 10, 11, 13, 14, 15 and 16	chr10	43607547	43607673
			43609006	43609126
			43609929	43610188
			43613820	43613930
			43607439	43607861
			43615528	43615653
			43617394	43617465
MEN1	Coding sequence	chr11		
AIP	Coding sequence	chr11		
HRAS	Exons 1, 2 and 3	chr11	535390	535557
			534210	534383
			533764	533954
CDKN1B	Exons	chr12		
KRAS	Exons 1, 2 and 3	chr12	25377149	25377925
			25377149	25377925
			25377149	25377925
PTEN	Exons 5, 6, 7 and 8	chr12	25377149	25377925
			25377149	25377925
			25377149	25377925
			25377149	25377925
TSHR	Exon 10	chr14	81606023	81606211
AKT1	Exon 3	chr14	105246196	105246630
TP53	Coding sequence	chr17		
GNAS	Exons 8 and 9	chr20	57468736	57476426
			57468736	57476426

regions of interest (**Table 13**), divided in two primer pools of 91 and 97 amplicons. Briefly, 10 ng of DNA per reaction of multiplex Polymerase Chain Reaction (PCR) was amplified using the premixed primer pool and the Ion AmpliSeq™ HiFi Master Mix (Ion AmpliSeq™ Library Kit 2.0). Amplified amplicons were partially digested and purified. The obtained libraries were then barcoded and quantified for further clonal PCR. Emulsion PCR was carried out for clonal amplification using the Ion Sphere™ particles scaffold (Ion PGM HI-Q View OT2). The obtained template was purified and later sequenced with the Personal Genome Machine™ Sequencer (Ion Torrent) using the Ion PGM HI-Q View Sequencing reagent according to manufacturer’s instructions.

After library quality control 56 FNA (34 benign nodules, 14 PTC and 8 FTC) were successfully sequenced and the raw signal data were analysed with the Torrent Suite v5.10 which included signalling processing, base calling, alignment to human genome 19 reference and variant calling. For quality control, samples with a genotyping rate >95% and <2 missing genotypes were included for further analysis.

Determining Sensitivity, Specificity, and Predictive Values

To evaluate the performance of the NGS panel as diagnostic test, we calculated several key parameters, including positive predictive value (PPV), negative predictive value (NPV), sensitivity, specificity, and accuracy, which are better explained in **Table 14**.

Table 14 *Definition of performance parameters used to describe diagnostic tests*

Sensitivity	Proportion of true positive results among all positive cases. It indicates the ability of the test to correctly identify positive cases.
Specificity	Proportion of true negative results among all negative cases. It indicates the ability of the test to correctly identify negative cases.
Positive predictive value (PPV)	Proportion of true positive results among all test results that are positive. It indicates the likelihood that a positive test result is a true positive.
Negative predictive value (NPV)	Proportion of true negative results among all test results that are negative. It indicates the likelihood that a negative test result is a true negative.
Accuracy	Proportion of true results (both positive and negative) among all results. It indicates the overall reliability of the test.

Calculations were performed with the aid of 2x2 contingency **Table 15**.

PPV and NPV were calculated using the following formulas:

$$PPV = a / (a+b) \text{ and } NPV = c / (c+d).$$

Sensitivity and specificity were calculated as:

$$\text{Sensitivity} = a / (a + d) \text{ and } \text{Specificity} = c / (c + d).$$

Finally, the accuracy was calculated with the following formula:

$$\text{Accuracy} = (a + c) / (a + b + c + d)$$

Table 15 Contingency matrix used for deriving sensitivity, specificity, PPV and NPV

	Malignant TN	Benign TN
Positive test	True positives a	False positives b
Negative test	True negatives c	False negatives d

Principal Component Analysis

We performed principal component analysis (PCA) using the PLINK software (196). PLINK is a widely used tool for the analysis of large-scale genetic data sets, and it has built-in functions for performing PCA. To begin the analysis, we first imported the genotypic data into PLINK. This data consisted of single nucleotide polymorphisms (SNPs) genotyped in a sample of individuals. We then used the "pca" command in PLINK to compute the principal components of the data. The "pca" command has a number of optional parameters that can be used to customize the analysis, such as the number of principal components to compute and the method used to centre and scale the data. We used the default settings for these parameters in our analysis. The output of the PCA was a set of principal components, which we visualized using a scatterplot. The scatterplot allowed us to examine the distribution of the individuals in the sample along the different principal components, and to identify any patterns or trends in the data.

Logistic regression

PLINK and R software (197) were used to compute logistic regression, two widely used software packages for statistical analysis. Overall, logistic regression is a powerful tool for examining the association between a genetic data set and disease status, and it can provide valuable insights into the underlying biological mechanisms involved in the development of a particular disease. The "logistic" command was used in PLINK to fit a logistic regression model to the data. The output of the logistic regression analysis included estimates of the odds ratios and p-values for each SNP, which allowed us to assess the strength of the association between each SNP and disease status. To perform the analysis in R, we first imported the genotypic data and disease status into the software as a data frame. We then used the "glm" function in R to fit a logistic regression model to the data. The output of the logistic regression analysis included estimates of the coefficients and p-values for each SNP that were used to compute the odds ratio.

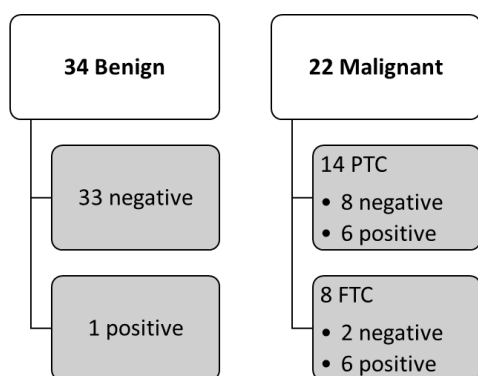
RESULTS

NGS panel as rule-out test

We evaluated the performance of our NGS-based panel as a diagnostic tool through the estimation of the performance parameters sensitivity, specificity, PPV, NPV, and accuracy. The results are summarized in the table below (**Table 16**). The histological status of the 56 samples analysed was known: 34 nodules were benign and 22 were malignant (14 PTC and 8 FTC). Among malignant nodules 8 PTC were negative and 6 were positive for genetic mutations, whereas in the FTC group 6 were true positives and 2 were negative. Only one benign sample resulted mutated in the benign group (**Figure 25**).

The calculated sensitivity in detecting TN malignancy was 54%, meaning that it was able to correctly identify 12 out of the 22 malignant nodules. Of these, 6 were PTC and 6 were FTC. In terms of specificity, the used panel was able to correctly identify 33 out of the 34 benign nodules, which means a specificity of 97% **Table 16**.

Figure 25
Schematic representation of the test results



Note: PTC=papillary thyroid carcinoma, FTC=follicular thyroid carcinoma.

Table 16 Performance of the NGS panel used as a diagnostic tool

Performance Parameter	Value (%)
Sensitivity	54.54
Specificity	97.06
PPV	92.31
NPV	76.74
Accuracy	80.36

Logistic regression results

Our analysis using logistic regression found strong associations between genetic data and TN phenotype. As expected, the single nucleotide polymorphism (SNP) rs113488022 (BRAF V600E variant) was found to be strongly associated with PTC, with an odds ratio (OR) of 41 ($p=0.002$). In fact, 5 of the 6 mutated PTC had this genetic variant. On the other hand, FTC did not associate with any known RAS variant; only 2 of the 6 mutated FTC presented the NRAS Q61 variant described by rs121913254 SNP. However, FTC was found to be associated with three SNPs: rs2699895, rs540012, and an intronic non-reported variant of the HRAS gene. The odds ratios for these SNPs were 3.97, 3.328, and 43.27, respectively, with corresponding p-values of 0.01, 0.03, and 0.005.

The magnitude of the odds ratios observed in our analysis suggest a strong association between these genetic variants and respective phenotype. It is worth noting that rs2699895

refers to an intronic variant (intron 5) of PI3K gene, which belong to a haplotype block that has been reported in triple-negative breast cancer in women from North-eastern Mexico (198). Along with the non-reported intronic variant of HRAS gene, these variants could have a potential role as long non-coding RNA and could be further analysed.

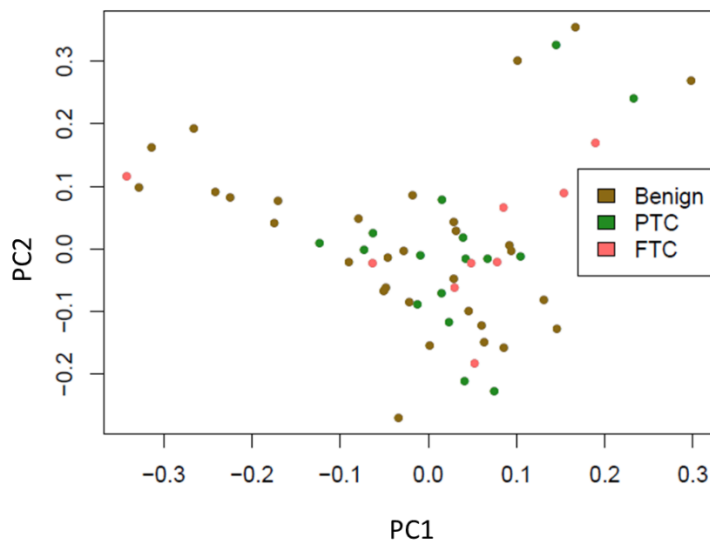
Overall, these findings provide valuable insight into the genetic basis of thyroid diseases and may have implications for the development of personalized treatment approaches. Further studies will be necessary to replicate and expand upon these results.

PCA results

PCA was performed to verify if there were distinct genetic patterns that would allow for differentiating the three phenotypes considered. Notwithstanding the different genetic variants associated with each phenotype, PTC, FTC, and benign nodules share common variants, and the differences found were not able to specifically describe them (**Figure 26**).

Figure 26

Principal component analysis



CONCLUSIONS

Thyroid Nodules are lumps that can form in the thyroid gland, which are usually benign and do not cause any symptoms. However, some TNs may be cancerous and need to be treated. The TBSRTC system is a standardised classification system used to report the results of FNA biopsy of TNs. The Bethesda III category, also known as the "grey zone," is used to describe TNs with FNA biopsy results that are indeterminate and cannot be confidently classified as benign or malignant based on the cytological features observed.

In this study, we aimed to evaluate the performance of our NGS-based panel as a diagnostic tool for thyroid nodules. Various performance parameters including sensitivity, specificity, positive predictive value, negative predictive value, and accuracy were calculated. We found that the panel had a sensitivity of 54% for detecting malignancy in TNs, meaning it was able to correctly identify 12 out of the 22 malignant nodules in our sample. It also had a high specificity of 97%, correctly identifying 33 out of the 34 benign nodules, and therefore could be a useful "rule-out" tool in the diagnosis of TN malignancy, allowing it to eliminate the need for further testing or treatment. This is an important consideration in the management of TN, as it can help reduce unnecessary interventions and improve patient outcomes. Further studies with larger sample sizes and a wider range of TN types may be needed to fully evaluate the utility of NGS in this setting.

In addition to evaluating the performance of the panel, we also analysed the genetic basis of thyroid diseases by examining the associations between genetic variants and TC phenotypes. We found strong associations between certain genetic variants and specific TC phenotypes, which may have implications for the development of personalized treatment approaches. However, further research is needed to replicate and expand upon these findings.

We also conducted a PCA to determine if there were distinct genetic patterns that would allow for differentiation between the three TN phenotypes considered in this study. PCA did not show any significant variation between PTC, FTC, and benign nodules, indicating the heterogeneous nature of TNs. However, we did find genetic alterations in intronic regions of PI3KCA and HRAS genes that were significantly associated with our population of FTCs, showing an odds ratio >15 and $p > 0.001$. Further analysis, including the use of additional genetic markers, may be needed to fully understand the genetic basis of thyroid diseases.

Our results indicate that FNA samples with Bethesda III or IV cytological analysis show genetic alterations in intronic regions of PI3KCA and HRAS genes in 16% of the samples and associate with a final histology consistent with FTCs. Several groups have developed Genetic Classifiers for thyroid cancer in order to increase sensitivity and specificity of molecular testing. However, unknown and/or intronic genetic alterations are usually discarded. We found an intronic HRAS point mutation that was strongly and positively associated with FTC phenotype that should be investigated for its' potential predictive value. Overall, the results of this study demonstrate the utility of NGS in the diagnosis of TN malignancy, particularly in the identification of benign nodules. Further research is needed to determine the optimal use of NGS in clinical practice and to explore the potential for improved sensitivity and specificity.

OVERALL CONCLUSIONS

The three chapters of this thesis have addressed different aspects of molecular biology in BCs, TNs, and the mechanism of action of a small inhibitor called Compound 5. Through the examination of various molecular and cellular processes, this research aimed to gain a deeper understanding of the underlying mechanisms driving the development and progression of these diseases.

Chapter one focused on the challenges of treating resistant BC and the differences between TBC and ABC. We found that concomitant targeting of PI3K/mTOR and TGF- β pathways in TBC may improve the progression-free survival in patients with advanced typical carcinoids. Chapter two examined the mechanism of action of a chemical inhibitor, Compound 5, which has shown to enhance the sensitivity of chemoresistant cells to pro-apoptotic stimuli. Our findings indicated that Compound 5 may sensitize cells to pro-apoptotic stimuli by disrupting the physical interaction between Tim16 and Tim14. Chapter three explored the use of next- NGS to diagnose TNs and identified genetic alterations in intronic regions of the PI3KCA and HRAS genes in samples with Bethesda III or IV cytological analysis, which associated with the FTC phenotype. These results highlight the potential for NGS in the diagnosis of TNs and the importance of considering unknown or intronic genetic alterations in molecular testing.

In summary, while these three topics may initially seem unrelated, they highlight the importance of targeting specific proteins and pathways, identifying ways to overcome chemoresistance, and utilizing advanced technologies such as NGS to improve the treatment and diagnosis of cancer, which might have important implications for the development of new therapeutic strategies and diagnostic tools for BCs, TNs and other cancer types.

REFERENCES

1. Pearse AGE. The diffuse neuroendocrine system: an extension of the APUD concept. *Co-Transmission* 1982. (doi:10.1007/978-1-349-06239-3_10)
2. Montuenga LM, Guembe L, Burrell MA, Bodegas ME, Calvo A, Sola JJ, Sesma P, & Villaro AC. The diffuse endocrine system: From embryogenesis to carcinogenesis. *Progress in Histochemistry and Cytochemistry* 2003. (doi:10.1016/s0079-6336(03)80004-9)
3. Basu B, Sirohi B, & Corrie P. Systemic therapy for neuroendocrine tumours of gastroenteropancreatic origin. *Endocrine-Related Cancer* 2010. (doi:10.1677/ERC-09-0108)
4. Rosai J. The origin of neuroendocrine tumors and the neural crest saga. *Modern Pathology* 2011. (doi:10.1038/modpathol.2010.166)
5. Pearse AGE, Polak JM, Rost FWD, Fontaine J, Lièvre C Le, & Douarin N Le. Demonstration of the neural crest origin of type I (APUD) cells in the avian carotid body, using a cytochemical marker system. *Histochemie* 1973. (doi:10.1007/BF00303435)
6. Day R & Salzet M. The neuroendocrine phenotype, cellular plasticity, and the search for genetic switches: Redefining the diffuse neuroendocrine system. *Neuroendocrinology Letters* 2002.
7. Champaneria MC, Modlin IM, Kidd M, & Eick GN. Friedrich Feyrter: A precise intellect in a diffuse system. *Neuroendocrinology* 2006. (doi:10.1159/000096050)
8. Herrera-Martínez AD, Hofland LJ, Gálvez Moreno MA, Castaño JP, Herder WW De, & Feelders RA. Neuroendocrine neoplasms: Current and potential diagnostic, predictive and prognostic markers. *Endocrine-Related Cancer* 2019. (doi:10.1530/ERC-18-0354)
9. Modlin I, Oberg K, & Chung D. Gastroenteropancreatic neuroendocrine tumours. *The lancet oncology* 2008. pp 61–72.

10. Oberndorfer S. Frankfurter Zeitschrift für Pathologie: Karzinoide Tumoren des Dünndarms. *Search* 1907.
11. Modlin IM, Shapiro MD, & Kidd M. Siegfried oberndorfer: Origins and perspectives of carcinoid tumors. *Human Pathology* 2004. (doi:10.1016/j.humpath.2004.09.018)
12. Williams ED & Sandler M. THE CLASSIFICATION OF CARCINOID TUMOURS. *The Lancet* 1963. (doi:10.1016/S0140-6736(63)90951-6)
13. Masson P. Carcinoids (Argentaffin-Cell Tumors) and Nerve Hyperplasia of the Appendicular Mucosa. *The American journal of pathology* 1928.
14. Barnard WG. The nature of the “oat-celled sarcoma” of the mediastinum. *The Journal of Pathology and Bacteriology* 1926. (doi:10.1002/path.1700290304)
15. MCKEOWN F. Oat-cell carcinoma of the oesophagus. *The Journal of pathology and bacteriology* 1952. (doi:10.1002/path.1700640420)
16. Hajdu SI & Tang P. A note from history: The saga of carcinoid and oat-cell carcinoma. *Annals of Clinical and Laboratory Science* 2008.
17. Bensch KG, Corrin B, Pariente R, & Spencer H. Oat-cell carcinoma of the lung. Its origin and relationship to bronchial carcinoid. *Cancer* 1968. (doi:10.1002/1097-0142(196811))
18. Pearse AG. The cytochemistry and ultrastructure of polypeptide hormone-producing cells of the APUD series and the embryologic, physiologic and pathologic implications of the concept. *The journal of histochemistry and cytochemistry : official journal of the Histochemistry Society* 1969. (doi:10.1177/17.5.303)
19. Sippel RS & Chen H. Carcinoid Tumors. *Surgical Oncology Clinics of North America* 2006. (doi:10.1016/j.soc.2006.05.002)
20. Savu C, Melinte A, Diaconu C, Stiru O, Gherghiceanu F, Tudorica Ștefan, Dumitrașcu O, Bratu A, Balescu I, & Bacalbasa N. Lung neuroendocrine tumors: A systematic literature review (Review). *Experimental and Therapeutic Medicine* 2021. (doi:10.3892/etm.2021.11099)

21. Hirsch F, Hansen HH, Dombernowsky P, & Hainau B. Bone-marrow examination in the staging of small-cell anaplastic carcinoma of the lung with special reference to subtyping: An evaluation of 203 consecutive patients. *Cancer* 1977. (doi:10.1002/1097-0142(197706).)
22. Hattori S, Matsuda M, Tateishi R, Nishihara H, & Horai T. Oat-cell carcinoma of the lung. Clinical and morphological studies in relation to its histogenesis. *Cancer* 1972. (doi:10.1002/1097-0142(197210))
23. Rosai J, Levine G, Weber WR, & Higa E. Carcinoid tumors and oat cell carcinomas of the thymus. *Pathology Annual* 1976.
24. Mills SE, Cooper PH, Walker AN, & Kron IL. Atypical carcinoid tumor of the lung. A clinicopathologic study of 17 cases. *American Journal of Surgical Pathology* 1982. (doi:10.1097/00000478-198210000-00006)
25. Warren WH, Memoli VA, & Gould VE. Immunohistochemical and ultrastructural analysis of bronchopulmonary neuroendocrine neoplasms. II. Well-differentiated neuroendocrine carcinomas. *Ultrastructural Pathology* 1984. (doi:10.3109/01913128409141476)
26. Soga J & Tazawa K. Pathologic analysis of carcinoids Histologic re evaluation of 62 cases. *Cancer* 1971. (doi:10.1002/1097-0142)
27. Ito T, Nakatani Y, Nagahara N, Ogawa T, Shibagaki T, & Kanisawa M. Quantitative study of pulmonary endocrine cells in anencephaly. *Lung* 1987. (doi:10.1007/BF02714446)
28. Williams ED & Sandler M. The Classification of Carcinoid Tumours. *The Lancet* 1963. (doi:10.1016/S0140-6736(63)90951-6)
29. Williams ED. Histological Typing of Endocrine Tumours. edn 1st, Ed WHO WHOWHFWO. 1980.
30. Capella C, Heitz PU, Höfler H, Solcia E, & Klöppel G. Revised classification of neuroendocrine tumours of the lung, pancreas and gut. *Virchows Archiv* 1995. (doi:10.1007/BF00199342)

31. Solcia E, Klöppel G, & Sobin LH. Histological Typing of Endocrine Tumours. In *Histological Typing of Endocrine Tumours*,2000.
32. Rindi G. 3. The ENETS Guidelines: The New TNM Classification System. *Tumori Journal* 2010 **96** 806–809. (doi:10.1177/030089161009600532)
33. Rindi G, Klöppel G, Alhman H, Caplin M, Couvelard A, Herder WW de, Eriksson B, Falchetti A, Falconi M, Komminoth P, Körner M, Lopes JM, McNicol AM, Nilsson O, Perren A, Scarpa A, Scoazec JY, & Wiedenmann B. TNM staging of foregut (neuro)endocrine tumors: a consensus proposal including a grading system. *Virchows Archiv* 2006 **449** 395–401. (doi:10.1007/s00428-006-0250-1)
34. Rindi G. 3. The ENETS Guidelines: The New TNM Classification System. *Tumori Journal* 2010 **96** 806–809. (doi:10.1177/030089161009600532)
35. Klöppel G. Classification and pathology of gastroenteropancreatic neuroendocrine neoplasms. *Endocrine-Related Cancer* 2011. (doi:10.1530/ERC-11-0013)
36. Pape U, Jann H, Müller-Nordhorn J, Bockelbrink A, Berndt U, Willich SN, Koch M, Röcken C, Rindi G, & Wiedenmann B. Prognostic relevance of a novel TNM classification system for upper gastroenteropancreatic neuroendocrine tumors. *Cancer* 2008 **113** 256–265. (doi:10.1002/cncr.23549)
37. Scarpa A, Mantovani W, Capelli P, Beghelli S, Boninsegna L, Bettini R, Panzuto F, Pederzoli P, Fave G delle, & Falconi M. Pancreatic endocrine tumors: improved TNM staging and histopathological grading permit a clinically efficient prognostic stratification of patients. *Modern Pathology* 2010 **23** 824–833. (doi:10.1038/modpathol.2010.58)
38. Dolcetta-Capuzzo A, Villa V, Albarello L, Franchi GM, Gemma M, Scavini M, Palo S di, Orsenigo E, Bosi E, Doglioni C, & Manzoni MF. Gastroenteric neuroendocrine neoplasms classification: Comparison of prognostic models. *Cancer* 2013 **119** 36–44. (doi:10.1002/cncr.27716)
39. Metovic J, Barella M, Bianchi F, Hofman P, Hofman V, Rimmelinck M, Kern I, Carvalho L, Pattini L, Sonzogni A, Veronesi G, Harari S, Forest F, Papotti M, & Pelosi G. Morphologic and molecular classification of lung neuroendocrine neoplasms. *Virchows Archiv* 2021 **478** 5–19. (doi:10.1007/s00428-020-03015-z)

40. The World Health Organization histological typing of lung tumors. *American Journal of Clinical Pathology* 1982. (doi:10.1093/ajcp/77.2.123)
41. Travis WD. Pathology of lung cancer. *Clinics in Chest Medicine* 2002. (doi:10.1016/S0272-5231(03)00061-3)
42. Travis WD, Colby T V., Corrin B, Shimosato Y, & Brambilla E. Histological Typing of Lung and Pleural Tumours. In *Histological Typing of Lung and Pleural Tumours*, 1999.
43. Travis WD Müller-Hermelink HK BE. Pathology and Genetics: Tumours of the Lung, Pleura, Thymus and Heart. *International agency for research on cancer* 2004.
44. Travis WD, Brambilla E, Burke AP, Marx A, & Nicholson AG. Introduction to the 2015 World Health Organization Classification of Tumors of the Lung, Pleura, Thymus, and Heart. *Journal of Thoracic Oncology* 2015. (doi:10.1097/JTO.0000000000000663)
45. Nicholson AG, Tsao MS, Beasley MB, Borczuk AC, Brambilla E, Cooper WA, Dacic S, Jain D, Kerr KM, Lantuejoul S, Noguchi M, Papotti M, Rekhtman N, Scagliotti G, Schil P van, Sholl L, Yatabe Y, Yoshida A, & Travis WD. The 2021 WHO Classification of Lung Tumors: Impact of Advances Since 2015. *Journal of Thoracic Oncology* 2022 **17** 362–387. (doi:10.1016/j.jtho.2021.11.003)
46. Rindi G, Mete O, Uccella S, Basturk O, Rosa S la, Brosens LAA, Ezzat S, Herder WW de, Klimstra DS, Papotti M, & Asa SL. Overview of the 2022 WHO Classification of Neuroendocrine Neoplasms. *Endocrine Pathology* 2022 **33** 115–154. (doi:10.1007/s12022-022-09708-2)
47. Yao JC, Hassan M, Phan A, Dagohoy C, Leary C, Mares JE, Abdalla EK, Fleming JB, Vauthey JN, Rashid A, & Evans DB. One Hundred Years After “Carcinoid”: Epidemiology of and Prognostic Factors for Neuroendocrine Tumors in 35,825 Cases in the United States. *Journal of Clinical Oncology* 2008 **26** 3063–3072. (doi:10.1200/JCO.2007.15.4377)
48. Hallet J, Law CHL, Cukier M, Saskin R, Liu N, & Singh S. Exploring the rising incidence of neuroendocrine tumors: A population-based analysis of epidemiology,

- metastatic presentation, and outcomes. *Cancer* 2015 **121** 589–597. (doi:10.1002/cncr.29099)
49. US National Cancer Institute. SEER Database. <http://seer.cancer.gov/>.
50. White BE, Rous B, Chandrakumaran K, Wong K, Bouvier C, Hemelrijck M van, George G, Russell B, Srirajskanthan R, & Ramage JK. Incidence and survival of neuroendocrine neoplasia in England 1995–2018: A retrospective, population-based study. *The Lancet Regional Health - Europe* 2022 **23** 100510. (doi:10.1016/j.lanepe.2022.100510)
51. Dasari A, Shen C, Halperin D, Zhao B, Zhou S, Xu Y, Shih T, & Yao JC. Trends in the incidence, prevalence, and survival outcomes in patients with neuroendocrine tumors in the United States. *JAMA Oncology* 2017. (doi:10.1001/jamaoncol.2017.0589)
52. Hauso O, Gustafsson BI, Kidd M, Waldum HL, Drozdov I, Chan AKC, & Modlin IM. Neuroendocrine tumor epidemiology: Contrasting Norway and North America. *Cancer* 2008 **113** 2655–2664. (doi:10.1002/cncr.23883)
53. Hallet J, Law CHL, Cukier M, Saskin R, Liu N, & Singh S. Exploring the rising incidence of neuroendocrine tumors: A population-based analysis of epidemiology, metastatic presentation, and outcomes. *Cancer* 2015 **121** 589–597. (doi:10.1002/cncr.29099)
54. Yao JC, Hassan M, Phan A, Dagohoy C, Leary C, Mares JE, Abdalla EK, Fleming JB, Vauthey JN, Rashid A, & Evans DB. One Hundred Years After “Carcinoid”: Epidemiology of and Prognostic Factors for Neuroendocrine Tumors in 35,825 Cases in the United States. *Journal of Clinical Oncology* 2008 **26** 3063–3072. (doi:10.1200/JCO.2007.15.4377)
55. Hallet J, Law CHL, Cukier M, Saskin R, Liu N, & Singh S. Exploring the rising incidence of neuroendocrine tumors: A population-based analysis of epidemiology, metastatic presentation, and outcomes. *Cancer* 2015 **121** 589–597. (doi:10.1002/cncr.29099)
56. Yao JC, Hassan M, Phan A, Dagohoy C, Leary C, Mares JE, Abdalla EK, Fleming JB, Vauthey JN, Rashid A, & Evans DB. One hundred years after ‘carcinoid’:

- Epidemiology of and prognostic factors for neuroendocrine tumors in 35,825 cases in the United States. *Journal of Clinical Oncology* 2008 **26** 3063–3072. (doi:10.1200/JCO.2007.15.4377)
57. Genus TSE, Bouvier C, Wong KF, Srirajaskanthan R, Rous BA, Talbot DC, Valle JW, Khan M, Pearce N, Elshafie M, Reed NS, Morgan E, Deas A, White C, Huws D, & Ramage J. Impact of neuroendocrine morphology on cancer outcomes and stage at diagnosis: a UK nationwide cohort study 2013–2015. *British Journal of Cancer* 2019 **121** 966–972. (doi:10.1038/s41416-019-0606-3)
58. Pape UF, Berndt U, Muller-Nordhorn J, Bohmig M, Roll S, Koch M, Willich SN, & Wiedenmann B. Prognostic factors of long-term outcome in gastroenteropancreatic neuroendocrine tumours. *Endocrine Related Cancer* 2008 **15** 1083–1097. (doi:10.1677/ERC-08-0017)
59. Ter-Minassian M, Chan JA, Hooshmand SM, Brais LK, Daskalova A, Heafield R, Buchanan L, Qian ZR, Fuchs CS, Lin X, Christiani DC, & Kulke MH. Clinical presentation, recurrence, and survival in patients with neuroendocrine tumors: results from a prospective institutional database. *Endocrine-Related Cancer* 2013 **20** 187–196. (doi:10.1530/ERC-12-0340)
60. Hallet J, Law CHL, Cukier M, Saskin R, Liu N, & Singh S. Exploring the rising incidence of neuroendocrine tumors: A population-based analysis of epidemiology, metastatic presentation, and outcomes. *Cancer* 2015 **121** 589–597. (doi:10.1002/cncr.29099)
61. Singh S, Granberg D, Wolin E, Warner R, Sissons M, Kolarova T, Goldstein G, Pavel M, Öberg K, & Leyden J. Patient-Reported Burden of a Neuroendocrine Tumor (NET) Diagnosis: Results From the First Global Survey of Patients With NETs. *Journal of Global Oncology* 2017 **3** 43–53. (doi:10.1200/JGO.2015.002980)
62. Leoncini E, Carioli G, Vecchia C la, Boccia S, & Rindi G. Risk factors for neuroendocrine neoplasms: a systematic review and meta-analysis. *Annals of Oncology* 2016 **27** 68–81. (doi:10.1093/annonc/mdv505)
63. Pacheco M. Multiple Endocrine Neoplasia: A Genetically Diverse Group of Familial Tumor Syndromes. *Journal of Pediatric Genetics* 2016 **05** 089–097. (doi:10.1055/s-0036-1579758)

64. Tirosh A, Sadowski SM, Linehan WM, Libutti SK, Patel D, Nilubol N, & Kebebew E. Association of *VHL* Genotype With Pancreatic Neuroendocrine Tumor Phenotype in Patients With von Hippel–Lindau Disease. *JAMA Oncology* 2018 **4** 124. (doi:10.1001/jamaoncol.2017.3428)
65. Marcos HB, Libutti SK, Alexander HR, Lubensky IA, Bartlett DL, Walther MM, Linehan WM, Glenn GM, & Choyke PL. Neuroendocrine Tumors of the Pancreas in von Hippel–Lindau Disease: Spectrum of Appearances at CT and MR Imaging with Histopathologic Comparison. *Radiology* 2002 **225** 751–758. (doi:10.1148/radiol.2253011297)
66. Mowrey K, Northrup H, Rougeau P, Hashmi SS, Krueger DA, Ebrahimi-Fakhari D, Towbin AJ, Trout AT, Capal JK, Franz DN, & Rodriguez-Buritica D. Frequency, Progression, and Current Management: Report of 16 New Cases of Nonfunctional Pancreatic Neuroendocrine Tumors in Tuberous Sclerosis Complex and Comparison With Previous Reports. *Frontiers in Neurology* 2021 **12**. (doi:10.3389/fneur.2021.627672)
67. Hofland J, Zandee WT, & Herder WW de. Role of biomarker tests for diagnosis of neuroendocrine tumours. *Nature Reviews Endocrinology* 2018 **14** 656–669. (doi:10.1038/s41574-018-0082-5)
68. Rindi G, Mete O, Uccella S, Basturk O, Rosa S la, Brosens LAA, Ezzat S, Herder WW de, Klimstra DS, Papotti M, & Asa SL. Overview of the 2022 WHO Classification of Neuroendocrine Neoplasms. *Endocrine Pathology* 2022 **33** 115–154. (doi:10.1007/s12022-022-09708-2)
69. Yasuhiro Goto MG de SATBSPALN and MSL. A novel human insulinoma-associated cDNA, IA-1, encodes a protein with ‘zinc-finger’ DNA-binding motifs. *The Journal of Biological Chemistry* 1992 **267** 15252–15257.
70. Lan MS & Breslin MB. Structure, expression, and biological function of INSM1 transcription factor in neuroendocrine differentiation. *The FASEB Journal* 2009 **23** 2024–2033. (doi:10.1096/fj.08-125971)
71. Sansone A, Lauretta R, Vottari S, Chiefari A, Barnabei A, Romanelli F, & Appetecchia M. Specific and Non-Specific Biomarkers in Neuroendocrine

- Gastroenteropancreatic Tumors. *Cancers* 2019 **11** 1113. (doi:10.3390/cancers11081113)
72. Vicentini C, Fassan M, D'Angelo E, Corbo V, Silvestris N, Nuovo G, & Scarpa A. Clinical Application of MicroRNA Testing in Neuroendocrine Tumors of the Gastrointestinal Tract. *Molecules* 2014 **19** 2458–2468. (doi:10.3390/molecules19022458)
73. Blázquez-Encinas R, Moreno-Montilla MT, García-Vioque V, Gracia-Navarro F, Alors-Pérez E, Pedraza-Arevalo S, Ibáñez-Costa A, & Castaño JP. The uprise of RNA biology in neuroendocrine neoplasms: altered splicing and RNA species unveil translational opportunities. *Reviews in Endocrine and Metabolic Disorders* 2022. (doi:10.1007/s11154-022-09771-4)
74. Raveh E, Matouk IJ, Gilon M, & Hochberg A. The H19 Long non-coding RNA in cancer initiation, progression and metastasis – a proposed unifying theory. *Molecular Cancer* 2015 **14** 184. (doi:10.1186/s12943-015-0458-2)
75. Narayanan D, Mandal R, Hardin H, Chanana V, Schwalbe M, Rosenbaum J, Buehler D, & Lloyd R v. Long Non-coding RNAs in Pulmonary Neuroendocrine Neoplasms. *Endocrine Pathology* 2020 **31** 254–263. (doi:10.1007/s12022-020-09626-1)
76. Moris D, Ntanasis-Stathopoulos I, Tsilimigras DI, Adam MA, Yang CJ, Harpole D, & Theoharis S. Insights into novel prognostic and possible predictive biomarkers of lung neuroendocrine tumors. *Cancer Genomics and Proteomics* 2018. (doi:10.21873/cgp.20073)
77. Prisciandaro M, Antista M, Raimondi A, Corti F, Morano F, Centonze G, Sabella G, Mangogna A, Randon G, Pagani F, Prinzi N, Niger M, Corallo S, Castiglioni di Caronno E, Massafra M, Bartolomeo M di, Braud F de, Milione M, & Pusceddu S. Biomarker Landscape in Neuroendocrine Tumors With High-Grade Features: Current Knowledge and Future Perspective. *Frontiers in Oncology* 2022 **12**. (doi:10.3389/fonc.2022.780716)
78. Burak GI, Ozge S, Cem M, Gulgun B, Zeynep DY, & Atil B. The emerging clinical relevance of genomic profiling in neuroendocrine tumours. *BMC Cancer* 2021 **21** 234. (doi:10.1186/s12885-021-07961-y)

79. Yachida S, Totoki Y, Noë M, Nakatani Y, Horie M, Kawasaki K, Nakamura H, Saito-Adachi M, Suzuki M, Takai E, Hama N, Higuchi R, Hirono S, Shiba S, Kato M, Furukawa E, Arai Y, Rokutan H, Hashimoto T, Mitsunaga S, Kanda M, Tanaka H, Takata S, Shimomura A, Oshima M, Hackeng WM, Okumura T, Okano K, Yamamoto M, ... Shibata T. Comprehensive Genomic Profiling of Neuroendocrine Carcinomas of the Gastrointestinal System. *Cancer Discovery* 2022 **12** 692–711. (doi:10.1158/2159-8290.CD-21-0669)
80. Bi WL, Horowitz P, Greenwald NF, Abedalthagafi M, Agarwalla PK, Gibson WJ, Mei Y, Schumacher SE, Ben-David U, Chevalier A, Carter S, Tiao G, Brastianos PK, Ligon AH, Ducar M, MacConaill L, Laws ER, Santagata S, Beroukhi R, & Dunn IF. Landscape of genomic alterations in pituitary adenomas. *Clinical Cancer Research* 2017 **23** 1841–1851. (doi:10.1158/1078-0432.CCR-16-0790)
81. Scarpa A, Chang DK, Nones K, Corbo V, Patch AM, Bailey P, Lawlor RT, Johns AL, Miller DK, Mafficini A, Rusev B, Scardoni M, Antonello D, Barbi S, Sikora KO, Cingarlini S, Vicentini C, McKay S, Quinn MCJ, Bruxner TJC, Christ AN, Harliwong I, Idrisoglu S, McLean S, Nourse C, Nourbakhsh E, Wilson PJ, Anderson MJ, Fink JL, ... Grimmond SM. Whole-genome landscape of pancreatic neuroendocrine tumours. *Nature* 2017. (doi:10.1038/nature21063)
82. Kidd M, Modlin IM, & Drozdov I. Gene network-based analysis identifies two potential subtypes of small intestinal neuroendocrine tumors. *BMC Genomics* 2014 **15** 595. (doi:10.1186/1471-2164-15-595)
83. Duerr EM, Mizukami Y, Ng A, Xavier RJ, Kikuchi H, Deshpande V, Warshaw AL, Glickman J, Kulke MH, & Chung DC. Defining molecular classifications and targets in gastroenteropancreatic neuroendocrine tumors through DNA microarray analysis. *Endocrine Related Cancer* 2008 **15** 243–256. (doi:10.1677/ERC-07-0194)
84. Modlin IM, Drozdov I, & Kidd M. The Identification of Gut Neuroendocrine Tumor Disease by Multiple Synchronous Transcript Analysis in Blood. *PLoS ONE* 2013 **8** e63364. (doi:10.1371/journal.pone.0063364)
85. Treijen MJC van, Korse CM, Leeuwaarde RS van, Saveur LJ, Vriens MR, Verbeek WHM, Tesselaar MET, & Valk GD. Blood Transcript Profiling for the Detection of

- Neuroendocrine Tumors: Results of a Large Independent Validation Study. *Frontiers in Endocrinology* 2018 **9**. (doi:10.3389/fendo.2018.00740)
86. Modlin IM, Kidd M, Malczewska A, Drozdov I, Bodei L, Matar S, & Chung KM. The NETest. *Endocrinology and Metabolism Clinics of North America* 2018 **47** 485–504. (doi:10.1016/j.ecl.2018.05.002)
87. Liu E, Paulson S, Gulati A, Freudman J, Grosh W, Kafer S, Wickremesinghe PC, Salem RR, & Bodei L. Assessment of NETest Clinical Utility in a U.S. Registry-Based Study. *The Oncologist* 2019 **24** 783–790. (doi:10.1634/theoncologist.2017-0623)
88. Kaufman HL, Russell J, Hamid O, Bhatia S, Terheyden P, D'Angelo SP, Shih KC, Lebbé C, Linette GP, Milella M, Brownell I, Lewis KD, Lorch JH, Chin K, Mahnke L, Heydebreck A von, Cuillerot JM, & Nghiem P. Avelumab in patients with chemotherapy-refractory metastatic Merkel cell carcinoma: a multicentre, single-group, open-label, phase 2 trial. *The Lancet Oncology* 2016 **17** 1374–1385. (doi:10.1016/S1470-2045(16)30364-3)
89. Mathieu L, Shah S, Pai-Scherf L, Larkins E, Vallejo J, Li X, Rodriguez L, Mishra-Kalyani P, Goldberg KB, Kluetz PG, Theoret MR, Beaver JA, Pazdur R, & Singh H. FDA Approval Summary: Atezolizumab and Durvalumab in Combination with Platinum-Based Chemotherapy in Extensive Stage Small Cell Lung Cancer. *The Oncologist* 2021 **26** 433–438. (doi:10.1002/onco.13752)
90. Gosney JR, Sissons MC, & Allibone RO. Neuroendocrine cell populations in normal human lungs: a quantitative study. *Thorax* 1988 **43** 878–882. (doi:10.1136/thx.43.11.878)
91. Gosney JR. Neuroendocrine cell populations in postnatal human lungs: Minimal variation from childhood to old age. *The Anatomical Record* 1993 **236** 177–180. (doi:10.1002/ar.1092360121)
92. Lauweryns JM, Lommel AT van, & Dom RJ. Innervation of rabbit intrapulmonary neuroepithelial bodies. *Journal of the Neurological Sciences* 1985 **67** 81–92. (doi:10.1016/0022-510X(85)90024-3)

93. Cutz E, Yeger H, Pan J, & Ito T. Pulmonary Neuroendocrine Cell System in Health and Disease. *Current Respiratory Medicine Reviews* 2008 **4** 174–186. (doi:10.2174/157339808785161314)
94. Awadalla M, Miyawaki S, Abou Alaiwa MH, Adam RJ, Bouzek DC, Michalski AS, Fuld MK, Reynolds KJ, Hoffman EA, Lin CL, & Stoltz DA. Early Airway Structural Changes in Cystic Fibrosis Pigs as a Determinant of Particle Distribution and Deposition. *Annals of Biomedical Engineering* 2014 **42** 915–927. (doi:10.1007/s10439-013-0955-7)
95. Gustafsson BI, Kidd M, Chan A, Malfertheiner M V., & Modlin IM. Bronchopulmonary Neuroendocrine Tumors. *Cancer* 2008 **113** 5–21. (doi:10.1002/cncr.23542)
96. Travis WD. Lung tumours with neuroendocrine differentiation. *European Journal of Cancer* 2009 **45** 251–266. (doi:10.1016/S0959-8049(09)70040-1)
97. Modlin IM, Lye KD, & Kidd M. A 5-decade analysis of 13,715 carcinoid tumors. *Cancer* 2003 **97** 934–959. (doi:10.1002/cncr.11105)
98. Swarts DRA, Ramaekers FCS, & Speel EJM. Molecular and cellular biology of neuroendocrine lung tumors: Evidence for separate biological entities. *Biochimica et Biophysica Acta (BBA) - Reviews on Cancer* 2012 **1826** 255–271. (doi:10.1016/j.bbcan.2012.05.001)
99. Simbolo M, Mafficini A, Sikora KO, Fassan M, Barbi S, Corbo V, Mastracci L, Rusev B, Grillo F, Vicentini C, Ferrara R, Pilotto S, Davini F, Pelosi G, Lawlor RT, Chilosi M, Tortora G, Bria E, Fontanini G, Volante M, & Scarpa A. Lung neuroendocrine tumours: deep sequencing of the four World Health Organization histotypes reveals chromatin-remodelling genes as major players and a prognostic role for TERT, RB1, MEN1 and KMT2D. *Journal of Pathology* 2017. (doi:10.1002/path.4853)
100. Araujo-Castro M, Pascual-Corrales E, Molina-Cerrillo J, Moreno Mata N, & Alonso-Gordoa T. Bronchial Carcinoids: From Molecular Background to Treatment Approach. *Cancers* 2022 **14** 520. (doi:10.3390/cancers14030520)

101. Bora M & Vithiavathi S. Primary bronchial carcinoid: A rare differential diagnosis of pulmonary koch in young adult patient. *Lung India* 2012 **29** 59. (doi:10.4103/0970-2113.92366)
102. Caplin ME, Baudin E, Ferolla P, Filosso P, Garcia-Yuste M, Lim E, Oberg K, Pelosi G, Perren A, Rossi RE, Travis WD, Bartsch D, Capdevila J, Costa F, Cwikla J, Herder W de, Delle Fave G, Eriksson B, Falconi M, Ferone D, Gross D, Grossman A, Ito T, Jensen R, Kaltsas G, Kelestimur F, Kianmanesh R, Knigge U, Kos-Kudla B, ... Zheng-Pei Z. Pulmonary neuroendocrine (carcinoid) tumors: European Neuroendocrine Tumor Society expert consensus and recommendations for best practice for typical and atypical pulmonary carcinoids. *Annals of Oncology* 2015 **26** 1604–1620. (doi:10.1093/annonc/mdv041)
103. Zatelli MC, Fanciulli G, Malandrino P, Ramundo V, Faggiano A, & Colao A. Predictive factors of response to mTOR inhibitors in neuroendocrine tumours. *Endocrine-Related Cancer* 2016. (doi:10.1530/ERC-15-0413)
104. Zatelli MC, Grossrubatscher EM, Guadagno E, Sciammarella C, Faggiano A, & Colao A. Circulating tumor cells and mirnas as prognostic markers in neuroendocrine neoplasms. *Endocrine-Related Cancer* 2017. (doi:10.1530/ERC-17-0091)
105. Herrera-Martínez AD, Hofland J, Hofland LJ, Brabander T, Eskens FALM, Gálvez Moreno MA, Luque RM, Castaño JP, Herder WW de, & Feelders RA. Targeted Systemic Treatment of Neuroendocrine Tumors: Current Options and Future Perspectives. *Drugs* 2019. (doi:10.1007/s40265-018-1033-0)
106. Oronsky B, Ma PC, Morgensztern D, & Carter CA. Nothing But NET: A Review of Neuroendocrine Tumors and Carcinomas. *Neoplasia* 2017 **19** 991–1002. (doi:10.1016/j.neo.2017.09.002)
107. Travis WD, Brambilla E, Nicholson AG, Yatabe Y, Austin JHM, Beasley MB, Chirieac LR, Dacic S, Duhig E, Flieder DB, Geisinger K, Hirsch FR, Ishikawa Y, Kerr KM, Noguchi M, Pelosi G, Powell CA, Tsao MS, & Wistuba I. The 2015 World Health Organization Classification of Lung Tumors: Impact of Genetic, Clinical and Radiologic Advances since the 2004 Classification. *Journal of Thoracic Oncology* 2015. (doi:10.1097/JTO.0000000000000630)

108. Hauso O, Gustafsson BI, Kidd M, Waldum HL, Drozdov I, Chan AKC, & Modlin IM. Neuroendocrine tumor epidemiology. *Cancer* 2008 **113** 2655–2664. (doi:10.1002/cncr.23883)
109. Fisseler-Eckhoff A & Demes M. Neuroendocrine Tumors of the Lung. *Cancers* 2012 **4** 777–798. (doi:10.3390/cancers4030777)
110. Jeung MY, Gasser B, Gangi A, Charneau D, Ducroq X, Kessler R, Quoix E, & Roy C. Bronchial Carcinoid Tumors of the Thorax: Spectrum of Radiologic Findings. *RadioGraphics* 2002 **22** 351–365. (doi:10.1148/radiographics.22.2.g02mr01351)
111. Jeung MY, Gasser B, Gangi A, Charneau D, Ducroq X, Kessler R, Quoix E, & Roy C. Bronchial Carcinoid Tumors of the Thorax: Spectrum of Radiologic Findings. *RadioGraphics* 2002 **22** 351–365. (doi:10.1148/radiographics.22.2.g02mr01351)
112. Ferolla P, Brizzi MP, Meyer T, Mansoor W, Mazieres J, Cao C do, Léna H, Berruti A, Damiano V, Buikhuisen W, Grønbaek H, Lombard-Bohas C, Grohé C, Minotti V, Tiseo M, Castro J de, Reed N, Gislimberti G, Singh N, Stankovic M, Öberg K, & Baudin E. Efficacy and safety of long-acting pasireotide or everolimus alone or in combination in patients with advanced carcinoids of the lung and thymus (LUNA): an open-label, multicentre, randomised, phase 2 trial. *The Lancet Oncology* 2017 **18** 1652–1664. (doi:10.1016/S1470-2045(17)30681-2)
113. Shrager JB, Wright CD, Wain JC, Torchiana DF, Grillo HC, & Mathisen DJ. Bronchopulmonary carcinoid tumors associated with cushing’s syndrome: A more aggressive variant of typical carcinoid. *The Journal of Thoracic and Cardiovascular Surgery* 1997 **114** 367–375. (doi:10.1016/S0022-5223(97)70182-X)
114. Athanassiadi K, Exarchos D, Tsagarakis S, & Bellenis I. Acromegaly caused by ectopic growth hormone–releasing hormone secretion by a carcinoid bronchial tumor: A rare entity. *The Journal of Thoracic and Cardiovascular Surgery* 2004 **128** 631–632. (doi:10.1016/j.jtcvs.2004.02.033)
115. Bozkurt MF, Virgolini I, Balogova S, Beheshti M, Rubello D, Decristoforo C, Ambrosini V, Kjaer A, Delgado-Bolton R, Kunikowska J, Oyen WJG, Chiti A, Giammarile F, & Fanti S. Guideline for PET/CT imaging of neuroendocrine neoplasms with 68Ga-DOTA-conjugated somatostatin receptor targeting peptides

- and 18F–DOPA. *European Journal of Nuclear Medicine and Molecular Imaging* 2017 **44** 1588–1601. (doi:10.1007/s00259-017-3728-y)
116. Morandi U, Casali C, & Rossi G. Bronchial Typical Carcinoid Tumors. *Seminars in Thoracic and Cardiovascular Surgery* 2006 **18** 191–198. (doi:10.1053/j.semtcvs.2006.08.005)
 117. Namasivayam S. Imaging of liver metastases: MRI. *Cancer Imaging* 2007 **7** 2–9. (doi:10.1102/1470-7330.2007.0002)
 118. Hope TA, Bergsland EK, Bozkurt MF, Graham M, Heaney AP, Herrmann K, Howe JR, Kulke MH, Kunz PL, Mailman J, May L, Metz DC, Millo C, O’Dorisio S, Reidy-Lagunes DL, Soulen MC, & Strosberg JR. Appropriate Use Criteria for Somatostatin Receptor PET Imaging in Neuroendocrine Tumors. *Journal of Nuclear Medicine* 2018 **59** 66–74. (doi:10.2967/jnumed.117.202275)
 119. Kruger S, Buck AK, Blumstein NM, Pauls S, Schelzig H, Kropf C, Schumann C, Mottaghy FM, Hombach V, & Reske SN. Use of integrated FDG PET/CT imaging in pulmonary carcinoid tumours. *Journal of Internal Medicine* 2006 **260** 545–550. (doi:10.1111/j.1365-2796.2006.01729.x)
 120. García-Yuste M, Matilla JM, Cañizares MA, Molins L, & Guijarro R. Surgical treatment of low and intermediate grade lung net. *Journal of Thoracic Disease* 2017 **9** S1435–S1441. (doi:10.21037/jtd.2017.09.83)
 121. Caplin ME, Baudin E, Ferolla P, Filosso P, Garcia-Yuste M, Lim E, Oberg K, Pelosi G, Perren A, Rossi RE, Travis WD, Bartsch D, Capdevila J, Costa F, Cwikla J, Herder W de, Delle Fave G, Eriksson B, Falconi M, Ferone D, Gross D, Grossman A, Ito T, Jensen R, Kaltsas G, Kelestimur F, Kianmanesh R, Knigge U, Kos-Kudla B, ... Zheng-Pei Z. Pulmonary neuroendocrine (carcinoid) tumors: European Neuroendocrine Tumor Society expert consensus and recommendations for best practice for typical and atypical pulmonary carcinoids. *Annals of Oncology* 2015 **26** 1604–1620. (doi:10.1093/annonc/mdv041)
 122. Pavel M, O’Toole D, Costa F, Capdevila J, Gross D, Kianmanesh R, Krenning E, Knigge U, Salazar R, Pape UF, & Öberg K. ENETS consensus guidelines update for the management of distant metastatic disease of intestinal, pancreatic, bronchial

- neuroendocrine neoplasms (NEN) and NEN of unknown primary site. *Neuroendocrinology* 2016. (doi:10.1159/000443167)
123. Cives M & Strosberg J. The expanding role of somatostatin analogs in gastroenteropancreatic and lung neuroendocrine tumors. *Drugs* 2015. pp 847–858. (doi:10.1007/s40265-015-0397-7)
 124. Zatelli MC, Minoia M, Martini C, Tagliati F, Ambrosio MR, Schiavon M, Buratto M, Calabrese F, Gentilin E, Cavallesco G, Berdondini L, Rea F, & Degli Uberti EC. Everolimus as a new potential antiproliferative agent in aggressive human bronchial carcinoids. *Endocrine-Related Cancer* 2010. (doi:10.1677/ERC-10-0097)
 125. Duran I, Siu LL, Oza AM, Chung TB, Sturgeon J, Townsley CA, Pond GR, Seymour L, & Niroumand M. Characterisation of the lung toxicity of the cell cycle inhibitor temsirolimus. *European Journal of Cancer* 2006. (doi:10.1016/j.ejca.2006.03.015)
 126. Gagliano T, Bellio M, Gentilin E, Molè D, Tagliati F, Schiavon M, Cavallesco NG, Andriolo LG, Ambrosio MR, Rea F, Uberti ED, & Zatelli MC. MTOR, p70S6K, AKT, and ERK1/2 levels predict sensitivity to mTOR and PI3K/mTOR inhibitors in human bronchial carcinoids. *Endocrine-Related Cancer* 2013. (doi:10.1530/ERC-13-0042)
 127. Pavel ME, Hainsworth JD, Baudin E, Peeters M, Hörsch D, Winkler RE, Klimovsky J, Lebwohl D, Jehl V, Wolin EM, Öberg K, Cutsem E Van, & Yao JC. Everolimus plus octreotide long-acting repeatable for the treatment of advanced neuroendocrine tumours associated with carcinoid syndrome (RADIANT-2): A randomised, placebo-controlled, phase 3 study. *The Lancet* 2011. (doi:10.1016/S0140-6736(11)61742-X)
 128. Yao JC, Fazio N, Singh S, Buzzoni R, Carnaghi C, Wolin E, Tomasek J, Raderer M, Lahner H, Voi M, Pacaud LB, Rouyrre N, Sachs C, Valle JW, Fave GD, Cutsem E Van, Tesselaar M, Shimada Y, Oh DY, Strosberg J, Kulke MH, & Pavel ME. Everolimus for the treatment of advanced, non-functional neuroendocrine tumours of the lung or gastrointestinal tract (RADIANT-4): A randomised, placebo-controlled, phase 3 study. *The Lancet* 2016. (doi:10.1016/S0140-6736(15)00817-X)
 129. Peri M & Fazio N. Clinical Evaluation of Everolimus in the Treatment of Neuroendocrine Tumors of the Lung: Patient Selection and Special Considerations.

130. Breuleux M, Klopfenstein M, Stephan C, Doughty CA, Barys L, Maira S michel, Kwiatkowski D, & Lane HA. Increased AKT S473 phosphorylation after mTORC1 inhibition is rictor dependent and does not predict tumor cell response to PI3K/mTOR inhibition. 2009 **8** 742–753. (doi:10.1158/1535-7163.MCT-08-0668)
131. Fazio N. Neuroendocrine tumors resistant to mammalian target of rapamycin inhibitors: A difficult conversion from biology to the clinic. *World Journal of Clinical Oncology* 2015. (doi:10.5306/wjco.v6.i6.194)
132. O'Reilly KE, Rojo F, She QB, Solit D, Mills GB, Smith D, Lane H, Hofmann F, Hicklin DJ, Ludwig DL, Baselga J, & Rosen N. mTOR inhibition induces upstream receptor tyrosine kinase signaling and activates Akt. *Cancer Research* 2006. (doi:10.1158/0008-5472.CAN-05-2925)
133. Uprety D, Halfdanarson TR, Molina JR, & Leventakos K. Pulmonary Neuroendocrine Tumors: Adjuvant and Systemic Treatments. *Current Treatment Options in Oncology* 2020 **21** 86. (doi:10.1007/s11864-020-00786-0)
134. Strosberg JR, Caplin ME, Kunz PL, Ruszniewski PB, Bodei L, Hendifar A, Mittra E, Wolin EM, Yao JC, Pavel ME, Grande E, Cutsem E van, Seregni E, Duarte H, Gericke G, Bartalotta A, Mariani MF, Demange A, Mutevelic S, & Krenning EP. 177Lu-Dotatate plus long-acting octreotide versus high-dose long-acting octreotide in patients with midgut neuroendocrine tumours (NETTER-1): final overall survival and long-term safety results from an open-label, randomised, controlled, phase 3 trial. *The Lancet Oncology* 2021 **22** 1752–1763. (doi:10.1016/S1470-2045(21)00572-6)
135. Shan YS, Hsu HP, Lai MD, Hung YH, Wang CY, Yen MC, & Chen YL. Cyclin D1 overexpression correlates with poor tumor differentiation and prognosis in gastric cancer. *Oncology Letters* 2017 **14** 4517–4526. (doi:10.3892/ol.2017.6736)
136. Biliran H, Wang Y, Banerjee S, Xu H, Heng H, Thakur A, Bollig A, Sarkar FH, & Liao JD. Overexpression of cyclin D1 promotes tumor cell growth and confers resistance to cisplatin-mediated apoptosis in an elastase-myc transgene-expressing pancreatic tumor cell line. *Clinical Cancer Research* 2005 **11** 6075–6086. (doi:10.1158/1078-0432.CCR-04-2419)

137. Imrali A, Mao X, Yeste-Velasco M, Shamash J, & Lu Y. Rapamycin inhibits prostate cancer cell growth through cyclin D1 and enhances the cytotoxic efficacy of cisplatin. *American journal of cancer research* 2016 **6** 1772–1784.
138. Chen G, Ding XF, Bouamar H, Pressley K, & Sun LZ. Everolimus induces G1 cell cycle arrest through autophagy-mediated protein degradation of cyclin D1 in breast cancer cells. *American Journal of Physiology-Cell Physiology* 2019 **317** C244–C252. (doi:10.1152/ajpcell.00390.2018)
139. Lawrence MS, Stojanov P, Mermel CH, Robinson JT, Garraway LA, Golub TR, Meyerson M, Gabriel SB, Lander ES, & Getz G. Discovery and saturation analysis of cancer genes across 21 tumour types. *Nature* 2014 **505** 495–501. (doi:10.1038/nature12912)
140. Yao JC, Pavel M, Lombard-Bohas C, Cutsem E van, Voi M, Brandt U, He W, Chen D, Capdevila J, Vries EGE de, Tomassetti P, Hobday T, Pommier R, & Öberg K. Everolimus for the Treatment of Advanced Pancreatic Neuroendocrine Tumors: Overall Survival and Circulating Biomarkers From the Randomized, Phase III RADIANT-3 Study. *Journal of Clinical Oncology* 2016 **34** 3906–3913. (doi:10.1200/JCO.2016.68.0702)
141. Yao JC, Fazio N, Singh S, Buzzoni R, Carnaghi C, Wolin E, Tomasek J, Raderer M, Lahner H, Voi M, Pacaud LB, Rouyrre N, Sachs C, Valle JW, Fave GD, Cutsem E van, Tesselaar M, Shimada Y, Oh DY, Strosberg J, Kulke MH, & Pavel ME. Everolimus for the treatment of advanced, non-functional neuroendocrine tumours of the lung or gastrointestinal tract (RADIANT-4): a randomised, placebo-controlled, phase 3 study. *The Lancet* 2016 **387** 968–977. (doi:10.1016/S0140-6736(15)00817-X)
142. Saxton RA & Sabatini DM. mTOR Signaling in Growth, Metabolism, and Disease. *Cell* 2017 **168** 960–976. (doi:10.1016/j.cell.2017.02.004)
143. Hsieh AC, Liu Y, Edlind MP, Ingolia NT, Janes MR, Sher A, Shi EY, Stumpf CR, Christensen C, Bonham MJ, Wang S, Ren P, Martin M, Jessen K, Feldman ME, Weissman JS, Shokat KM, Rommel C, & Ruggero D. The translational landscape of mTOR signalling steers cancer initiation and metastasis. *Nature* 2012 **485** 55–61. (doi:10.1038/nature10912)

144. Ortolani S, Ciccarese C, Cingarlini S, Tortora G, & Massari F. Suppression of mTOR pathway in solid tumors: lessons learned from clinical experience in renal cell carcinoma and neuroendocrine tumors and new perspectives. *Future Oncology* 2015 **11** 1809–1828. (doi:10.2217/fon.15.81)
145. Laplante M & Sabatini DM. mTOR Signaling in Growth Control and Disease. *Cell* 2012 **149** 274–293. (doi:10.1016/j.cell.2012.03.017)
146. Zhou H, Luo Y, & Huang S. Updates of mTOR Inhibitors. *Anti-Cancer Agents in Medicinal Chemistry* 2010 **10** 571–581. (doi:10.2174/187152010793498663)
147. Syed V. TGF- β Signaling in Cancer. *Journal of cellular biochemistry* 2016. (doi:10.1002/jcb.25496)
148. Liu Y, Liu H, Meyer C, Li J, Nadalin S, Königsrainer A, Weng H, Dooley S, & Dijke P ten. Transforming Growth Factor- β (TGF- β)-mediated Connective Tissue Growth Factor (CTGF) Expression in Hepatic Stellate Cells Requires Stat3 Signaling Activation. *Journal of Biological Chemistry* 2013 **288** 30708–30719. (doi:10.1074/jbc.M113.478685)
149. Aoki CA, Borchers AT, Li M, Flavell RA, Bowlus CL, Ansari AA, & Gershwin ME. Transforming growth factor β (TGF- β) and autoimmunity. *Autoimmunity Reviews* 2005 **4** 450–459. (doi:10.1016/j.autrev.2005.03.006)
150. Tzavlaki K & Moustakas A. TGF- β Signaling. *Biomolecules* 2020 **10** 487. (doi:10.3390/biom10030487)
151. Datto MB, Li Y, Panus JF, Howe DJ, Xiong Y, & Wang XF. Transforming growth factor beta induces the cyclin-dependent kinase inhibitor p21 through a p53-independent mechanism. *Proceedings of the National Academy of Sciences* 1995 **92** 5545–5549. (doi:10.1073/pnas.92.12.5545)
152. Pasche B. Role of transforming growth factor beta in cancer. *Journal of Cellular Physiology* 2001 **186** 153–168. (doi:10.1002/1097-4652(200002)186:2<153::AID-JCP1016>3.0.CO;2-J)
153. Teicher BA. TGF β -Directed Therapeutics: 2020. *Pharmacology & Therapeutics* 2021 **217** 107666. (doi:10.1016/j.pharmthera.2020.107666)

154. Dash S, Sarashetti PM, Rajashekar B, Chowdhury R, & Mukherjee S. TGF- β -induced EMT is dampened by inhibition of autophagy and TNF- α treatment. *Oncotarget* 2018. (doi:10.18632/oncotarget.23942)
155. Ikushima H & Miyazono K. TGF β 2 signalling: A complex web in cancer progression. *Nature Reviews Cancer* 2010. (doi:10.1038/nrc2853)
156. Kalluri R & Weinberg RA. The basics of epithelial-mesenchymal transition. *Journal of Clinical Investigation* 2009 **119** 1420–1428. (doi:10.1172/JCI39104)
157. Lamouille S & Derynck R. Cell size and invasion in TGF- β -induced epithelial to mesenchymal transition is regulated by activation of the mTOR pathway. *Journal of Cell Biology* 2007 **178** 437–451. (doi:10.1083/jcb.200611146)
158. Morris JC, Tan AR, Olencki TE, Shapiro GI, Dezube BJ, Reiss M, Hsu FJ, Berzofsky JA, & Lawrence DP. Phase I Study of GC1008 (Fresolimumab): A Human Anti-Transforming Growth Factor-Beta (TGF β) Monoclonal Antibody in Patients with Advanced Malignant Melanoma or Renal Cell Carcinoma. *PLoS ONE* 2014 **9** e90353. (doi:10.1371/journal.pone.0090353)
159. Vincenti F, Fervenza FC, Campbell KN, Diaz M, Gesualdo L, Nelson P, Praga M, Radhakrishnan J, Sellin L, Singh A, Thornley-Brown D, Veronese FV, Accomando B, Engstrand S, Ledbetter S, Lin J, Neylan J, & Tumlin J. A Phase 2, Double-Blind, Placebo-Controlled, Randomized Study of Fresolimumab in Patients With Steroid-Resistant Primary Focal Segmental Glomerulosclerosis. *Kidney International Reports* 2017 **2** 800–810. (doi:10.1016/j.ekir.2017.03.011)
160. Teicher BA. TGF β -Directed Therapeutics: 2020. *Pharmacology & Therapeutics* 2021 **217** 107666. (doi:10.1016/j.pharmthera.2020.107666)
161. Huang CY, Chung CL, Hu TH, Chen JJ, Liu PF, & Chen CL. Recent progress in TGF- β inhibitors for cancer therapy. *Biomedicine & Pharmacotherapy* 2021 **134** 111046. (doi:10.1016/j.biopha.2020.111046)
162. Yi JY, Shin I, & Arteaga CL. Type I Transforming Growth Factor β Receptor Binds to and Activates Phosphatidylinositol 3-Kinase. *Journal of Biological Chemistry* 2005 **280** 10870–10876. (doi:10.1074/jbc.M413223200)

163. Torrealba N, Vera R, Fraile B, Martínez-Onsurbe P, Paniagua R, & Royuela M. TGF- β /PI3K/AKT/mTOR/NF-kB pathway. Clinicopathological features in prostate cancer. *The Aging Male* 2020 **23** 801–811. (doi:10.1080/13685538.2019.1597840)
164. Zhai XX, Tang ZM, Ding JC, & Lu XL. Expression of TGF- β 1/mTOR signaling pathway in pathological scar fibroblasts. *Molecular Medicine Reports* 2017. (doi:10.3892/mmr.2017.6437)
165. Cheng KY & Hao M. Mammalian target of rapamycin (mTOR) regulates transforming growth factor- β 1 (TGF- β 1)-induced epithelial-mesenchymal transition via decreased pyruvate kinase M2 (PKM2) expression in cervical cancer cells. *Medical Science Monitor* 2017. (doi:10.12659/MSM.901542)
166. Fazio N, Buzzoni R, Delle Fave G, Tesselaar ME, Wolin E, Cutsem E van, Tomassetti P, Strosberg J, Voi M, Bubuteishvili-Pacaud L, Ridolfi A, Herbst F, Tomasek J, Singh S, Pavel M, Kulke MH, Valle JW, & Yao JC. Everolimus in advanced, progressive, well-differentiated, non-functional neuroendocrine tumors: RADIANT-4 lung subgroup analysis. *Cancer Science* 2018 **109** 174–181. (doi:10.1111/cas.13427)
167. Tagliati F, Gentilin E, Buratto M, Molè D, Degli Uberti EC, & Zatelli MC. Magmas, a gene newly identified as overexpressed in human and mouse ACTH-secreting pituitary adenomas, protects pituitary cells from apoptotic stimuli. *Endocrinology* 2010 **151** 4635–4642. (doi:10.1210/en.2010-0441)
168. Schneider CA, Rasband WS, & Eliceiri KW. NIH Image to ImageJ: 25 years of image analysis. *Nature Methods* 2012 **9** 671–675. (doi:10.1038/nmeth.2089)
169. Mohammadzadeh F, Hani M, Ranaee M, & Bagheri M. Role of cyclin D1 in breast carcinoma. *Journal of research in medical sciences : the official journal of Isfahan University of Medical Sciences* 2013 **18** 1021–1025.
170. Worsley SD, Ponder BAJ, & Davies BR. Overexpression of Cyclin D1 in Epithelial Ovarian Cancers. *Gynecologic Oncology* 1997 **64** 189–195. (doi:10.1006/gyno.1996.4569)
171. Albasri AM, Elkablawy MA, Ansari IA, & Alhujaily AS. Prognostic Significance of Cyclin D1 Over-expression in Colorectal Cancer: An Experience from Madinah,

- Saudi Arabia. *Asian Pacific Journal of Cancer Prevention* 2019 **20** 2471–2476. (doi:10.31557/APJCP.2019.20.8.2471)
172. Igarashi T, Jiang SX, Kameya T, Asamura H, Sato Y, Nagai K, & Okayasu I. Divergent cyclin B1 expression and Rb/p16/cyclin D1 pathway aberrations among pulmonary neuroendocrine tumors. *Modern Pathology* 2004 **17** 1259–1267. (doi:10.1038/modpathol.3800176)
173. Lamouille S, Connolly E, Smyth JW, Akhurst RJ, & Derynck R. TGF- β -induced activation of mTOR complex 2 drives epithelial–mesenchymal transition and cell invasion. *Journal of Cell Science* 2012 **125** 1259–1273. (doi:10.1242/jcs.095299)
174. Zhou M, Liu X, Li Z, Huang Q, Li F, & Li CY. Caspase-3 regulates the migration, invasion and metastasis of colon cancer cells. *International Journal of Cancer* 2018 **143** 921–930. (doi:10.1002/ijc.31374)
175. Tyson JJ & Novak B. Control of cell growth, division and death: information processing in living cells. *Interface Focus* 2014 **4** 20130070. (doi:10.1098/rsfs.2013.0070)
176. Plati J, Bucur O, & Khosravi-Far R. Apoptotic cell signaling in cancer progression and therapy. *Integrative Biology* 2011 **3** 279–296. (doi:10.1039/c0ib00144a)
177. Elmore S. Apoptosis: A Review of Programmed Cell Death. *Toxicologic Pathology* 2007 **35** 495–516. (doi:10.1080/01926230701320337)
178. Bukowski K, Kciuk M, & Kontek R. Mechanisms of Multidrug Resistance in Cancer Chemotherapy. *International Journal of Molecular Sciences* 2020 **21** 3233. (doi:10.3390/ijms21093233)
179. Peng J, Huang CH, Short MK, & Jubinsky PT. Magmas gene structure and evolution. *In Silico Biol* 2005. (doi:2004050024 [pii])
180. Jubinsky PT, Messer A, Bender J, Morris RE, Ciruolo GM, Witte DP, Hawley RG, & Short MK. Identification and characterization of Magmas, a novel mitochondria-associated protein involved in granulocyte-macrophage colony-stimulating factor signal transduction. *Experimental Hematology* 2001 **29** 1392–1402. (doi:10.1016/S0301-472X(01)00749-4)

181. Di K, Lomeli N, Bota DA, & Das BC. Magmas inhibition as a potential treatment strategy in malignant glioma. *Journal of Neuro-Oncology* 2019. (doi:10.1007/s11060-018-03040-8)
182. Jubinsky PT, Short MK, Mutema G, Morris RE, Ciruolo GM, & Li M. Magmas expression in neoplastic human prostate. *Journal of Molecular Histology* 2005. (doi:10.1007/s10735-004-3840-8)
183. Vijver MJ van de, He YD, 't Veer LJ van, Dai H, Hart AAM, Voskuil DW, Schreiber GJ, Peterse JL, Roberts C, Marton MJ, Parrish M, Atsma D, Witteveen A, Glas A, Delahaye L, Velde T van der, Bartelink H, Rodenhuis S, Rutgers ET, Friend SH, & Bernards R. A Gene-Expression Signature as a Predictor of Survival in Breast Cancer. *New England Journal of Medicine* 2002 **347** 1999–2009. (doi:10.1056/NEJMoa021967)
184. Srivastava S, Sinha D, Saha PP, Marthala H, & D'Silva P. Magmas functions as a ROS regulator and provides cytoprotection against oxidative stress-mediated damages. *Cell Death & Disease* 2014 **5** e1394–e1394. (doi:10.1038/cddis.2014.355)
185. Tagliati F, Gagliano T, Gentilin E, Minoia M, Molè D, Delgi Uberti EC, & Zatelli MC. Magmas Overexpression Inhibits Staurosporine Induced Apoptosis in Rat Pituitary Adenoma Cell Lines. *PLoS ONE* 2013 **8** 1–13. (doi:10.1371/journal.pone.0075194)
186. Jubinsky PT, Short MK, Ghanem M, & Das BC. Design, synthesis, and biological activity of novel Magmas inhibitors. *Bioorganic and Medicinal Chemistry Letters* 2011 **21** 3479–3482. (doi:10.1016/j.bmcl.2011.03.050)
187. Zatelli MC, Gagliano T, Pelà M, Bianco S, Bertolasi V, Tagliati F, Guerrini R, Degli Uberti E, Salvadori S, & Trapella C. N-carbamidoyl-4-((3-ethyl-2,4,4-trimethylcyclohexyl)methyl)benzamide enhances staurosporine cytotoxic effects likely inhibiting the protective action of Magmas toward cell apoptosis. *Journal of Medicinal Chemistry* 2014 **57** 4606–4614. (doi:10.1021/jm5000535)
188. Zatelli MC, Gagliano T, Pelà M, Bianco S, Bertolasi V, Tagliati F, Guerrini R, Degli Uberti E, Salvadori S, & Trapella C. N-carbamidoyl-4-((3-ethyl-2,4,4-trimethylcyclohexyl)methyl)benzamide enhances staurosporine cytotoxic effects

- likely inhibiting the protective action of Magmas toward cell apoptosis. *Journal of Medicinal Chemistry* 2014. (doi:10.1021/jm5000535)
189. Pronobis MI, Deutch N, & Peifer M. The Miraprep: A Protocol that Uses a Miniprep Kit and Provides Maxiprep Yields. *PLOS ONE* 2016 **11** e0160509. (doi:10.1371/journal.pone.0160509)
 190. D'Silva PR, Schilke B, Walter W, & Craig E a. Role of Pam16's degenerate J domain in protein import across the mitochondrial inner membrane. *Proceedings of the National Academy of Sciences of the United States of America* 2005 **102** 12419–12424. (doi:10.1073/pnas.0505969102)
 191. Cibas ES & Ali SZ. The 2017 Bethesda System for Reporting Thyroid Cytopathology. *Thyroid* 2017 **27** 1341–1346. (doi:10.1089/thy.2017.0500)
 192. Borowczyk M, Szczepanek-Parulska E, Olejarz M, Więckowska B, Verburg FA, Dębicki S, Budny B, Janicka-Jedyńska M, Ziemnicka K, & Ruchała M. Evaluation of 167 Gene Expression Classifier (GEC) and ThyroSeq v2 Diagnostic Accuracy in the Preoperative Assessment of Indeterminate Thyroid Nodules: Bivariate/HROC Meta-analysis. *Endocrine Pathology* 2019 **30** 8–15. (doi:10.1007/s12022-018-9560-5)
 193. Nikiforov YE, Carty SE, Chiosea SI, Coyne C, Duvvuri U, Ferris RL, Gooding WE, LeBeau SO, Ohori NP, Seethala RR, Tublin ME, Yip L, & Nikiforova MN. Impact of the Multi-Gene ThyroSeq Next-Generation Sequencing Assay on Cancer Diagnosis in Thyroid Nodules with Atypia of Undetermined Significance/Follicular Lesion of Undetermined Significance Cytology. *Thyroid* 2015 **25** 1217–1223. (doi:10.1089/thy.2015.0305)
 194. Nikiforov YE, Ohori NP, Hodak SP, Carty SE, LeBeau SO, Ferris RL, Yip L, Seethala RR, Tublin ME, Stang MT, Coyne C, Johnson JT, Stewart AF, & Nikiforova MN. Impact of mutational testing on the diagnosis and management of patients with cytologically indeterminate thyroid nodules: A prospective analysis of 1056 FNA samples. *Journal of Clinical Endocrinology and Metabolism* 2011. (doi:10.1210/jc.2011-1469)
 195. Taye A, Gurciullo D, Miles BA, Gupta A, Owen RP, Inabnet WB, Beyda JN, & Marti JL. Clinical performance of a next-generation sequencing assay (ThyroSeq v2) in the

- evaluation of indeterminate thyroid nodules. *Surgery* 2018 **163** 97–103. (doi:10.1016/j.surg.2017.07.032)
196. Purcell S, Neale B, Todd-Brown K, Thomas L, Ferreira MAR, Bender D, Maller J, Sklar P, Bakker PIW de, Daly MJ, & Sham PC. PLINK: A Tool Set for Whole-Genome Association and Population-Based Linkage Analyses. *The American Journal of Human Genetics* 2007 **81** 559–575. (doi:10.1086/519795)
197. R Core Team (2018). R: A language and environment for statistical computing. R Foundation for Statistical Computing, Vienna, Austria. Available online at <https://www.R-project.org/>.
198. Uscanga-Perales G, Santuario-Facio S, Sanchez-Dominguez C, Cardona-Huerta S, Muñoz-Maldonado G, Ruiz-Flores P, Barcenas-Walls J, Osuna-Rosales L, Rojas-Martinez A, Gonzalez-Guerrero J, Valero-Gomez J, Gomez-Macias G, Barbosa-Quintana A, Barboza-Quintana O, Garza-Guajardo R, & Ortiz-Lopez R. Genetic alterations of triple negative breast cancer (TNBC) in women from Northeastern Mexico. *Oncology Letters* 2019. (doi:10.3892/ol.2019.9984)